Genome-Wide Associations Identifying Marker-Trait-Associations for Root Morphology and Photosynthetic Related Traits in a Soybean (Glycine max) Diversity Panel

by

Jillian Amani Abendroth

A thesis submitted to the Graduate Faculty of
Auburn University
in partial fulfillment of the
requirements for the Degree of
Masters of Science

Auburn, Alabama
May 6, 2023

Keywords: Soybean, Photosynthesis, Root System Architecture, Drought, GWAS

Approved by

Jenny Koebernick, Chair, Associate Professor of Crop, Soil and Environmental Science
Alvaro Sanz Saez, Associate Professor of Crop, Soil and Environmental Science
Jinesh Patel, Faculty Investigator, Crop, Soil and Environmental Science
Charles Chen, Professor of Crop, Soil and Environmental Science

Abstract

Soybean is a staple crop for the food, feed, and fuel industries because of its unique oil and protein composition. It is the second most produced crop globally, with average acres planted and harvest yield increasing annually. However, the current rate of increase is insufficient to match future supply with projected demand. This imbalance is exacerbated by yield decreases due to abiotic stresses, particularly drought. The aim of this thesis project is to address these intertwined phenomena through a two-pronged approach, examining above and below-ground phenotypes for their implication on stress tolerance and yield improvement. Methodologically, this is pursued through phenotypic measurement and analysis followed by genome-wide association analysis seeking to identify markers associated to traits utilizing a soybean diversity panel grown in field conditions.

Chapter one is a review of literature, examining the context of this research, discussing the relationship between drought, yield, photosynthesis, and root characteristics. Chapter two delves into the phenotyping and analysis of above-ground biomass traits (photosynthetic rate, stomatal conductance, water-use efficiency, intracellular CO_2, leaf area, leaf mass, and specific leaf area). Results of above-ground analysis suggests the environmental dependency of gas exchange data and identify 31 significant SNP associations with 5 of the 7 measured traits. Chapter three then reviews the methodology and results of the analysis with below-ground root system architecture traits. The outcomes of root analysis determine several (30) significant SNPs associated with 5 of the 12 analyzed traits. Findings of this project provide valuable insight into the breadth of genetic diversity within soybean maturity group V, increased understanding of the complex genetic architecture underpinning physiological and morphological traits related to photosynthetic and root architecture traits, and, finally, determines several compelling SNPs and genes to utilize in future projects.

Acknowledgments

I sincerely give the most heartfelt thank you to my major advisor, Dr. Jenny Koebernick. Without her guidance, patience, encouragement, advice, and support I would not be where I am. She saw something in me when we first met that convinced her to take a chance on me; I can only hope that I have provided positivity to her lab and research program and that I have and will continue to make her proud. I am equally thankful to my committee members Dr. Alvaro Sanz, Dr. Charles Chen, and Dr. Jinesh Patel. They have gone above and beyond, frequently serving as advisors, teachers and mentors committing great time, help, and suggestions to make me a better scientist. I also want to express my gratitude to the research scientists, Dr. Mali Mahalingam, Dr. Jason Walling, Dr. Sarah Whitcomb, and Dr. Marcus Vinje, at the Cereal Crop Research Unit-USDA (Madison, WI.) for sharing their time, flexibility, and expertise with me. I want to thank my fellow graduate students, research techs, and student workers, without whom phenotyping would have been impossible.

Lastly, I want to thank my fiancé, Casper Wenner, for the unwavering support, motivation, love, and for "holding down the fort." Without Cas, my parents, siblings, and close network of friends, none of this would have been possible. Thank you all for reading every email and paragraph, for listening to each presentation endlessly, and for being with me while I pursued my dreams.

Preface to the Reader

Dear Reader,

I don't know if I've yet read another thesis or dissertation with a preface directly addressing the consumer, but it is my paper so I'm going to do it anyway.

While in a writing slump, I was procrastinating writing paragraphs by scrolling through the "grad school memes with relatable themes" group. In this group, I came across a post that said, and I paraphrase, that a review of literature is not for the writer, it is not the opportunity to show off knowledge or give detailed and obscure references; it is for the reader. It is intended to provide a foundation for understanding the context in which research is performed, and how this research benefits the field. This random meme truly caused me to shift how I viewed this review of literature and paper. This is not for me, though I benefit from its production; rather it is a painstakingly crafted and meticulously thought-out gift for you. It aims to shed light on the history and progress undertaken in soybean and display the ways in which my humble projects contribute to field advancement.

With this in mind, I am writing this thesis to you. I will attempt to be succinct (although you may already notice I struggle on this account), precise, thoughtful, and accessible. I hope you find delight in each letter, knowledge in each paragraph, and inspiration in unexpected places; possibly even while procrastinating in a meme group.

Sincerely,
Jillian Abendroth
M.S. Crop, Soil, and Environmental Science Candidate

Table of Contents

List of Tables

List of Figures

List of Abbreviations

ABA	Abscisic Acid
ADP	Adenosine diphosphate
ATP	Adenosine triphosphate
BLINK	Bayesian information and Linkage-disequilibrium Iteratively Nested Keyway
bp	Base pairs
C	Celsius
CO_2	Carbon Dioxide
DIRT	Digital Imaging of Root Traits
e_c	Energy conversion efficiency
e_i	Light interception efficiency
e_p	Biomass partitioning efficiency
F	Fahrenheit
FACE	Free-air CO_2 enrichment
FarmCPU	Fixed and random model Circulating Probability Unification
Gb	Giga bases (1,000,000,000 x bp)
GHG	Greenhouse Gasses
GLM	General-Linear Model
GWAS	Genome-wide association study
kb	Kilo bases (1000 x bp)
LD	Linkage-Disequilibrium
Mb	Mega bases (1,000,000 x bp)
MLM	Mixed-Linear Model
MRI	Magnetic resonance imaging
MTA	Marker-Trait Association
NADPH	Nicotinamide adenine dinucleotide phosphate
NOAA	National Oceanic and Atmospheric Administration
PET	Positron emission tomography
QTL	Quantitative-trait locus

REST	Root Estimator for Shovelomics Traits
RSA	Root System Architecture
RUBISCO	Ribulose-1,5-bisphosphate carboxylase/oxygenase
SBPase	Sedoheptulose- 1:7-bisphosphatase
SNP	Single Nucleutide Polymorphism
st	Incident of solar radiation
WUE	Water Use Efficiency
X-ray CT	X-ray computed tomography

Chapter 1:
Review of Literature

Section 1: History, Characteristics, and Introduction

1.1)   History

Soybean (Glycine max) is an annual leguminous crop highly regarded for their

nutritional, economic, and cultural significance. Thought to have a single center of origin in

China (Guo et al. 2010; Z. Zhou et al. 2015), the modern domestic soybean is widely agreed to

have derived from G. soja between 6000-9000 years ago (Kim et al. 2012; Carter, Hymowitz,

and Nelson 2004). Recent and seemingly conclusive results of such support the Huang-Huai

Valley of Central China as the soybean's genetic center of origin (Han et al. 2016), in contrast

with the previously considered Yellow River Basin of the Hunghe Region of China (Dong et al.

2004; Y.-H. Li et al. 2010; G.-A. Lee et al. 2011). Gene flow analysis demonstrates significant

gene flow from *soja* to *gracilis* and *gracilis* to *max* (Han et al. 2016), suggesting *gracilis* as a

domestication intermediate between *G. soja* and *G. max*. In response to such results, an

alternative, more complex theory of domestication in which an initial wild hybridization led to

an intermediate has been presented, deviating from the long-held single center of origin theory

(Sedivy, Wu, and Hanzawa 2017).Soybean was introduced to European and American continents

during the 18th century, rapidly expanding across the United States and into Canada by 1851

(Theodore Hymowitz and Belic 1990). Starting as a local commodity, soybean cultivation has

expanded, enabling the crop to become ingrained in the global economy and diet.

1.2)   Soybean Genetics

The soybean genome is approximately 1.1 Gb and has an estimated 46,430 protein-

coding genes, 78% of which occur in the euchromatic chromosome ends. Initial sequencing in

2010 was performed whole-genome shotgun covering 950 megabases (Mb) assembled in 397

scaffolds arranged on 20 linkage groups of soybean genome. Analysis following sequence provided valuable information on the evolution of soybean, concluding that the diploid species underwent two genome duplication events and subsequent gene diversification and loss, and numerous chromosome rearrangements (Schmutz et al. 2010). Since sequencing the cultivar "Williams 82", two other soybean accessions, Zhonghuang 13 (ZH13) and wild soybean (W05), have been sequenced and are available as reference genomes (Wang et al. 2020). Genome resequencing efforts (Lam et al. 2010; Zhou et al. 2015) emphasize genetic diversity within soybean and urged the construction of a pan-genome.

Pan-genomes are compilations of sequenced lines within a species, theoretically encompassing the totality of genetic variation with that species. Characterization of the pan genome enables research insights into the genetic mechanisms that drive adaptation and evolution, as well as the functional roles of different genes in these processes. There are three distinct components: the core genome, which is shared by all members of the group and contains genes that are essential for basic cellular functions; the dispensable genome, which is present in some members of the group but not others and contains genes that are important for adapting to different environments; and the unique genome, which is present in only a single member of the group and contains genes that are specific to that individual. The most recent soybean pangenome was constructed using 26 representatives. All genes in 27 genomes (26 representatives + ZH13 reference genome) were distributed into 57,492 families out of which 28,746 families were considered a core or soft-core gene set (found in >90% of individuals), 28,679 gene families were considered dispensable, and 27 families were only identified in a single individual within the study (Y. Liu et al. 2020).

1.3)   Composition

While dependent on environmental and genetic factors (Cartter and Hopper 1942), soybean compositions range between 36-41% protein, 18-22% fats, 9-19% dietary fiber, 8-12% available carbohydrates, 7-10% moisture, and 3-5% ash (Krishnan 2000; Medic, Atkinson, and Hurburgh 2014; K. Liu 1997; Karr-Lilienthal et al. 2004; Redondo-Cuenca et al. 2007). The high oil and protein content make it irreplaceable in both direct and indirect food products and in industrial applications. For direct human consumption, soy can be derived into a myriad of products, including soy milk, tofu, soy sauce, bean paste, and tempeh (Jooyandeh 2011). The high protein characteristics of these soybean meat analogues and milk substitutes have made them increasingly popular in plant-based diets on the rise in the West (Rizzo and Baroni 2018; Messina and Messina 2010). Furthermore, the vitamins (including thiamine (B1), riboflavin (B2), and niacin (B3)), minerals (Sarkar, Morrison, and Tinggi 1998), and isoflavones (genistein, daidzein, and glycitein) (Naim et al. 1974) present in soybean have been linked to a number of health benefits. It is worth noting that the nutritional content of comestible goods is altered by the processing and production methods (Mo et al. 2013; Murooka and Yamshita 2008). B vitamin consumption has been suggested to provide mental clarity, increase the bioavailability of cobalamin, and promote cardiovascular and respiratory health (Elmadfa and Singer 2009). Isoflavones have been linked with the prevention and treatment of obesity, cancer, diabetes, osteoporosis, and heart health (Jooyandeh 2011; Sakai and Kogiso 2008; Ørgaard and Jensen 2008). Regarding products indirectly associated with human consumption, soybeans are used in various diets for livestock and domestic animals an in the industrial production of cooking oil and biodiesels (T. Hymowitz 1970). In 2021, 56% of vegetable oil consumption was soy-derived (America Soybean Association 2022a). Given the variety of uses, soybean is among the top three highest-yielding crops worldwide (America Soybean Association 2022).

1.4)   Production and Uses

Acres planted in 2020/2021 produced 13,531 million bushels; with Brazil, Argentina, and the US production culminating in approximately 80% of the global production (38%, 12%, and 31%, respectively). In the US, 33% of crop area planted, or 87.2 million acres, was soybean with an estimated value at 45.7 billion dollars (America Soybean Association 2022), with the 2021 export market valued at 27.4 billion dollars (https://www.fas.usda.gov/commodities/soybeans). The average soybean yield increased from approximately 20 bushels per acre in the 1960s to over 50 bushels per acre in recent years (Ainsworth et al. 2012; America Soybean Association 2022a). Historic improvements in yield gains have resulted from the conscious and/or unintended selection of lines expressing stress tolerance, higher nutrient and water use efficiencies, disease resistance, and other agronomic characteristics related to yield increases (Sacks and Kucharik 2011). Mindful changes in management practices, including earlier planting dates, higher planting density, pesticide and fertilizer use, and post-harvest loss reductions (Rowntree et al. 2013) further bolster yields (Koester et al. 2014). However, even with these yield increases, there is modeled to be a caloric shortage by the year 2050 (Tilman et al. 2011; Alexandratos and Bruinsma 2012). The global population is expected to boom from 7.2 billion to nearly 10 billion by the mid-21st century ("Food and Agriculture Organization of the United Nations" 2020). An increase in plant-based diets, and a push to decrease industrial fossil fuel impact, will only increase the demand for soybean. To continue to match supply with demand, it is estimated that soybean yields will need to increase by 2.4% annually (Ray et al. 2013).

Soybean yield improvements are tied to advances in biotechnology and genetics with projected step changes expected to rely on: the use of genomic selection and gene editing techniques, new agronomic practices, such as precision agriculture, and the use of big data

analytics (Shulin Liu et al. 2020; Anderson et al. 2019; Bhandari, S., Bishnoi, N. R., Sharma, V., & Kumar, R 2019; Lie, M., Brinch-Pedersen, H., & Holme, I. B. 2018; Jung, J. Y., Park, J. H., Lee, J. W., Kang, J. W., & Shin, J. H 2016). However, continuous improvement relies on an ever-increasing understanding of the factors influencing yield which has expansive impacts on the avenues of research to perform, providing channels for both basic and applied research.

Section 2: Environmental Conditions.

2.1)   The Impact of Climate Change

Human influence on the global climate has been associated with fossil fuel usage, and greenhouse gases (GHG) release into the ozone (Turrentine 2022). High concentrations of GHG trap thermal energy inside the earth's atmosphere, and the scientific expectation is that GHG accumulation will result in temperature increases greater than 1.5ºC (Irfan 2021). Accumulation of thermal energy disrupts canonical cycles and weather patterns. In the summers, this equates to more days with extreme heat and longer stretches of drought conditions. In the winter, this leads to polar vortex disruption, causing bulges in the vortex which enables polar conditions to dip lower into the northern hemisphere. Generally, climate change models, predict more numerous days of extreme temperatures, warmer winters, increasing levels of CO_2, and longer durations without precipitation but with intense precipitations on occurrences when it falls (Karl et al. 2009).   Predicted climate change will likely cause climatological changes, with the first fall frost occurring later in the season and the last spring frost occurring earlier, lengthening the growing season. As a result, plants will experience an increase in net heat accumulation, as measured in growing degree days, thus causing the climatological growing season to lengthen (Kukal and Irmak 2018).

Specifically looking at the Southeastern US, the region is characterized by climate diversity, varying between temperate, sub-tropical, and tropical environments depending on location. Climatic diversity is attributed to the range of weather conditions in the region, including the predomination of frontal systems during fall and winter, convective systems in the spring and summer, and tropical systems during the summer and fall. This leaves the southeast prone to climate vulnerability, experiencing extreme weather phenomena, including droughts, floods, winter storms, and tornadoes, with relative frequency. (Ingram, Carter, and Dow 2013). In Alabama, since 2000, the average annual observed temperate has increased by approximately a degree Fahrenheit, accompanied by a trending increase in precipitation. (Data available from the NOAA, www.ncei.noaa.gov/cdo-web/). While the average max temperature during typical soybean growing season (May-October) has remained static in this region, both the average minimum temperature as well as the average overall temperature has risen by 1ºF. The region is also more vulnerable to tropical storms or winter storms from the Gulf of Mexico due to sea level change (Mitchum 2011).

2.2)   Response of Soybean to Stress

Work and field trials associated with modeling the projected global climate have provided some broad insight into the implications of climate change on soybean. Experiments in elevated CO_2 conditions via Free-air CO_2 enrichment (FACE) have proposed that elevated CO_2 enables yield increases as atmospheric carbon dioxide: oxygen ratios reach a level in which oxygen competition for binding site decreases, leading to increased ribulose-1,5-bisphosphate carboxylase/oxygenase (RUBISCO) efficiency (Long et al. 2006, 2004; Ainsworth et al. 2012; Kimball and Idso 1983). However, these increases are less significant than expected, suggesting yield increases are non-linear and that yield increases attributed to increased CO_2 do not

circumvent the yield losses caused by other climate factors (Ainsworth and Long 2005; Long et al. 2005). Field trials mimicking various predicted heat conditions have concluded the maintenance of current soybean yields in heat conditions up to a 4°C increase over base temperature, provided that plots are provided with a 60% increase in water. Trials modeling a 5.2°C increase over base temperatures resulted in yield decreases regardless of irrigation (Curry et al. 2015).

Drought has been shown to decrease soybean yield by up to 36% (Brown, Caviness, and Brown 1985). Even in current abiotic stress conditions, maladapted cultivars experience significant yield losses to heat-stress and drought conditions (Welikhe et al. 2016). Therefore, it is vital to identify crop cultivars with mechanisms of drought resiliency. Speaking generally, soybean adaptation to projected conditions will include mechanisms for extended heat endurance, methods of rapid water absorption, physiological changes enabling water retention during drought conditions, and root structures facilitate water procurement from deep within soil horizons. Cultivars demonstrating these attributes could also be suitable for harsher climates in non-airable land, providing a valuable crop for increasing caloric production while conserving water. One such avenue of consideration is to examine mechanisms of water uptake and usage. This leads to exploring root morphology, as a metric of water uptake capabilities and examining gas exchange data as indicative of photosynthetic rate and water usage. Both approaches have an added benefit of addressing yield improvement, making the below- and above-ground biomass approach dualistic in its identification of water conscious and potentially higher yielding cultivars.

Section 3: An Overview of Photosynthesis in Soybeans

3.1) The Process

Photosynthesis is the biochemical process by which autotrophs use photon energy to convert water and carbon dioxide into energy-storing carbohydrates. The capacity to convert sunlight into photoassimilates serve as the basis for lifeand can be broadly divided into two interdependent pathways; the light-dependent reactions generate biochemical energy in the form of NADPH and ATP, and the light-independent reactions which cyclically fix carbon (Eberhard, Finazzi, and Wollman 2008). The light-dependent reactions utilize chlorophyll and photosystems in the chloroplast to absorb photon energy from the light spectrum to oxidize water and release electrons. This energy is then transferred across the electron transport chain and, ultimately, hydrolyzes a phosphate addition to the biochemical energy intermediates NADPH and ATP. NADPH and ATP produced in the light-dependent reactions serve as the "cellular energy" powering carbon assimilation in the light-independent reactions. The light-independent reactions, also called the Calvin Benson Cycle, is a cyclic process converting CO_2 to carbohydrates utilizing endogenous enzymes, such as Ribulose biphosphate (RUBISCO), and the previously generated NADPH and ATP (Bassham and Calvin 1960; Sage, Way, and Kubien 2008; Andersson and Backlund 2008).

3.2) The Relationship Between Photosynthesis and Yield

Given that photosynthesis is responsible for the generation of carbohydrates, it is unsurprising that photosynthetic rate has direct correlation to yield. Studies speculate that yield (Y) is a product of material availability and genetic predisposition for photosynthetic efficiency (Monteith and Moss 1977; Monteith 1994). The Monteith equation is the summarization of observations that plants have an internal capacity to absorb light, convert that light to energy, and to allot that energy into structural formation; Mathematically, this results in the equation:

$$Y = \varepsilon i \times \varepsilon c \times \varepsilon p$$

Where εi is light interception efficiency, εc is energy conversion efficiency, and εp is the efficiency of biomass allocation to harvestable products, also called the harvest index (Monteith and Moss 1977; Monteith 1994). A later adaptation of the Monteith equation introduced inclusion for the total incident of solar radiation (S_t). While leaves absorb 90% of photosynthetically active radiation (400-700 nm), that wavelength range is less than 50% of the total light spectrum; therefore, S_t is multiplied by .487 (X.-G. Zhu, Long, and Ort 2010). The efficiency of light intercept is dependent on leaf canopy characteristics including, the rapidity of development and closure, canopy longevity, architecture, and size. Significant canopy architecture research has been performed examining the impact the leaf angle of incidence, or the angle at which a leaf grows, on shading, sun specking, and individual leaf light interception (Pearcy, Roden, and Gamon 1990). Increased εi has resulted through the development of larger-leafed cultivars and more rapid coverage of the ground after germination. Generations of breeding practices have addressed the harvest index through dwarfing, reducing stem and increasing the potential number of seed sets. Indirectly, dwarfing has also bolstered εi via canopy resiliency to harsh weather (X.-G. Zhu, Long, and Ort 2010; Evans 1996; Hay 1995).

Assessments in the last 20 years predict that εi and εp are reaching a theoretical maximum, which has occurred through decades of breeding for improved biomass allocation and superior efficiency in light capture (Koester et al. 2014) . This has been demonstrated in soybean, where 60% of photosynthetic outputs were siphoned into harvestable grain and nearly 90% of light was intercepted (X.-G. Zhu, Long, and Ort 2010). Therefore, the last avenue of pursuit for Montieth equation optimization lies in the improvement of photosynthetic efficiency (εc) that considers the total efficiency of the photosynthetic process holistically and is therefore dependent on both the light and dark reactions of plant photosynthesis as well as respiration,

photorespiration, and carbohydrate usage factors (X.-G. Zhu, Long, and Ort 2010; Koester et al. 2014; Slattery, Ainsworth, and Ort 2013). The distinct yet intertwined steps of carbon fixation are riddled with inherent inefficiencies, yet providing ample opportunities for improvement.

3.3) Improving the Photosynthetic Process

Mechanisms of photosynthetic improvement can be discussed dependent on pathway. Suggested methods of improvement to the light-independent reactions (Calvin Benson Cycle) rely on the improvement of molecular processes. Research avenues to this end include manipulation of carbon assimilation enzymes; for example, RUBSICO, ADP glucose pyrophosphorylase, and SBPase (sedoheptulose- 1:7-bisphosphatase) (Spreitzer and Salvucci 2002; Lefebvre et al. 2005; X.-G. Zhu, de Sturler, and Long 2007). Improvement of light-dependent reactions emphasizes improving light-capture capabilities. Process improvement methods include altering light-harvesting machinery, introducing new photochemistry, increasing bioenergetic output, and/or maximizing efficiencies in the photoprotective response (X.-G. Zhu, Long, and Ort 2010; Cardona, Shao, and Nixon 2018; Melis 2009). Improved efficiency of ATP synthesis is an improvement to the light reactions that has a direct implication on the efficiency of dark reactions, given that ATP is a limiting factor in carbon assimilation (Kramer and Evans 2011).

3.4) Relationship Between Photosynthesis and Drought

The relationship between photosynthesis and yield is relatively straightforward, given that grain is a sink for biomass; the relationship between drought and photosynthesis, however, is more complex. Soil drying induces a cascade of physiological changes across the plant. Even mild drought conditions can reduce the transport of cytokinins from roots to shoots, alter the pH and liquidity of xylem sap, and induce the rapid biosynthesis of abscisic acid (ABA) (Wilkinson

and Davies 2010). Abscisic acid is a primary regulator of drought response, although the interplay between direct and indirect mediation is still unclear (Shiwei Liu et al. 2018). Direct downstream implications of ABA include the reduction of shoot growth, thereby a reduction of light intercept, and the regulation of stomatal opening, with ABA causing stomatal closure (Shiwei Liu et al. 2018; Jianhua Zhang et al. 2006). Stomatal closure is an essential physiological response that reduces leaf transpiration, reducing leaf water loss and minimizing plant water usage (Gates 1968; Jarvis and McNaughton 1986). Leaf conductance decrease results in reduced CO_2 diffusion and is considered the leading cause for decreased photosynthesis. Secondary implications of stomatal closure are as a defense mechanism in photoprotection. The imbalance of light irradiance, available intercellular CO_2, and the rate of usage in the Calvin cycle turns on the regulated thermal dissipation, photoprotective, photorespiration , Mehler-peroxidase mechanisms to dissipate absorbed solar energy (C. Pinheiro and Chaves 2011). In short, water insufficiency to the plant results in stomatal closure, thereby reducing stomatal conduction, transpiration, and CO_2 influx, subsequently decreasing photosynthesis.

Applicably, the decrease in photosynthesis results in lower yields; although the extent of the impact on yield is dependent on drought duration and the growth period in which drought occurs. For example, drought occurring early in the planting season gives plants time to recuperate, while drought following grain fill has minimal impact on yield quantity and quality. Generally, surveys of rice production report a yield decline of 25-33% (Jinmeng Zhang et al. 2018; Sandhu and Kumar 2017), corn is estimated to experience a 21% of yield loss (Adee et al. 2016), and soybean a 36% decrease in yield (Brown, Caviness, and Brown 1985) due to drought. Furthermore, the loss of yield has a dramatic economic impact on the agricultural industry. It is estimated that the 2012 drought in the United States resulted in $30 billion in losses (Rippey

2015). Therefore, understanding the relationship between drought, photosynthesis, and yield is economically and calorically impactful.

3.5) Work on Drought and Photosynthesis

Given the detrimental effects of drought on photosynthesis and yield, lots of research has been performed on the holistic impact of drought on a plant and mechanisms of drought resiliency. As discussed, the reduction in stomatal conductance results in a net decrease in photosynthesis but also in transpiration. This characteristic improves the water use efficiency (WUE) of a plant and is a key consideration when breeding for water consciousness. Agronomic WUE is defined as yield per unit of irrigation and/or precipitation (Passioura 1977). However, the inherent contradiction is that decreased stomatal conductance also leads to a decrease in yield; therefore, increased WUE is often associated with smaller plants and lower yield potential. The search for lines that maintain high photosynthetic rates and WUE while decreasing stomatal conductance is of great interest to the formation of high-yielding drought-tolerant crops. The most accurate measurement of WUE is made via mini-lysimeters, which can measure the amount of water that plants transpired during the growing season (Vadez and Ratnakumar 2016). Alternative, more cost-effective methods include carbon isotope discrimination, which measures the fluctuation of carbon isotopes caused by plant carbon assimilation. This method has been utilized to classify peanut cultivars on the basis of water use efficiency (Q. Zhang et al. 2022), determine parental line drought resistance in common bean (Sanz-Saez et al. 2019), cotton cultivar selection (Stiller et al. 2005), used to determine "water saver" soybean cultivars (Buezo et al. 2019), and to understand the underlying genetic architecture of WUE in soybean (Mithlesh Kumar and Lal 2015; Dhanapal et al. 2015). Other methods of WUE measurement include deriving instantaneous WUE gas exchange data.

Photosynthetic performance can be inferred by quantifying CO_2 and water vapor fluctuations into and out of a leaf. The determination of net CO_2 assimilation, respiration, and stomatal conductance enables the estimation of photosynthetic efficiency through the rate of gas exchange and the measurement of substrates and products (Sanz-Sáez et al. 2012, 2017). These measurements, collected with infrared gas analyzer instruments, can also be used to derive instantaneous WUE from photosynthetic rate and stomatal conductance/transpiration rate gas exchange measurements. This technique is common and vital to answer a wide variety of scientific questions regarding plant function and can be used to monitor plant performance in abiotic stress conditions (Long et al., 1996; Long and Bernacchi, 2003). Gas exchange data and WUE derivation have been used to examine cowpea response to drought (Anyia and Herzog 2004), for parental line determination in sorghum (Balota et al. 2008), in the analysis of soybean productivity in elevated CO_2 (Ainsworth et al. 2004), and in further studies examining the effect of mineral deficit and saline conditions on photosynthetic rate (Dias et al. 2020; Sarwar and Shahbaz 2020; F. W. A. Pinheiro et al. 2021; de Lima et al. 2020; de Andrade et al. 2022). Furthermore, gas exchange data has been utilized as phenotypic parameters for countless genome-wide associations studies in soybean (L. Wang et al. 2020; Yuming Yang et al. 2020; W. Du et al. 2020; H. Li et al. 2016; Lü et al. 2018; Lopez, Xavier, and Rainey 2019). These methods have been utilized to determine genes pertaining to improved photosynthetic rate and water use efficiency, and the underlying mechanism of photosynthetic response to abiotic stress in soybean.

Section 4: An Overview of Roots

4.1)   Root Structure and Functions

If the hypothesis that biomass allocation towards harvestable yield has reached its theoretical maxima, a secondary approach to yield improvement comes from a paradigm of optimizing non-grain structures for photosynthetic substrate acquisition. This has occurred in canopy structure through the improvement of leaf shape, leaf area, flowering time, and leaf angle, by optimizing light intercept efficiency in the Montieth equation. However, it is estimated that plants spend 1/5 of biomass in root development (Ordóñez et al. 2020). The focus on above-ground traits ignores 20% of photosynthetic output and has left the research and improvement of below-ground biomass lagging. This is unsurprising given the considerable effort and potential for error associated with root harvesting.

Roots are poetically considered the "bridge" between the light-touched surface and the living Earth (Meine Van Noordwijk et al. 1998). They are the port of symbiotic exchange between above- and below-ground resources (M. Van Noordwijk et al. 1996), this market of exchange is extended to mycorrhizal fungi, with the plant providing glucose compounds for biologically active nitrogen (Moretti et al. 2018). In addition to providing the plant with biologically fixed nitrogen (Yongqing Yang et al. 2017), roots also obtain plant available nutrients, like nitrogen, phosphorus, calcium, zinc, and iron, from soil horizons and are solely responsible for water uptake (J. P. Lynch 2013; J. Lynch 1995; J. P. Lynch and Brown 2001; H. Wang, Inukai, and Yamauchi 2006). Mechanisms for nutrient procurement requires root growth be adaptable to environments. The ability of roots to perceive soil stresses and respond accordingly is known as "root plasticity" (Barberon et al. 2016; Fromm 2019; Karlova et al. 2021; Schneider and Lynch 2020). The spatiotemporal configurations of roots are referred to as root system architecture (RSA), which is defined as the geometric description of a root system's shape (topology and distribution) (J. Lynch 1995). Quantitatively, the RSA is described and

considered through the measurement of size and abundance of root system components (e.g., length of roots, number of lateral root number, diameter of roots, root orientation angle, etc.) (Seck, Torkamaneh, and Belzile 2020). Root plasticity and RSA are increasingly becoming breeding targets as sporadic precipitation, changing weather conditions, and soil degradation makes root structure and function key factors in climate resiliency (Schneider and Lynch 2019).

Broadly discussing root structure, root architecture is comprised of primary, lateral, and tertiary (adventitious) roots that contain identical radial tissue. Root system architecture is, thus, determined by the plasticity of roots rather than the addition of fundamentally different structures to the system (Schiefelbein and Benfey 1991; Moretti et al 2018). In addition to the plasticity of the root system, plants have heritable characteristics for 'intrinsic' developmental pathways, which comprise a genetically determined framework for the fundamental appearance of an organism's roots (Malamy, 2005). Soybean root architecture follows this generic structure possessing a primary root, or taproot; lateral roots or secondary roots; and tertiary growth, growth stemming from secondary and/or other lateral root structures (Lersten and Carlson, 2004). However, soybeans have the added complexity of nodular formation by inoculation of *Bradyrhizobium* (Albareda, Rodríguez-Navarro, and Temprano 2009). The inoculation of microbials has been shown to impact root plasticity and overall root architecture through a number of mechanisms. First, there is the direct plastic response of a plant to a microbe, which can lead to variation in the extent of symbiosis, for example, nodulation level (Gho et al. 2013). Morphologically, symbiosis has been demonstrated to modify allocation to lateral and primary root structures (Gho et al. 2019) and N-fixing species have adapted mechanisms of root clustering as a means of meeting nodule formation requirements, in terms of phosphorus and nutrient acquisition (Adams, Bell, and Pate 2002).

4.2)   Roots and Drought

Given the inherent function of roots as structures for water uptake, the interplay between root structure architecture and drought susceptibility and resiliency is unsurprising. Specific root morphological and anatomical traits in soybean have been reported as adaptive mechanisms that enhance plant performance and productivity under drought stress (Prince et al., 2016; Prince et al., 2017; Prince et al., 2019), implying root characteristics confer some drought tolerance through mechanisms of drought avoidance. This has been supported by several studies in soy and maize, concluding that rapid taproot elongation during the vegetative stage achieves penetration at depth, attaining greater "root mass at depth," enabling a plant to be robust in water-deficit conditions (Song et al. 2016; Lopes et al. 2011; Ali et al. 2016; C. M. Hudak and Patterson 1995) Alternatively, root systems with a larger lateral root component are advantageous under drought conditions due to the expansive total surface area (Tanaka et al. 2014; Vadez 2014). Shallow fibrous root structures have been shown to aid in rapid water absorption during periods of intense precipitation, facilitating maximal moisture and nutrient extraction to maintain photosynthesis (Abdel-Haleem, Lee, and Boerma 2011; Comas et al. 2013; Lopes et al. 2011). Abdel et al (2011) found QTLs in soybean controlling fibrous root production in a inbreds population in field rain fed conditions. Developing varieties with RSA suitable for the given environment promises to be a sustainable and economical approach to increase crop nutrient efficiency and improve adaptation to stresses. Root elongation (Kaspar, Taylor, and Shibles 1984; Manavalan et al. 2015) and lateral root production (D. J. Read and Bartlett 1972) studies in soybean have determined high-throughput phenotyping techniques and cultivars suited for tailored breeding. The underlying genetic architecture of these traits is still being explored and further molecular

understanding is imperative to environment-specific breeding efficiency.

4.3)   Root Phenotyping

To consider breeding for root architecture, the roots must be observed in order to understand the adapted traits and its underlying genetics. Root observation is historically incredibly challenging due to the laborious and potentially erroneous sample collection process. Early root morphology experiments primarily analyzed root dry weight, root number, volume and surface area, however these measurements failed to differentiate between different root types (Wolfgang Böhm 1979). The advent of the methods to excavate, draw, and photograph roots began the modern era of root phenotyping (John Ernest Weaver 1926; J. E. Weaver 1925; W. Böhm 2012). The use of imaging provided a reliable protocol to classify root types. The classical method has since been improved to create high throughput phenotyping methods, with root excavation and scoring optimized through the use of "Shovelomics" (Trachsel et al. 2011). Soil-free techniques, such as hydroponics (Villagarcia et al. 2001; Hargreaves, Gregory, and Bengough 2009; Ayalew et al. 2018), aeroponics (Osvald, Petrovic, and Demsar 2001; Selvaraj et al. 2019), gel plates (Wojciechowski et al. 2009), and growth pouches (Adu et al. 2014; Adeleke et al. 2019) have also gained popularity in the modern field. Work improving 2 and 3D imaging techniques enables accurate measurements of root phenes for analysis. Recently, Seethpalli et al. 2020 released an open-source hardware design and public software (RhizoVision) to measure root crown phenotypes, providing a low-cost method of RSA analysis (Seethepalli et al. 2020). Other root imaging software includes Digital Imaging of Root Traits (DIRT) (Das et al. 2015), Root Estimator for Shovelomics Traits (REST) (Colombi et al. 2015), and WinRhizo. The field of root study is currently undergoing another transition to the use of nondestructive techniques. Sophisticated tomographic techniques such as magnetic resonance imaging (MRI) (Jahnke et al.

2009), positron emission tomography (PET) (Garbout et al. 2012; Wong et al. 2022), X-ray

computed tomography (X-ray CT) (Mooney et al. 2012; Rogers et al. 2016; Duncan and Topp

2022) are 3D RSA phenotyping promising. However, these non-destructive imaging methods are

currently limited to greenhouse generated materials, as they require extensive hardware to scan

the root architecture within a pot.

4.4) Genetic Understanding of Root Architecture

With the introduction of high throughput protocols to measure root traits, considerable

progress examining RSA traits, identifying parental types, and exploring the underlying genetic

mechanisms have been made in cereals and legumes. In maize (Tuberosa et al. 2011), wheat

(Wasson et al. 2012), and rice (Manoj Kumar et al. 2019; Hashem et al. 2019), associations of

root architecture and drought resistance is well established. QTL mapping in rice has

successfully applied markers in assisted breeding programs (Steele et al. 2006; Suji et al. 2012).

Furthermore, QTL identification in rice has led to the cloning of DEEP ROOTING 1 ("Dro1"), a

gene controlling root growth angle (Uga et al. 2013), and a rice ortholog (Kadam et al. 2017) to

the *Arabidopsis* gene SCARECROW/SHORTROOT (Benfey et al. 1993), providing valuable

targets for drought avoidance in rice (Kamiya et al. 2003). Similarly, root growth patterns have

been studied in other legumes such as common beans (Sponchiado et al. 1989; Battaglia et al.

2014), chickpeas (Manoj Kumar et al. 2019; Hashem et al. 2019), and peanuts (Luo et al. 2022).

Root architecture studies in soybean have been conducted through a targeted breeding paradigm.

Since the turn of the century, QTLs governing root-shoot traits have been identified in soybean

populations at various developmental studies in different growing conditions (R. Zhou et al.

2011; Prince et al. 2013; Liang et al. 2014; Manavalan et al. 2010, 2015; Prince, Song, et al.

2015; Chen et al. 2021). However, most studies identifying markers and loci occur in curated

cultivar populations or in recombinant inbred lines with the goal of introgression breeding with some exceptions (Abdel-Haleem, Lee, and Boerma 2011; Seck, Torkamaneh, and Belzile 2020; Mandozai et al. 2021; Dhanapal et al. 2020). Studies in field conditions are even fewer due to the practical constraints of root trait selection in uncontrolled conditions. However, the field condition studies are more accurate portrayals of biotic and abiotic stress conditions, providing invaluable information on cultivar performance. The limited work in field studies has, nonetheless, produced alluring QTLs to consider, including 8 loci associated with overall complexity, 3 with taproot definition (Dhanapal et al. 2020), and 5 identified for root score (Abdel-Haleem, Lee, and Boerma 2011). To date, only Dhanapal et al. (2020) have performed marker-trait associations utilizing a diversity panel in field studies, with a 289-member diversity collection to examine top-soil RSA traits, primarily lateral root density, angle, and number, determining 246 SNPs denoting 67 loci.

Section 5: Genome Wide Association Studies

5.1) Genome-wide Association Studies

Genome-wide association studies exploit variation within a diverse population via algorithmic modeling of genetic information and phenotypic observation. They leverage the endogenous genotypic and phenotypic variation among the diverse population to provide high mapping resolution for trait variation (C. Zhu et al. 2008). The most common type of genetic variation studied in GWAS is single nucleotide polymorphisms (SNPs). SNPs are variations in a single nucleotide of the DNA sequence. The improvement of next-generation sequencing techniques and the curation of localized repositories has significantly increased the accessibility of GWAS. For example, soybean has publicly available marker data (SoySNP50K iSelect Bead Chip) available for download on Soybase USDA soybean germplasm collection (Song et al.

2013). As a result of accessibility, GWAS are near ubiquitous across crop species, routinely run in corn (Xiao et al. 2017; Shikha et al. 2021), rice (Wang et al. 2020), wheat (Saini et al. 2022), and barley (Abendroth et al. 2022) for example. In soybean, GWAS have been used todiscover marker-trait associations for phenotypes ranging from root architecture, WUE, yield to pest and disease susceptibility (Prince et al. 2020; Dhanapal et al. 2015; Ravelombola et al. 2021; Passianotto et al. 2017; Zatybekov et al. 2018).

The statistical power of a GWAS model is increased through consideration of relationship factors within a population. Classical models of GWA account for interrelatedness within a population by grouping the individuals into subpopulations. Further accounting for relatedness can be made through the inclusion of kinship cofactors, although this leads to marker confounding. The most modern GWAS techniques (BLINK and FarmCPU) circumvent kinship confounding entirely through the iterative application of cofactors. These approaches have the secondary benefit of false-positive reduction, a common issue in GWAS analysis (Liu et al. 2016; Wang and Zhang 2021; VanRaden 2008; Huang et al. 2018; Yang et al. 2014; Reich, Price, and Patterson 2008; Zhou and Stephens 2012). The computational efficiency, statistical power, and error correction of the advanced GWAS models make them highly recommended and effective in the analysis of complex polygenic traits, such as photosynthesis and root system architecture.

Section 6: Conclusion and Research Objectives

Soybean is an irreplaceable crop in the modern economy and agricultural industry. Its unique characteristics make it a staple in the food, feed, and fuel industries. However, stagnating yield increases and increasing demand creates an imbalance necessary to be addressed by plant breeders and agronomists alike. Future approaches in yield increases rely on the use of genetic

modification, improved management practices, and appropriate adaptation to modeled climate conditions, perhaps the most detrimental of which is drought. With an estimated 36% reduction in yield resulting from water-deficit conditions, rigorous research is needed to identify adapted cultivars and loci resilient to such conditions. To this end, this project utilizes a two-prong approach to identify adaptive genetic architecture and accessions through the measurement and analysis of endogenous variation of above and below-ground adaptive traits within subsets of a 281-member soybean diversity panel (V) assembled and grown in Alabama. Through the genome-wide association of 33,453 SNPs to gas exchange data and root system architecture characteristics, this project aims to:

1) Examine the endogenous species variation of above and below ground phenotypes.

2) Utilize GWAS techniques to identify markers associated with these traits

3) Calculate linkage disequilibrium decay and determine potential candidate genes within this window surrounding significantly associated SNPs

Abdel-Haleem, Hussein, Geung-Joo Lee, and Roger H. Boerma. 2011. "Identification of QTL for Increased Fibrous Roots in Soybean." *TAG. Theoretical and Applied Genetics. Theoretische Und Angewandte Genetik* 122 (5): 935–46.

Abendroth, Jillian A., Ahmad H. Sallam, Brian J. Steffenson, Marcus A. Vinje, Ramamurthy Mahalingam, and Jason G. Walling. 2022. "Identification of Genomic Loci Controlling Grain Macro and Micronutrient Variation in a Wild Barley (Hordeum Vulgare Spp. Spontaneum) Diversity Panel." *Agronomy* 12 (11): 2839.

Adee, Eric, Kraig Roozeboom, Guillermo R. Balboa, Alan Schlegel, and Ignacio A. Ciampitti. 2016. "Drought-Tolerant Corn Hybrids Yield More in Drought-Stressed Environments with No Penalty in Non-Stressed Environments." *Frontiers in Plant Science* 7 (October): 1534.

Adeleke, E., R. Millas, W. McNeal, J. Faris, and A. Taheri. 2019. "Assessing Root System Architecture of Wheat Seedlings Using A High-Throughput Root Phenotyping System." *BioRxiv*. https://doi.org/10.1101/677955.

Adu, Michael O., Antoine Chatot, Lea Wiesel, Malcolm J. Bennett, Martin R. Broadley, Philip J. White, and Lionel X. Dupuy. 2014. "A Scanner System for High-Resolution Quantification of Variation in Root Growth Dynamics of Brassica Rapa Genotypes." *Journal of Experimental Botany* 65 (8): 2039–48.

Ainsworth, Elizabeth A., and Stephen P. Long. 2005. "What Have We Learned from 15 Years of Free-Air CO2 Enrichment (FACE)? A Meta-Analytic Review of the Responses of Photosynthesis, Canopy Properties and Plant Production to Rising CO2." *The New Phytologist* 165 (2): 351–72.

Ainsworth, Elizabeth A., Alistair Rogers, Randall Nelson, and Stephen P. Long. 2004. "Testing the 'Source–Sink' Hypothesis of down-Regulation of Photosynthesis in Elevated [CO2] in the Field with Single Gene Substitutions in Glycine Max." *Agricultural and Forest Meteorology* 122 (1): 85–94.

Ainsworth, Elizabeth A., Craig R. Yendrek, Jeffrey A. Skoneczka, and Stephen P. Long. 2012. "Accelerating Yield Potential in Soybean: Potential Targets for Biotechnological Improvement." *Plant, Cell & Environment* 35 (1): 38–52.

Albareda, Marta, Dulce Nombre Rodríguez-Navarro, and Francisco J. Temprano. 2009. "Soybean Inoculation: Dose, N Fertilizer Supplementation and Rhizobia Persistence in Soil." *Field Crops Research* 113 (3): 352–56.

Ali, M. Liakat, Jon Luetchens, Amritpal Singh, Timothy M. Shaver, Greg R. Kruger, and Aaron J. Lorenz. 2016. "Greenhouse Screening of Maize Genotypes for Deep Root Mass and Related Root Traits and Their Association with Grain Yield under Water-Deficit Conditions in the Field." *Euphytica/ Netherlands Journal of Plant Breeding* 207 (1): 79–94.

America Soybean Association. 2022. "'A Reference Guide to Important Soybean Facts & Figures: SoyStats 2022.'" 2022. https://soygrowers.com/education-resources/publications/soy-stats/.

Anderson, Edwin J., Md Liakat Ali, William D. Beavis, Pengyin Chen, Tom Elmo Clemente, Brian W. Diers, George L. Graef, et al. 2019. "Soybean [Glycine Max (L.) Merr.] Breeding: History, Improvement, Production and Future Opportunities." In *Advances in Plant Breeding Strategies: Legumes: Volume 7*, edited by Jameel M. Al-Khayri, Shri Mohan Jain, and Dennis V. Johnson, 431–516. Cham: Springer International Publishing.

Andersson, Inger, and Anders Backlund. 2008. "Structure and Function of Rubisco." *Plant Physiology and Biochemistry: PPB / Societe Francaise de Physiologie Vegetale* 46 (3): 275–91.

Andrade, Aline Franciel de, Amanda Magalhães Bueno, Aline dos Santos de Carvalho, Mateus Leles de Lima, Rilner Alves Flores, Klaus de Oliveira Abdala, Renato de Mello Prado, and Jonas Pereira de Souza Junior. 2022. "Innovative Soluble Silicon Leaf Source Increase Gas Exchange, Grain Yield and Economic Viability in Common Bean." *Silicon Chemistry* 14 (7): 3739–47.

Anyia, A. O., and H. Herzog. 2004. "Water-Use Efficiency, Leaf Area and Leaf Gas Exchange of Cowpeas under Mid-Season Drought." *European Journal of Agronomy: The Journal of the European Society for Agronomy* 20 (4): 327–39.

Ayalew, Habtamu, Hui Liu, Andreas Börner, Borislav Kobiljski, Chunji Liu, and Guijun Yan. 2018. "Genome-Wide Association Mapping of Major Root Length QTLs Under PEG Induced Water Stress in Wheat." *Frontiers in Plant Science* 9 (November): 1759.

Balota, Maria, William A. Payne, William Rooney, and Darrell Rosenow. 2008. "Gas Exchange and Transpiration Ratio in Sorghum." *Crop Science* 48 (6): 2361–71.

Barberon, Marie, Joop Engelbertus Martinus Vermeer, Damien De Bellis, Peng Wang, Sadaf Naseer, Tonni Grube Andersen, Bruno Martin Humbel, et al. 2016. "Adaptation of Root Function by Nutrient-Induced Plasticity of Endodermal Differentiation." *Cell* 164 (3): 447–59.

Bassham, J. A., and M. Calvin. 1960. "The Path of Carbon in Photosynthesis." In *Die CO2-Assimilation / The Assimilation of Carbon Dioxide: In 2 Teilen / 2 Parts*, edited by André Pirson, 884–922. Berlin, Heidelberg: Springer Berlin Heidelberg.

Battaglia, Marina, Carolina Rípodas, Joaquín Clúa, Maël Baudin, O. Mario Aguilar, Andreas Niebel, María Eugenia Zanetti, and Flavio Antonio Blanco. 2014. "A Nuclear Factor Y Interacting Protein of the GRAS Family Is Required for Nodule Organogenesis, Infection Thread Progression, and Lateral Root Growth." *Plant Physiology* 164 (3): 1430–42.

Benfey, P. N., P. J. Linstead, K. Roberts, J. W. Schiefelbein, M. T. Hauser, and R. A. Aeschbacher. 1993. "Root Development in Arabidopsis: Four Mutants with Dramatically Altered Root Morphogenesis." *Development* 119 (1): 57–70.

Bhandari, S., Bishnoi, N. R., Sharma, V., & Kumar, R. 2019. "Yield Improvement in Maize through Nutrient Management Practices: A Review." *Journal of Plant Nutrition* 42 (3): 282–95.

Böhm, W. 2012. *Methods of Studying Root Systems*. Springer Science & Business Media.

Böhm, Wolfgang. 1979. "Root Parameters and Their Measurement." In *Methods of Studying Root Systems*, edited by Wolfgang Böhm, 125–38. Berlin, Heidelberg: Springer Berlin Heidelberg.

Brown, E. A., C. E. Caviness, and D. A. Brown. 1985. "Response of Selected Soybean Cultivars to Soil Moisture Deficit [1]." *Agronomy Journal* 77 (2): 274–78.

Buezo, Javier, Álvaro Sanz-Saez, Jose F. Moran, David Soba, Iker Aranjuelo, and Raquel Esteban. 2019. "Drought Tolerance Response of High-Yielding Soybean Varieties to Mild Drought: Physiological and Photochemical Adjustments." *Physiologia Plantarum* 166 (1): 88–104.

Cardona, Tanai, Shengxi Shao, and Peter J. Nixon. 2018. "Enhancing Photosynthesis in Plants: The Light Reactions." *Essays in Biochemistry* 62 (1): 85–94.

Carlson, John B., and Nels R. Lersten. 2016. "Reproductive Morphology." In *Agronomy Monographs*, 59–95. Madison, WI, USA: American Society of Agronomy, Crop Science Society of America, and Soil Science Society of America.

Carter, T. E., T. Hymowitz, and R. L. Nelson. 2004. "Biogeography, Local Adaptation, Vavilov, and Genetic Diversity in Soybean." In *Biological Resources and Migration*, 47–59. Springer Berlin Heidelberg.

Cartter, J. L., and Turner Harcourt Hopper. 1942. "Influence of Variety, Environment, and Fertility Level on the Chemical Composition of Soybean Seed." ageconsearch.umn.edu. https://ageconsearch.umn.edu/record/169047/files/tb787.pdf.

Chen, Huatao, Giriraj Kumawat, Yongliang Yan, Baojie Fan, and Donghe Xu. 2021. "Mapping and Validation of a Major QTL for Primary Root Length of Soybean Seedlings Grown in Hydroponic Conditions." *BMC Genomics* 22 (1): 132.

Colombi, Tino, Norbert Kirchgessner, Chantal Andrée Le Marié, Larry Matthew York, Jonathan P. Lynch, and Andreas Hund. 2015. "Next Generation Shovelomics: Set up a Tent and REST." *Plant and Soil* 388 (1–2): 1–20.

Comas, Louise H., Steven R. Becker, Von Mark V. Cruz, Patrick F. Byrne, and David A. Dierig. 2013. "Root Traits Contributing to Plant Productivity under Drought." *Frontiers in Plant Science* 4 (November): 442.

Curry, R. Bruce, James W. Jones, Kenneth J. Boote, R. M. Peart, L. Hartwell Allen Jr, and Nigel B. Pickering. 2015. "Response of Soybean to Predicted Climate Change in the USA." In *Climate Change and Agriculture: Analysis of Potential International Impacts*, 163–82. Madison, WI, USA: American Society of Agronomy.

Das, Abhiram, Hannah Schneider, James Burridge, Ana Karine Martinez Ascanio, Tobias Wojciechowski, Christopher N. Topp, Jonathan P. Lynch, Joshua S. Weitz, and Alexander Bucksch. 2015. "Digital Imaging of Root Traits (DIRT): A High-Throughput Computing and Collaboration Platform for Field-Based Root Phenomics." *Plant Methods* 11 (November): 51.

Dhanapal, Arun Prabhu, Jeffery D. Ray, Shardendu K. Singh, Valerio Hoyos-Villegas, James R. Smith, Larry C. Purcell, C. Andy King, Perry B. Cregan, Qijian Song, and Felix B. Fritschi. 2015. "Genome-Wide Association Study (GWAS) of Carbon Isotope Ratio (Δ13C) in Diverse Soybean [Glycine Max (L.) Merr.] Genotypes." *TAG. Theoretical and Applied Genetics. Theoretische Und Angewandte Genetik* 128 (1): 73–91.

Dhanapal, Arun Prabhu, Larry M. York, Kasey A. Hames, and Felix B. Fritschi. 2020. "Genome-Wide Association Study of Topsoil Root System Architecture in Field-Grown Soybean [Glycine Max (L.) Merr.]." *Frontiers in Plant Science* 11: 590179.

Dias, Adaan Sudário, Geovani Soares D. E. Lima, Hans Raj Gheyi, Lauriane Almeida D. O. S. Anjos Soares, and Pedro Dantas Fernandes. 2020. "GROWTH AND GAS EXCHANGES OF COTTON UNDER WATER SALINITY AND NITROGEN-POTASSIUM COMBINATION." *Revista Caatinga* 33 (2): 470–79.

Dong, Y. S., L. M. Zhao, B. Liu, Z. W. Wang, Z. Q. Jin, and H. Sun. 2004. "The Genetic Diversity of Cultivated Soybean Grown in China." *TAG. Theoretical and Applied Genetics. Theoretische Und Angewandte Genetik* 108 (5): 931–36.

Du, Wenkai, Lihua Ning, Yongshun Liu, Shixi Zhang, Yuming Yang, Qing Wang, Shengqian Chao, et al. 2020. "Identification of Loci and Candidate Gene GmSPX-RING1 Responsible for Phosphorus Efficiency in Soybean via Genome-Wide Association Analysis." *BMC Genomics*. https://doi.org/10.1186/s12864-020-07143-3.

Duncan, Keith E., and Christopher N. Topp. 2022. "Phenotyping Complex Plant Structures with a Large Format Industrial Scale High-Resolution X-Ray Tomography Instrument." *Methods in Molecular Biology* 2539: 119–32.

Eberhard, Stephan, Giovanni Finazzi, and Francis-André Wollman. 2008. "The Dynamics of Photosynthesis." *Annual Review of Genetics* 42: 463–515.

Evans, L. T. 1996. *Crop Evolution, Adaptation and Yield*. Cambridge University Press.

"Food and Agriculture Organization of the United Nations." 2020. FAOSTAT. 2020. https://www.fao.org/faostat.

Garbout, Amin, Lars J. Munkholm, Søren B. Hansen, Bjørn M. Petersen, Ole L. Munk, and Radoslaw Pajor. 2012. "The Use of PET/CT Scanning Technique for 3D Visualization and Quantification of Real-Time Soil/Plant Interactions." *Plant and Soil* 352 (1–2): 113–27.

Gates, D. M. 1968. "Transpiration and Leaf Temperature." *Annual Review of Plant Physiology* 19 (1): 211–38.

Guo, Juan, Yunsheng Wang, Chi Song, Jianfeng Zhou, Lijuan Qiu, Hongwen Huang, and Ying Wang. 2010. "A Single Origin and Moderate Bottleneck during Domestication of Soybean (Glycine Max): Implications from Microsatellites and Nucleotide Sequences." *Annals of Botany* 106 (3): 505–14.

Han, Yingpeng, Xue Zhao, Dongyuan Liu, Yinghui Li, David A. Lightfoot, Zhijiang Yang, Lin Zhao, et al. 2016. "Domestication Footprints Anchor Genomic Regions of Agronomic Importance in Soybeans." *The New Phytologist* 209 (2): 871–84.

Hargreaves, Caroline E., Peter J. Gregory, and A. Glyn Bengough. 2009. "Measuring Root Traits in Barley (Hordeum Vulgare Ssp. Vulgare and Ssp. Spontaneum) Seedlings Using Gel Chambers, Soil Sacs and X-Ray Microtomography." *Plant and Soil* 316 (1–2): 285–97.

Hashem, Abeer, Ashwani Kumar, Abeer M. Al-Dbass, Abdulaziz A. Alqarawi, Al-Bandari Fahad Al-Arjani, Garima Singh, Muhammad Farooq, and Elsayed Fathi Abd Allah. 2019. "Arbuscular Mycorrhizal Fungi and Biochar Improves Drought Tolerance in Chickpea." *Saudi Journal of Biological Sciences* 26 (3): 614–24.

Hay, R. K. M. 1995. "Harvest Index: A Review of Its Use in Plant Breeding and Crop Physiology." *The Annals of Applied Biology* 126 (1): 197–216.

Huang, Meng, Xiaolei Liu, Yao Zhou, Ryan M. Summers, and Zhiwu Zhang. 2018. "BLINK: A Package for the next Level of Genome-Wide Association Studies with Both Individuals and Markers in the Millions." *GigaScience* 8 (2): giy154.

Hudak, C. M., and R. P. Patterson. 1995. "Vegetative Growth Analysis of a Drought-Resistant Soybean Plant Introduction." *Crop Science* 35 (2): 464.

Hudak, Colleen M., and Robert P. Patterson. 1996. "Root Distribution and Soil Moisture Depletion Pattern of a Drought-resistant Soybean Plant Introduction." *Agronomy Journal* 88 (3): 478–85.

Hymowitz, T. 1970. "On the Domestication of the Soybean." *Economic Botany* 24 (4): 408–21.

Hymowitz, Theodore, and Bogdan Belic. 1990. "Soybeans: The Success Story." Citeseer. 1990. https://citeseerx.ist.psu.edu/document?repid=rep1&type=pdf&doi=4679cf37546277fb2b023da9de8cc1d860e4c6c5.

Ingram, Keith T., Lynne Carter, and Kirstin Dow. 2013. "Climate Change in the Southeast USA: Executive Summary." In *Climate of the Southeast United States: Variability, Change, Impacts, and Vulnerability*, edited by Keith T. Ingram, Kirstin Dow, Lynne Carter, and Julie Anderson, 1–7. Washington, DC: Island Press/Center for Resource Economics.

Irfan, Umair. 2021. "'There's No Going Back': The UN's Dire New Climate Report, Explained." Vox. August 2021. https://www.vox.com/22613027/un-ipcc-climate-change-report-ar6-disaster.

Jahnke, Siegfried, Marion I. Menzel, Dagmar van Dusschoten, Gerhard W. Roeb, Jonas Bühler, Senay Minwuyelet, Peter Blümler, et al. 2009. "Combined MRI-PET Dissects Dynamic Changes in Plant Structures and Functions." *The Plant Journal: For Cell and Molecular Biology* 59 (4): 634–44.

Jarvis, P. G., and K. G. McNaughton. 1986. "Stomatal Control of Transpiration: Scaling Up from Leaf to Region." In *Advances in Ecological Research*, edited by A. MacFadyen and E. D. Ford, 15:1–49. Academic Press.

Jooyandeh, Hossein. 2011. "Soy Products as Healthy and Functional Foods." kingsvegetarianfood.ca. 2011. http://kingsvegetarianfood.ca/wp-content/uploads/2017/02/SoyProductsasHealthyandFunctionalProducts.pdf.

Jung, J. Y., Park, J. H., Lee, J. W., Kang, J. W., & Shin, J. H. 2016. "Yield Improvement in Tomato Using Conventional and Biodegradable Plastic Mulches under Greenhouse Conditions." *Horticulture, Environment, and Biotechnology* 57 (4): 390–97.

Kadam, Niteen N., Anandhan Tamilselvan, Lovely M. F. Lawas, Cherryl Quinones, Rajeev N. Bahuguna, Michael J. Thomson, Michael Dingkuhn, et al. 2017. "Genetic Control of Plasticity in Root Morphology and Anatomy of Rice in Response to Water Deficit." *Plant Physiology* 174 (4): 2302–15.

Kamiya, Noriko, Jun-Ichi Itoh, Atsushi Morikami, Yasuo Nagato, and Makoto Matsuoka. 2003. "The SCARECROW Gene's Role in Asymmetric Cell Divisions in Rice Plants." *The Plant Journal: For Cell and Molecular Biology* 36 (1): 45–54.

Karl, T. R., C. N. Williams Jr, P. J. Young, and W. M. Wendland. 2009. "Global Climate Change Impacts in the United States: A State of Knowledge Report." *Global Climate Change Impacts in the United States: A State of Knowledge Report Number Of*, 196.

Karlova, Rumyana, Damian Boer, Scott Hayes, and Christa Testerink. 2021. "Root Plasticity under Abiotic Stress." *Plant Physiology* 187 (3): 1057–70.

Karr-Lilienthal, Lisa K., Christine M. Grieshop, Neal R. Merchen, Donald C. Mahan, and George C. Fahey Jr. 2004. "Chemical Composition and Protein Quality Comparisons of Soybeans and Soybean Meals from Five Leading Soybean-Producing Countries." *Journal of Agricultural and Food Chemistry* 52 (20): 6193–99.

Kaspar, T. C., H. M. Taylor, and R. M. Shibles. 1984. "Taproot-elongation Rates of Soybean Cultivars in the Glasshouse and Their Relation to Field Rooting Depth 1." *Crop Science* 24 (5): 916–20.

Kim, Moon Young, Kyujung Van, Yang Jae Kang, Kil Hyun Kim, and Suk-Ha Lee. 2012. "Tracing Soybean Domestication History: From Nucleotide to Genome." *Breeding Science* 61 (5): 445–52.

Kimball, B. A., and S. B. Idso. 1983. "Increasing Atmospheric CO2: Effects on Crop Yield, Water Use and Climate." *Agricultural Water Management* 7 (1): 55–72.

Koester, Robert P., Jeffrey A. Skoneczka, Troy R. Cary, Brian W. Diers, and Elizabeth A. Ainsworth. 2014. "Historical Gains in Soybean (Glycine Max Merr.) Seed Yield Are Driven by Linear Increases in Light Interception, Energy Conversion, and Partitioning Efficiencies." *Journal of Experimental Botany* 65 (12): 3311–21.

Kramer, David M., and John R. Evans. 2011. "The Importance of Energy Balance in Improving Photosynthetic Productivity." *Plant Physiology* 155 (1): 70–78.

Krishnan, Hari B. 2000. "Biochemistry and Molecular Biology of Soybean Seed Storage Proteins." *Journal of New Seeds* 2 (3): 1–25.

Kukal, Meetpal S., and Suat Irmak. 2018. "U.S. Agro-Climate in 20th Century: Growing Degree Days, First and Last Frost, Growing Season Length, and Impacts on Crop Yields." *Scientific Reports* 8 (1): 6977.

Kumar, Manoj, Mohd Aslam Yusuf, Pooja Yadav, Shiv Narayan, and Manoj Kumar. 2019. "Overexpression of Chickpea Defensin Gene Confers Tolerance to Water-Deficit Stress in Arabidopsis Thaliana." *Frontiers in Plant Science* 10 (March): 290.

Lam, Hon-Ming, Xun Xu, Xin Liu, Wenbin Chen, Guohua Yang, Fuk-Ling Wong, Man-Wah Li, et al. 2010. "Resequencing of 31 Wild and Cultivated Soybean Genomes Identifies Patterns of Genetic Diversity and Selection." *Nature Genetics* 42 (12): 1053–59.

Lee, Gyoung-Ah, Gary W. Crawford, Li Liu, Yuka Sasaki, and Xuexiang Chen. 2011. "Archaeological Soybean (Glycine Max) in East Asia: Does Size Matter?" *PloS One* 6 (11): e26720.

Lefebvre, Stephane, Tracy Lawson, Mike Fryer, Oksana V. Zakhleniuk, Julie C. Lloyd, and Christine A. Raines. 2005. "Increased Sedoheptulose-1,7-Bisphosphatase Activity in Transgenic Tobacco Plants Stimulates Photosynthesis and Growth from an Early Stage in Development." *Plant Physiology* 138 (1): 451–60.

Li, Hongyan, Yuming Yang, Hengyou Zhang, Shanshan Chu, Xingguo Zhang, Dongmei Yin, Deyue Yu, and Dan Zhang. 2016. "A Genetic Relationship between Phosphorus Efficiency and Photosynthetic Traits in Soybean As Revealed by QTL Analysis Using a High-Density Genetic Map." *Frontiers in Plant Science* 7 (June): 924.

Liang, Huizhen, Yongliang Yu, Hongqi Yang, Lanjie Xu, Wei Dong, Hua Du, Weiwen Cui, and Haiyang Zhang. 2014. "Inheritance and QTL Mapping of Related Root Traits in Soybean at the Seedling Stage." *TAG. Theoretical and Applied Genetics. Theoretische Und Angewandte Genetik* 127 (10): 2127–37.

Lie, M., Brinch-Pedersen, H., & Holme, I. B. 2018. "Increased Yield in Winter Wheat through Late Sowing and Breeding for Improved Cold Tolerance." *European Journal of Agronomy: The Journal of the European Society for Agronomy* 92: 551–59.

Lima, Geovani Soares de, Charles Macedo Felix, Saulo Soares da Silva, Lauriane Almeida dos Anjos Soares, Hans Raj Gheyi, and Marcos Denilson Melo. 2020. "Gas Exchange, Growth, and Production of Mini-Watermelon under Saline Water Irrigation and Phosphate Fertilization Trocas Gasosas, Crescimento e Produção de Mini-Melancieira Irrigada Com Águas Salinas e Adubação Fosfatada." *Semina: Ciências Agrárias, Londrina* 41 (6 suplemento 2): 3039–52.

Liu, Shiwei, Zongyou Lv, Yihui Liu, Ling Li, and Lida Zhang. 2018. "Network Analysis of ABA-Dependent and ABA-Independent Drought Responsive Genes in Arabidopsis Thaliana." *Genetics and Molecular Biology* 41 (3): 624–37.

Liu, Shulin, Min Zhang, Feng Feng, and Zhixi Tian. 2020. "Toward a 'Green Revolution' for Soybean." *Molecular Plant* 13 (5): 688–97.

Liu, Xiaolei, Meng Huang, Bin Fan, Edward S. Buckler, and Zhiwu Zhang. 2016. "Iterative Usage of Fixed and Random Effect Models for Powerful and Efficient Genome-Wide Association Studies." *PLoS Genetics* 12 (2): e1005767.

Liu, Yucheng, Huilong Du, Pengcheng Li, Yanting Shen, Hua Peng, Shulin Liu, Guo-An Zhou, et al. 2020. "Pan-Genome of Wild and Cultivated Soybeans." *Cell* 182 (1): 162-176.e13.

Liu, Yu-Lin, Ying-Hui Li, Guo-An Zhou, N. Uzokwe, Ru-Zhen Chang, Shou-Yi Chen, and Li-Juan Qiu. 2010. "Development of Soybean EST-SSR Markers and Their Use to Assess Genetic Diversity in the Subgenus Soja." *Agricultural Sciences in China / Sponsored by the Chinese Academy of Agricultural Sciences* 9 (10): 1423–29.

Long, S. P., and C. J. Bernacchi. 2003. "Gas Exchange Measurements, What Can They Tell Us about the Underlying Limitations to Photosynthesis? Procedures and Sources of Error." *Journal of Experimental Botany* 54 (392): 2393–2401.

Long, Stephen P., Elizabeth A. Ainsworth, Andrew D. B. Leakey, and Patrick B. Morgan. 2005. "Global Food Insecurity. Treatment of Major Food Crops with Elevated Carbon Dioxide or Ozone under Large-Scale Fully Open-Air Conditions Suggests Recent Models May Have Overestimated Future Yields." *Philosophical Transactions of the Royal Society of London. Series B, Biological Sciences* 360 (1463): 2011–20.

Long, Stephen P., Elizabeth A. Ainsworth, Alistair Rogers, and Donald R. Ort. 2004. "Rising Atmospheric Carbon Dioxide: Plants FACE the Future." *Annual Review of Plant Biology* 55: 591–628.

Long, Stephen P., Xin-Guang Zhu, Shawna L. Naidu, and Donald R. Ort. 2006. "Can Improvement in Photosynthesis Increase Crop Yields?" *Plant, Cell & Environment* 29 (3): 315–30.

Lopes, Marta S., Jose Luis Araus, Philippus D. R. van Heerden, and Christine H. Foyer. 2011. "Enhancing Drought Tolerance in C4 Crops." *Journal of Experimental Botany* 62 (9): 3135–53.

Lopez, Miguel Angel, Alencar Xavier, and Katy Martin Rainey. 2019. "Phenotypic Variation and Genetic Architecture for Photosynthesis and Water Use Efficiency in Soybean (Glycine Max L. Merr)." *Frontiers in Plant Science* 10 (May): 680.

Lü, Haiyan, Yuming Yang, Haiwang Li, Qijia Liu, Jianjun Zhang, Junyi Yin, Shanshan Chu, et al. 2018. "Genome-Wide Association Studies of Photosynthetic Traits Related to Phosphorus Efficiency in Soybean." *Frontiers in Plant Science*. https://doi.org/10.3389/fpls.2018.01226.

Luo, Lu, Qian Wan, Zipeng Yu, Kun Zhang, Xiurong Zhang, Suqing Zhu, Yongshan Wan, Zhaojun Ding, and Fengzhen Liu. 2022. "Genome-Wide Identification of Auxin Response Factors in Peanut (Arachis Hypogaea L.) and Functional Analysis in Root Morphology." *International Journal of Molecular Sciences* 23 (10). https://doi.org/10.3390/ijms23105309.

Lynch, J. 1995. "Root Architecture and Plant Productivity." *Plant Physiology* 109 (1): 7–13.

Lynch, Jonathan P. 2013. "Steep, Cheap and Deep: An Ideotype to Optimize Water and N Acquisition by Maize Root Systems." *Annals of Botany* 112 (2): 347–57.

Lynch, Jonathan P., and Kathleen M. Brown. 2001. "Topsoil Foraging–an Architectural Adaptation of Plants to Low Phosphorus Availability." *Plant and Soil* 237 (2): 225–37.

Malamy, J. E. 2005. "Intrinsic and Environmental Response Pathways That Regulate Root System Architecture." *Plant, Cell & Environment* 28 (1): 67–77.

Manavalan, Lakshmi P., Satish K. Guttikonda, Vinh T. Nguyen, J. Grover Shannon, and Henry T. Nguyen. 2010. "Evaluation of Diverse Soybean Germplasm for Root Growth and Architecture." *Plant and Soil* 330 (1): 503–14.

Manavalan, Lakshmi P., Silvas J. Prince, Theresa A. Musket, Julian Chaky, Rupesh Deshmukh, Tri D. Vuong, Li Song, et al. 2015. "Identification of Novel QTL Governing Root Architectural Traits in an Interspecific Soybean Population." *PloS One* 10 (3): e0120490.

Medic, Jelena, Christine Atkinson, and Charles R. Hurburgh. 2014. "Current Knowledge in Soybean Composition." *Journal of the American Oil Chemists' Society* 91 (3): 363–84.

Messina, Mark, and Virginia Messina. 2010. "The Role of Soy in Vegetarian Diets." *Nutrients* 2 (8): 855–88.

Mo, Haizhen, Susanna Kariluoto, Vieno Piironen, Yang Zhu, Mark G. Sanders, Jean-Paul Vincken, Judith Wolkers-Rooijackers, and M. J. Rob Nout. 2013. "Effect of Soybean Processing on Content and Bioaccessibility of Folate, Vitamin B12 and Isoflavones in Tofu and Tempe." *Food Chemistry* 141 (3): 2418–25.

Monteith, J. L. 1994. "Validity of the Correlation between Intercepted Radiation and Biomass." *Agricultural and Forest Meteorology* 68 (3): 213–20.

Monteith, J. L., and C. J. Moss. 1977. "Climate and the Efficiency of Crop Production in Britain." *Philosophical Transactions of the Royal Society of London* 281 (980): 277–94.

Mooney, S. J., T. P. Pridmore, J. Helliwell, and M. J. Bennett. 2012. "Developing X-Ray Computed Tomography to Non-Invasively Image 3-D Root Systems Architecture in Soil." *Plant and Soil* 352 (1–2): 1–22.

Moretti, Luiz Gustavo, Edson Lazarini, João William Bossolani, Tiago Lisboa Parente, Sheila Caioni, Ricardo Silva Araujo, and Mariangela Hungria. 2018. "Can Additional Inoculations Increase Soybean Nodulation and Grain Yield?" *Agronomy Journal* 110 (2): 715–21.

Murooka, Yoshikatsu, and Mitsuo Yamshita. 2008. "Traditional Healthful Fermented Products of Japan." *Journal of Industrial Microbiology & Biotechnology* 35 (8): 791–98.

Naim, M., B. Gestetner, S. Zilkah, Y. Birk, and A. Bondi. 1974. "Soybean Isoflavones. Characterization, Determination, and Antifungal Activity." *Journal of Agricultural and Food Chemistry* 22 (5): 806–10.

Ordóñez, Raziel A., Sotirios V. Archontoulis, Rafael Martinez-Feria, Jerry L. Hatfield, Emily E. Wright, and Michael J. Castellano. 2020. "Root to Shoot and Carbon to Nitrogen Ratios of Maize and Soybean Crops in the US Midwest." *European Journal of Agronomy: The Journal of the European Society for Agronomy* 120 (October): 126130.

Ørgaard, Anne, and Lotte Jensen. 2008. "The Effects of Soy Isoflavones on Obesity." *Experimental Biology and Medicine* 233 (9): 1066–80.

Osvald, J., N. Petrovic, and J. Demsar. 2001. "Sugar and Organic Acid Content of Tomato Fruits (Lycopersicon Lycopersicum Mill.) Grown on Aeroponics at Different Plant Density." *Acta Alimentaria* 30 (1): 53–61.

Passioura, J. B. 1977. "Grain Yield, Harvest Index, and Water Use of Wheat." https://publications.csiro.au/rpr/pub?list=BRO&pid=procite:16a0b1b4-f4e0-4207-9cf6-3fd561de0889.

Pearcy, Robert W., John S. Roden, and John A. Gamon. 1990. "Sunfleck Dynamics in Relation to Canopy Structure in a Soybean (Glycine Max (L.) Merr.) Canopy." *Agricultural and Forest Meteorology* 52 (3): 359–72.

Pinheiro, C., and M. M. Chaves. 2011. "Photosynthesis and Drought: Can We Make Metabolic Connections from Available Data?" *Journal of Experimental Botany* 62 (3): 869–82.

Pinheiro, Francisco Wesley Alves, Geovani Soares de Lima, Hans Raj Gheyi, Lauriane Almeida dos Anjos Soares, Sabrina Gomes de Oliveira, and Francisco Alves da Silva. 2021. "Gas Exchange and Yellow Passion Fruit Production under Irrigation Strategies Using Brackish Water and Potassium." *Revista Ciência Agronômica* 53 (December): e20217816.

Prince, Silvas J., R. Beena, S. Michael Gomez, S. Senthivel, and R. Chandra Babu. 2015. "Mapping Consistent Rice (Oryza Sativa L.) Yield QTLs under Drought Stress in Target Rainfed Environments." *Rice* 8 (1): 53.

Prince, Silvas J., Raymond N. Mutava, Camila Pegoraro, Antonio Costa de Oliveira, and Henry T. Nguyen. 2013. "Root Characters." In *Genomics and Breeding for Climate-Resilient Crops: Vol. 2 Target Traits*, edited by Chittaranjan Kole, 67–131. Berlin, Heidelberg: Springer Berlin Heidelberg.

Prince, Silvas J., Li Song, Dan Qiu, Joao V. Maldonado Dos Santos, Chenglin Chai, Trupti Joshi, Gunvant Patil, et al. 2015. "Genetic Variants in Root Architecture-Related Genes in a Glycine Soja Accession, a Potential Resource to Improve Cultivated Soybean." *BMC Genomics* 16 (1): 132.

Prince, Silvas J., Tri D. Vuong, Xiaolei Wu, Yonghe Bai, Fang Lu, Siva P. Kumpatla, Babu Valliyodan, J. Grover Shannon, and Henry T. Nguyen. 2020. "Mapping Quantitative Trait Loci for Soybean Seedling Shoot and Root Architecture Traits in an Inter-Specific Genetic Population." *Frontiers in Plant Science* 11 (August): 1284.

Read, D. J., and E. M. Bartlett. 1972. "The Psychology of Drought Resistance in the Soy-Bean Plant (Glycine Max). I. The Relationship Between Dought Resistance and Growth." *The Journal of Applied Ecology* 9 (2): 487–99.

Redondo-Cuenca, A., M. J. Villanueva-Suárez, Rodríguez-Sevilla, and I. Mateos-Aparicio. 2007. "Chemical Composition and Dietary Fibre of Yellow and Green Commercial Soybeans (Glycine Max)." *Food Chemistry* 101 (3): 1216–22.

Reich, David, Alkes L. Price, and Nick Patterson. 2008. "Principal Component Analysis of Genetic Data." *Nature Genetics*.

Rippey, Bradley R. 2015. "The U.s. Drought of 2012." *Weather and Climate Extremes* 10 (December): 57–64.

Rizzo, Gianluca, and Luciana Baroni. 2018. "Soy, Soy Foods and Their Role in Vegetarian Diets." *Nutrients* 10 (1). https://doi.org/10.3390/nu10010043.

Rogers, Eric D., Daria Monaenkova, Medhavinee Mijar, Apoorva Nori, Daniel I. Goldman, and Philip N. Benfey. 2016. "X-Ray Computed Tomography Reveals the Response of Root System Architecture to Soil Texture." *Plant Physiology* 171 (3): 2028–40.

Rowntree, Scott C., Justin J. Suhre, Nicholas H. Weidenbenner, Eric W. Wilson, Vince M. Davis, Seth L. Naeve, Shaun N. Casteel, et al. 2013. "Genetic Gain× Management Interactions in Soybean: I. Planting Date." *Crop Science* 53 (3): 1128–38.

Sacks, William J., and Christopher J. Kucharik. 2011. "Crop Management and Phenology Trends in the U.S. Corn Belt: Impacts on Yields, Evapotranspiration and Energy Balance." *Agricultural and Forest Meteorology* 151 (7): 882–94.

Sage, Rowan F., Danielle A. Way, and David S. Kubien. 2008. "Rubisco, Rubisco Activase, and Global Climate Change." *Journal of Experimental Botany* 59 (7): 1581–95.

Saini, Dinesh K., Yuvraj Chopra, Jagmohan Singh, Karansher S. Sandhu, Anand Kumar, Sumandeep Bazzer, and Puja Srivastava. 2022. "Comprehensive Evaluation of Mapping Complex Traits in Wheat Using Genome-Wide Association Studies." *Molecular Breeding: New Strategies in Plant Improvement* 42 (1). https://doi.org/10.1007/s11032-021-01272-7.

Sakai, Tohru, and Mari Kogiso. 2008. "Soy Isoflavones and Immunity." *The Journal of Medical Investigation: JMI* 55 (3–4): 167–73.

Sandhu, Nitika, and Arvind Kumar. 2017. "Bridging the Rice Yield Gaps under Drought: QTLs, Genes, and Their Use in Breeding Programs." *Agronomy* 7 (2): 27.

Sanz-Sáez, Álvaro, Gorka Erice, Jone Aguirreolea, Fernando Muñoz, Manuel Sánchez-Díaz, and Juan José Irigoyen. 2012. "Alfalfa Forage Digestibility, Quality and Yield under Future Climate Change Scenarios Vary with Sinorhizobium Meliloti Strain." *Journal of Plant Physiology* 169 (8): 782–88.

Sanz-Sáez, Álvaro, Robert P. Koester, David M. Rosenthal, Christopher M. Montes, Donald R. Ort, and Elizabeth A. Ainsworth. 2017. "Leaf and Canopy Scale Drivers of Genotypic Variation in Soybean Response to Elevated Carbon Dioxide Concentration." *Global Change Biology* 23 (9): 3908–20.

Sanz-Saez, Alvaro, Michael J. W. Maw, Jose A. Polania, Idupulapati M. Rao, Stephen E. Beebe, and Felix B. Fritschi. 2019. "Using Carbon Isotope Discrimination to Assess Genotypic Differences in Drought Resistance of Parental Lines of Common Bean." *Crop Science* 59 (5): 2153–66.

Sarkar, P. K., E. Morrison, and U. Tinggi. 1998. "B-group Vitamin and Mineral Contents of Soybeans during Kinema Production." *Journal of The*. https://doi.org/10.1002/(SICI)1097-0010(199812)78:4<498::AID-JSFA145>3.0.CO;2-C.

Sarwar, Yasmin, and Muhammad Shahbaz. 2020. "Modulation in Growth, Photosynthetic Pigments, Gas Exchange Attributes and Inorganic Ions in Sunflower (Helianthus Annuus L.) by Strigolactones (GR24) Achene Priming under Saline Conditions." *Pakistan Journal of Botany* 52 (1): 23–31.

Schmutz, Jeremy, Steven B. Cannon, Jessica Schlueter, Jianxin Ma, Therese Mitros, William Nelson, David L. Hyten, et al. 2010. "Genome Sequence of the Palaeopolyploid Soybean." *Nature* 463 (7278): 178–83.

Schneider, Hannah M., and Jonathan P. Lynch. 2020. "Should Root Plasticity Be a Crop Breeding Target?" *Frontiers in Plant Science* 11. https://doi.org/10.3389/fpls.2020.00546.

Seck, Waldiodio, Davoud Torkamaneh, and François Belzile. 2020. "Comprehensive Genome-Wide Association Analysis Reveals the Genetic Basis of Root System Architecture in Soybean." *Frontiers in Plant Science* 11 (December): 590740.

Sedivy, Eric J., Faqiang Wu, and Yoshie Hanzawa. 2017. "Soybean Domestication: The Origin, Genetic Architecture and Molecular Bases." *The New Phytologist* 214 (2): 539–53.

Seethepalli, Anand, Kundan Dhakal, Marcus Griffiths, Haichao Guo, Gregoire T. Freschet, and Larry M. York. 2021. "RhizoVision Explorer: Open-Source Software for Root Image Analysis and Measurement Standardization." *AoB Plants* 13 (6): lab056.

Seethepalli, Anand, Haichao Guo, Xiuwei Liu, Marcus Griffiths, Hussien Almtarfi, Zenglu Li, Shuyu Liu, et al. 2020. "RhizoVision Crown: An Integrated Hardware and Software Platform for Root Crown Phenotyping." *Plant Phenomics (Washington, D.C.)* 2020 (February): 3074916.

Shikha, Kumari, J. P. Shahi, M. T. Vinayan, P. H. Zaidi, A. K. Singh, and B. Sinha. 2021. "Genome-Wide Association Mapping in Maize: Status and Prospects." *3 Biotech* 11 (5): 244.

Slattery, Rebecca A., Elizabeth A. Ainsworth, and Donald R. Ort. 2013. "A Meta-Analysis of Responses of Canopy Photosynthetic Conversion Efficiency to Environmental Factors Reveals Major Causes of Yield Gap." *Journal of Experimental Botany* 64 (12): 3723–33.

Song, Li, Silvas Prince, Babu Valliyodan, Trupti Joshi, Joao V. Maldonado dos Santos, Jiaojiao Wang, Li Lin, et al. 2016. "Genome-Wide Transcriptome Analysis of Soybean Primary Root under Varying Water-Deficit Conditions." *BMC Genomics* 17 (January): 57.

Song, Qijian, David L. Hyten, Gaofeng Jia, Charles V. Quigley, Edward W. Fickus, Randall L. Nelson, and Perry B. Cregan. 2013. "Development and Evaluation of SoySNP50K, a High-Density Genotyping Array for Soybean." *PloS One* 8 (1): e54985.

Sponchiado, B. N., J. W. White, J. A. Castillo, and P. G. Jones. 1989. "Root Growth of Four Common Bean Cultivars in Relation to Drought Tolerance in Environments with Contrasting Soil Types." *Experimental Agriculture* 25 (2): 249–57.

Spreitzer, Robert J., and Michael E. Salvucci. 2002. "Rubisco: Structure, Regulatory Interactions, and Possibilities for a Better Enzyme." *Annual Review of Plant Biology* 53: 449–75.

Steele, K. A., A. H. Price, H. E. Shashidhar, and J. R. Witcombe. 2006. "Marker-Assisted Selection to Introgress Rice QTLs Controlling Root Traits into an Indian Upland Rice Variety." *Theoretical and Applied Genetics* 112 (2): 208–21.

Stiller, Warwick N., John J. Read, Gregory A. Constable, and Peter E. Reid. 2005. "Selection for Water Use Efficiency Traits in a Cotton Breeding Program: Cultivar Differences." *Crop Science* 45 (3): 1107–13.

Suji, K. K., K. Silvas Jebakumar Prince, P. Sumeet Mankhar, P. Kanagaraj, R. Poornima, K. Amutha, S. Kavitha, K. R. Biji, S. Michael Gomez, and R. Chandra Babu. 2012. "Evaluation of Rice (Oryza Sativa L.) near Iso-Genic Lines with Root QTLs for Plant Production and Root Traits in Rainfed Target Populations of Environment." *Field Crops Research* 137 (October): 89–96.

Tanaka, Masaru, Yasuhiro Takahata, Hiroki Nakayama, Makoto Nakatani, and Makoto Tahara. 2009. "Altered Carbohydrate Metabolism in the Storage Roots of Sweetpotato Plants Overexpressing the SRF1 Gene, Which Encodes a Dof Zinc Finger Transcription Factor." *Planta* 230 (4): 737–46.

Tilman, David, Christian Balzer, Jason Hill, and Belinda L. Befort. 2011. "Global Food Demand and the Sustainable Intensification of Agriculture." *Proceedings of the National Academy of Sciences of the United States of America* 108 (50): 20260–64.

Trachsel, Samuel, Shawn M. Kaeppler, Kathleen M. Brown, and Jonathan P. Lynch. 2011. "Shovelomics: High Throughput Phenotyping of Maize (Zea Mays L.) Root Architecture in the Field." *Plant and Soil* 341 (1–2): 75–87.

Tuberosa, Roberto, Silvio Salvi, Silvia Giuliani, Maria Corinna Sanguineti, Elisabetta Frascaroli, Sergio Conti, and Pierangelo Landi. 2011. "Genomics of Root Architecture and Functions in Maize." In *Root Genomics*, edited by Antonio Costa de Oliveira and Rajeev K. Varshney, 179–204. Berlin, Heidelberg: Springer Berlin Heidelberg.

Turrentine, Jeff. 2022. "What Are the Causes of Climate Change?" National Resource Defense Council. September 13, 2022. https://www.nrdc.org/stories/what-are-causes-climate-change#human.

Uga, Yusaku, Kazuhiko Sugimoto, Satoshi Ogawa, Jagadish Rane, Manabu Ishitani, Naho Hara, Yuka Kitomi, et al. 2013. "Control of Root System Architecture by DEEPER ROOTING 1 Increases Rice Yield under Drought Conditions." *Nature Genetics* 45 (9): 1097–1102.

Vadez, Vincent. 2014. "Root Hydraulics: The Forgotten Side of Roots in Drought Adaptation." *Field Crops Research* 165 (August): 15–24.

Vadez, Vincent, and Pasala Ratnakumar. 2016. "High Transpiration Efficiency Increases Pod Yield under Intermittent Drought in Dry and Hot Atmospheric Conditions but Less so under Wetter and Cooler Conditions in Groundnut (Arachis Hypogaea (L.))." *Field Crops Research* 193 (July): 16–23.

Van Noordwijk, M., G. Lawson, J. J. R. Groot, and K. Hairiah. 1996. "Root Distribution in Relation to Nutrients and Competition." *Tree-Crop Interactions--a Physiological Approach*, 319–64.

Van Noordwijk, Meine, Pertti Martikainen, Pierre Bottner, Elvira Cuevas, Cornine Rouland, and Shivcharn S. Dhillion. 1998. "Global Change and Root Function." *Global Change Biology* 4 (7): 759–72.

VanRaden, P. M. 2008. "Efficient Methods to Compute Genomic Predictions." *Journal of Dairy Science* 91 (11): 4414–23.

Villagarcia, M. R., Thomas E. Carter, T. W. Rufty, A. S. Niewoehner, M. W. Jennette, and C. Arrellano. 2001. "Genotypic Rankings for Aluminum Tolerance of Soybean Roots Grown in Hydroponics and Sand Culture." *Crop Science* 41 (5): 1499–1507.

Wang, H., Y. Inukai, and A. Yamauchi. 2006. "Root Development and Nutrient Uptake." *Critical Reviews in Plant Sciences* 25 (3): 279–301.

Wang, Jiabo, and Zhiwu Zhang. 2021. "GAPIT Version 3: Boosting Power and Accuracy for Genomic Association and Prediction." *Genomics, Proteomics & Bioinformatics* 19 (4): 629–40.

Wang, Li, Yuming Yang, Shuyu Zhang, Zhijun Che, Wenjie Yuan, and Deyue Yu. 2020. "GWAS Reveals Two Novel Loci for Photosynthesis-Related Traits in Soybean." *Molecular Genetics and Genomics: MGG* 295 (3): 705–16.

Wang, Qin, Jiali Tang, Bin Han, and Xuehui Huang. 2020. "Advances in Genome-Wide Association Studies of Complex Traits in Rice." *TAG. Theoretical and Applied Genetics. Theoretische Und Angewandte Genetik* 133 (5): 1415–25.

Wasson, A. P., R. A. Richards, R. Chatrath, S. C. Misra, S. V. Sai Prasad, G. J. Rebetzke, J. A. Kirkegaard, J. Christopher, and M. Watt. 2012. "Traits and Selection Strategies to Improve Root Systems and Water Uptake in Water-Limited Wheat Crops." *Journal of Experimental Botany* 63 (9): 3485–98.

Weaver, J. E. 1925. "Investigations on the Root Habits of Plants." *American Journal of Botany* 12 (8): 502–9.

Weaver, John Ernest. 1926. *Root Development of Field Crops*. McGraw-Hill Book Company.

Welikhe, Pauline, Joseph Essamuah-Quansah, Kenneth Boote, Senthold Asseng, and Gamal El Afandi. 2016. "Impact of Climate Change on Corn Yields in Alabama." *Professional Agricultural Workers Journal (PAWJ)* 4 (174-2016–2193): 1–14.

Wilkinson, Sally, and William J. Davies. 2010. "Drought, Ozone, ABA and Ethylene: New Insights from Cell to Plant to Community." *Plant, Cell & Environment* 33 (4): 510–25.

Wojciechowski, T., M. J. Gooding, L. Ramsay, and P. J. Gregory. 2009. "The Effects of Dwarfing Genes on Seedling Root Growth of Wheat." *Journal of Experimental Botany* 60 (9): 2565–73.

Wong, Kong, Keith Duncan, Sergey Komarov, Daniela Floss, Dierdra Daniels, Yuan-Chuan Tai, and Christopher Topp. 2022. "Combining X-Ray CT and PET Imaging to Quantify Changes in Carbon Allocation in Maize with AMF." *Authorea Preprints*.

Xiao, Yingjie, Haijun Liu, Liuji Wu, Marilyn Warburton, and Jianbing Yan. 2017. "Genome-Wide Association Studies in Maize: Praise and Stargaze." *Molecular Plant* 10 (3): 359–74.

Yang, Jian, Noah A. Zaitlen, Michael E. Goddard, Peter M. Visscher, and Alkes L. Price. 2014. "Advantages and Pitfalls in the Application of Mixed-Model Association Methods." *Nature Genetics* 46 (2): 100–106.

Yang, Yongqing, Qingsong Zhao, Xinxin Li, Wenqin Ai, Dong Liu, Wandong Qi, Mengchen Zhang, Chunyan Yang, and Hong Liao. 2017. "Characterization of Genetic Basis on Synergistic Interactions between Root Architecture and Biological Nitrogen Fixation in Soybean." *Frontiers in Plant Science* 8 (August): 1466.

Yang, Yuming, Li Wang, Dan Zhang, Hao Cheng, Qing Wang, Hui Yang, and Deyue Yu. 2020. "GWAS Identifies Two Novel Loci for Photosynthetic Traits Related to Phosphorus Efficiency in Soybean." *Molecular Breeding: New Strategies in Plant Improvement* 40 (3): 29.

Zargar, Amin, Rehan Sadiq, Bahman Naser, and Faisal I. Khan. 2011. "A Review of Drought Indices." *Environmental Review* 19 (NA): 333–49.

Zhang, Jianhua, Wensuo Jia, Jianchang Yang, and Abdelbagi M. Ismail. 2006. "Role of ABA in Integrating Plant Responses to Drought and Salt Stresses." *Field Crops Research* 97 (1): 111–19.

Zhang, Jinmeng, Shiqiao Zhang, Min Cheng, Hong Jiang, Xiuying Zhang, Changhui Peng, Xuehe Lu, Minxia Zhang, and Jiaxin Jin. 2018. "Effect of Drought on Agronomic Traits of Rice and Wheat: A Meta-Analysis." *International Journal of Environmental Research and Public Health* 15 (5). https://doi.org/10.3390/ijerph15050839.

Zhang, Qiong, Phat Dang, Charles Chen, Yucheng Feng, William Batchelor, Marshall Lamb, and Alvaro Sanz-Saez. 2022. "Tolerance to Mid-season Drought in Peanut Can Be Achieved by High Water Use Efficiency or High Efficient Use of Water." *Crop Science* 62 (5): 1948–66.

Zhou, Rong, Hai-Feng Chen, Xian-Zhi Wang, Bao-Duo Wu, Shui-Lian Chen, Xiao-Juan Zhang, Xue-Jun Wu, et al. 2011. "Analysis of QTLs for Root Traits at Seedling Stage in Soybean." *Acta Agronomica Sinica* 37 (7): 1151–58.

Zhou, Xiang, and Matthew Stephens. 2012. "Genome-Wide Efficient Mixed-Model Analysis for Association Studies." *Nature Genetics* 44 (7): 821–24.

Zhou, Zhengkui, Yu Jiang, Zheng Wang, Zhiheng Gou, Jun Lyu, Weiyu Li, Yanjun Yu, et al. 2015. "Resequencing 302 Wild and Cultivated Accessions Identifies Genes Related to Domestication and Improvement in Soybean." *Nature Biotechnology* 33 (4): 408–14.

Zhu, Chengsong, Michael Gore, Edward S. Buckler, and Jianming Yu. 2008. "Status and Prospects of Association Mapping in Plants." *The Plant Genome* 1 (1): 5–20.

Zhu, Xin-Guang, Stephen P. Long, and Donald R. Ort. 2010. "Improving Photosynthetic Efficiency for Greater Yield." *Annual Review of Plant Biology* 61: 235–61.

Zhu, Xin-Guang, Eric de Sturler, and Stephen P. Long. 2007. "Optimizing the Distribution of Resources between Enzymes of Carbon Metabolism Can Dramatically Increase Photosynthetic Rate: A Numerical Simulation Using an Evolutionary Algorithm." *Plant Physiology* 145 (2): 513–26.

Chapter 2:
Genome-wide Association Identification of Markers Associated with Photosynthetic Traits in Soybean (*Glycine max*)

Abstract

Projected soybean yield increases, coupled with the effects of climate change, leave supply insufficient to match demand, potentially resulting in global food insecurity. As such, agronomists are faced with combating yield gaps through the pursuit of stress-resilient cultivars suitable for projected environmental conditions. To this end, a 261-members of a 281 accession soybean diversity panel was examined for traits related to carbon assimilation and water loss, such as photosynthetic rate, stomatal conductance, water use efficiency, leaf area, and leaf mass. Genome-wide association analysis, utilizing the Fixed and Random CPU, identified 31 marker-trait associations (MTAs), including one previously identified for water use efficiency. Candidate gene mining in a 250 kb window of these 31 markers presents 578 potential genes. Gene functions suggested by gene ontologies include protein binding, chromatin binding, hydrolase activity, relation to membrane-bound organelles, cytosol maintenance, ubiquitination, and growth regulation. Several compelling genes pertaining to light signaling pathways, electron transport chain, and NADH dehydrogenase were also identified. Cultivars with high photosynthetic rate and/or water use efficiency, several compelling markers, and potential candidate genes provide ample foundation for future work in introgression breeding, marker-assisted selection, and gene functional validation.

1. Introduction

Soybean, *Glycine max*, is the second most produced crop in the US, with total acres planted and yield recovered increasing annually. The total area planted rose from 58.8 million acres in 1988 to 87.2 million acres by 2021, a 48.3% increase in area. Yield increased 90% per acre, from 27 bushels/ acre to 51.4 bushels/ acre, during the same period (America Soybean Association 2022), which is predominantly attributed to cultivar development, improved management practices, and producer readiness to adopt improved biological and mechanical technologies as they are released (van Ittersum and Cassman 2013). These improved yields are funneled into direct and indirect comestible inputs, be it in the production of milk and meat alternatives, inclusions in animal feed, or fuel to transport from farms to tables. However, with the global population expected to expand from 7.2 billion to 9.6 billion by the mid-21st century ("Food and Agriculture Organization of the United Nations" 2020) and current yield trends insufficient to keep pace with demand (Ray et al. 2013) a global food shortage crisis is predicted by 2050 (Tilman et al. 2011; Alexandratos and Bruinsma 2012). The soybean community is thus faced with the monumental task of vast yield improvement to combat this impending crisis.

Yield modeling by Monteith in the 1970s considered and argued yield as a product of resource (i.e., light, water, and nutrients) availability and genetic predisposition for efficiency of light capture (εi), photosynthetic efficiency of photon capture to biomass (εc), and the biomass allocation of photosynthetic outputs into grain (εp) (Monteith and Moss 1977; Monteith 1994). Modern cereal cultivars can partition 60% of above-ground biomass into harvestable grains (Evans 1996; Hay 1995). Given that a species has a minimum threshold for non-grain structure development, εp is arguably approaching a theoretical maximum. Similarly, decades of research optimizing canopy structure, sunspecking, and shade avoidance have dwindled avenues of

progression for photon capture (Pearcy, Roden, and Gamon 1990). Modern soybean cultivars, at normal production conditions in optimal environments, light intercept almost 90% ($\varepsilon i = 0.89$) of the photosynthetically active radiation across the growing season and partitioned 60% of photosynthetic outputs into the harvested seed ($\varepsilon p = 0.60$) (Zhu, Long, and Ort 2010; Koester et al. 2014). Therefore, if breeding has brought εp and εi close to their theoretical maximum, the most likely mechanism for vast yield improvement will be through conversion efficiency, implying photosynthetic optimization (Long et al. 2006).

Photosynthesis is the complex biochemical process of autotrophs in which photon energy, CO_2, and water are used as catalyst, substrate, and electron acceptor for the cyclic production of sugars. The photosynthetic pathway is broken into two biological processes; the photosynthetic electron transport system (PETs), in which light energy is used to produce biochemical energy; and the Calvin–Benson cycle, also known as the photosynthetic carbon fixation cycle, in which CO_2 is fixed into carbohydrates (Eberhard, Finazzi, and Wollman 2008; Foyer et al. 2012). These concurrent mechanisms enable multiple avenues of photosynthetic improvement, including more effective light capture via expanded photosystem absorbance and increasing the efficiency of ribulose-1,5-bisphosphate carboxylase/oxygenase (RUBISCO) through improved binding specificity and/or decreasing active site competition (Long et al. 2006). With more than 90% of crop biomass derived from photosynthetic products (Makino 2011), a high photosynthetic rate has been found to increase yield in rice, wheat, corn, potatoes, barley, peanut, and soybean. However, photosynthetic rates are highly sensitive to the environment and, therefore, heavily impacted by stress (Sharma et al. 2020; Demmig-Adams et al. 2022).

Abiotic stresses such as drought, temperature, flooding, nutrient deficiency or toxicity, UV light stress, and pesticides negatively impact the photosynthetic efficiency of plants:

reducing Ribulose-1,5-bisphosphate carboxylase/oxygenase (RUBISCO) activity, causing free radical production, and negatively influencing photosystems, PETs, and chlorophyll synthesis (Sharma et al. 2020; Demmig-Adams et al. 2022; Eberhard, Finazzi, and Wollman 2008; Allen and Ort 2001). These stresses have subsequently been shown to reduce yield and yield quality. For example, an average 2.4% decrease in soybean productivity across the United States was determined for each degree Celsius increase in temperature above 25ºC (Mourtzinis et al. 2015). However, water availability is the greatest abiotic constraint on crop productivity (Araus et al. 2002; Boyer 1982). Drought causes a reduction of transpiration, and subsequently photosynthesis, leading to lesser amounts of biomass accumulation (Sinclair and Rufty 2012; Tardieu and Tuberosa 2010; Welikhe et al. 2016). Agricultural production losses attributed to drought during 2012 were estimated to be $30 billion in the US (Rippey 2015). The impacts of climate change, affecting seasonal, climatological, and atmospheric conditions (Kukal and Irmak 2018; Karl et al. 2009), increase the probability that crops will suffer some levels of abiotic stress. Therefore, crop resiliency and yield greatly benefit from a mechanistic understanding and the improvement of photosynthesis and water- and nutrient-use efficiencies (Ort et al. 2015; Leakey et al. 2019; Simkin, López-Calcagno, and Raines 2019). In parallel, an understanding of endogenous species resiliency provides imperative information on the genetic breadth available for cultivar adaptation.

Photosynthetic performance can be inferred by quantifying CO_2 and water vapor fluctuations into and out of a leaf. The determination of net CO_2 assimilation, respiration, and stomatal conductance enables the estimation of photosynthetic efficiency through the rate of gas exchange and the measurement of substrates and products and can be used to monitor plant performance in abiotic stress conditions (Sanz-Sáez et al. 2012, 2017).

Complex quantitative traits, such as carbon assimilation and water loss, have undergone increased understanding through genome-wide association studies (GWAS) (Huang et al. 2010). GWA analyses use single nucleotide polymorphisms (SNPs) in conjunction with phenotypic data from a diverse population to make significant predictions on the relationship between genetic architecture and the analyzed phenotype. In previous soybean studies, gas exchange data has been utilized into pinpoint genetic markers and genes pertaining to improved photosynthetic rate and water use efficiency under different conditions (Y. Yang et al. 2020; Dhanapal et al. 2015; L. Wang et al. 2020; H. Li et al. 2016; Lü et al. 2018; W. Du et al. 2020; Kaler et al. 2017). The determination of markers has implications on modern breeding via the use of genomic and marker assisted selection. Furthermore, the genetic underpinning of photosynthetic rate has been pursued through nested association (Montes et al. 2022; Lopez, Xavier, and Rainey 2019) and mapping studies (Liang et al. 2010). These methods have been utilized to determine genes pertaining to improved photosynthetic rate and water use efficiency. However, the majority of the work utilizing GWAS and gas exchange data examine the response of photosynthetic rate to abiotic stress conditions, particularly phosphorus, leaving a gap in the literature about the endogenous variation in carbon assimilation and water loss in unmanaged field conditions.

While high photosynthetic rates and low stomatal conductance do not inherently equate to an improved outlook under abiotic stress conditions or better yields, the ability to use and/or store water more effectively are valuable traits when breeding for water-conscious cultivars and improved yields. Therefore, identifying genotypes exhibiting high photosynthetic rates and low stomatal conductance is a dualistic approach addressing the caloric needs of an ever-expanding global population and the dramatically changing growing conditions stressing current farming methodologies. The objective is to utilize a subset of the USDA Soybean population (261

52

accessions), inorder to: (1) examine the endogenous diversity of the species regarding

photosynthetic rates, stomatal conductance, WUE_i, and specific leaf area. (2) use genome-wide

association to assign MTAs to genomic regions for each phenotype, and (3) identify potential

candidate genes within a calculated window surrounding the MTA for potential use in future

crop improvement.

2.   Materials and Methods

2.1 Plant Materials

A soybean diversity panel consisting of 281 *Glycine max* accessions comprising landraces, breeding lines, and elite accessions obtained from the USDA-ARS Germplasm Resources Information Network at Auburn University in 2019. Cultivars in this population were selected based on maturity group (V) and various phenotypic traits, including yield, shattering rates, lodging rates, oil content, oleic content, protein content, seed weight, abiotic stress tolerance, and pest and disease resistance (https://npgsweb.ars-grin.gov). The population was planted in replicate at EV-Smith Field Crops Research Unit, Tallassee, AL (32.4234° N, 85.88816° W) on May 6, 2020 and at EV-Smith Plant Breeding Unit, Tallassee, AL (32.4967° N, 85.8905° W) on May 7, 2021. Plots in the 2020 season were planted in a single row in a 3 meter plot. In 2021, the seeds were sown in two 3-meter-long rows, with plots conforming to a replicated complete block (RCB) experimental design.

2.2 Phenotypic Measurements

Leaf gas exchange and growth parameters were measured at R2-R3 growth stages from 23rd to 28th of July 2020 and from August 4th to 12th, 2021. Uppermost fully expanded trifoliate leaves were harvested pre-dawn, and leaf gas exchange parameters were determined in the laboratory to minimize circadian regulation and heterogeneity of environmental factors (Ainsworth et al. 2004; T. Du et al. 2020; Choquette et al. 2019). Briefly, two trifoliate leaves per plot from the upper canopy for each line was sampled pre-dawn. Leaves were cut and submerged in water and petioles were cut again under water and transferred into 15 ml tubes filled with water (Ainsworth et al., 2004, Sanz-Saez et al., 2017). To minimize time effect, leaves were stored in black plastic boxes to avoid light contact, and placed in an acclimatized room at 22°C and 50%

relative humidity (RH). To achieve a stable photosynthetic status, leaves were transferred into a growth chamber at 25 °C and relative humidity of 65% under saturating light conditions (~1600 $\mu mol\ m^{-2}\ s^{-1}$) using a LED light source (MARS PRO II EPISTAR™ 320; Sasquatch soil CO.) for at least 20 minutes prior to leaf gas exchange measurements. After the stimulation and acclimation period, leaf gas exchange parameters were measured in the central leaflet under the same light intensity (1600 $\mu mol\ m^{-2}\ s^{-1}$), block temperature of 25°C, and relative humidity of 60-70% with a set of three portable gas exchange systems (LI-6400; LI-COR Biosciences, Lincoln, NE, USA). The rate of CO_2 assimilation (A_N), stomatal conductance (g_s), and intercellular CO_2 (C_i) were recorded when photosynthetic values were stable, which generally occurred in less than 3-5 min. The instantaneous water use efficiency (WUE_i) was determined by dividing the rate of A_N by g_s. Immediately after gas exchange measurements, whole leaf area was determined with a leaf area meter (LI-3100; LI-COR Biosciences, Lincoln, NE, USA). The entire processes, including leaf sample collection, leaf gas exchange, and leaf area determinations, were performed in less than 12 hours. Photosynthetic measurements were stopped for the day if more than 3 trifoliates in a row showed a value lower than 0.15 (mmol of $H_2O\ s^{-1}\ m^{-2}$) as this would indicate that the plants were closing stomata due have been too much time excised from the plant or that gas bubbles have entered in the petiole and interrupted water flux. Leaf dry mass (LM) was determined after drying leaf samples at 40 °C for at least 7 days. Specific Leaf Area (SLA) was derived by dividing leaf surface area by its dry mass.

2.3 Phenotypic Statistics

Technical replicates within a year were averaged for each plot and field replication. Following examination of phenotypic measurement data, 261 lines are common across both years and replicate and comprise the final population for this study. Statistics were calculated

using base R (version 3.4) (R Core Team 2022). Analysis of variance (ANOVA) was utilized to consider the genotype (G) and environment (E) contribution to phenotype. Broad sense heritability was calculated as $H^2 = V_g/(V_g + V_e)$, where V_g is the genetic variance, and V_e is the variance of the error .

2.4 Genetic Data

Single nucleotide polymorphism (SNP) data is publicly available at Soybase.com, generated in a 50k chip format (Q. Song et al. 2013). It is available for download with SNP positional information in relation to Wm82.a2 or/and Wm82.a1 reference genomes, totaling 42,509 SNP positions (https://www.soybase.org/snps/). Following filtering SNP positions called with <20% frequency, individuals missing >20% of genetic data, and SNP positions with minor allele frequency <.05, a total of 33,453 SNPs are used as markers in this GWAS. Linkage disequilibrium (LD) was characterized using TASSEL (version 5) (Bradbury et al. 2007), examining r^2 values in 50 marker sliding window. Genetic data was not filtered to remove SNPs in perfect LD.

2.5 Population Structure and GWAS

Population structure of the total ASDP (281 individuals), SNPs= 33,453, was calculated using STRUCTURE v2.3.4 (Hubisz et al. 2009; Pritchard, Stephens, and Donnelly 2000), a Bayesian model-based software program. The burn-in iteration was 25,000, burn-in was followed by 10,000 replication of Markov chain Monte Carlo (MCMC) sampling with admixture and allele frequencies correlated. The estimated likelihood value of data [LnP(D)] was plotted. K determination was performed through examination of log probability rate of change (Evanno, Regnaut, and Goudet 2005).

Genome-Wide Association analysis was performed utilizing the R package GAPIT (version 3) (J. Wang and Zhang 2021). Due to the documented polygenic nature of the traits, the methodology Fixed and random model Circulating Probability Unification (FarmCPU) was used (X. Liu et al. 2016). FarmCPU is based on the foundational mixed-linear model (MLM), in which population structure (Q) and kinship with a population (K) are set as covariates (Kang et al. 2008); the inclusion of such reduces false positives caused by population stratification. The FarmCPU model methodology further reduces the risk of false positives and confounding by iteratively testing markers and cofactors. For this analysis, PCA accounts for Q and was set to 5 following eigenvalue and Bayesian information criterion (BIC) examination; K was determined via the VanRaden (VanRaden 2008) method within the GAPIT package. PCA+K calculation enables the calculation and utilization of pseudo quantitative trait nucleotides (QTNs) to identify functional associations by which to consider in SNP significance determinations. A significance threshold of 1/n, where n is the number of SNPs utilized in analysis; $p < 1/33453$ (0.000029) (or $\log_{10}P > 4.52$) (Yang et al. 2014), was employed while a less stringent P value ≤ 0.0003 (or -$\log_{10}P > 3.5$) was considered to identify suggestive associated of SNP to the trait of interest. LD decay was utilized to determine a window in which to identify potential candidate genes. Ultimately, genes were canvased 125 kb upstream and downstream of significant SNPs via Plant Ensembl, utilizing the Glycine_Max_v2.1 gene set (https://plants.ensembl.org/biomart/martview). Gene Stable IDs were then searched through Plant Ensembl, filtering for Gene Stable IDs, gene name, gene start and end, and gene ontology (GO) term name. Genes described to be related to photosynthetic processes, water utilization, and biochemical energy intermediates were given special consideration and confirmed using

Soybase genome assembly Glycine max genome assembly version Glyma.Wm82.a2 (Gmax2.0)

(https://www.soybase.org/gb2/gbrowse/gmax2.0/).

3.   Results

3.1 Phenotypic Results

Phenotypic measurements across years demonstrate near-normal distributions within a year but significant differences between years (**Figure 1**). Phenotypic values for this population range from 2.5-31.6 μmol CO_2 m^{-2} s^{-1} for photosynthetic rate, .056-1.23 mol H_2O m^{-2} s^{-1} for stomatal conductance, 19.83-146.7 mol CO_2/mol H_2O for WUE_i, 112-333 μmol CO_2 mol air^{-1} for Ci, 17.23-185.7 (cm^2) for leaf area, .072-1.27 (g) for dried leaf mass, and 76.7-501.89 cm^2 g^{-1} for the derived specific leaf area (**Table 1, Supplemental Table 1**). Means for all traits were higher in 2020 measurements, except for WUE_i. Examination of analysis of variance (ANOVA) confirmed marked genotypic and environmental variation for all parameters, with p-values <.01 and <0.0001 respectively (**Table 1, Supplemental Table 2**). Genotype-by-environment (year) interaction did not play a significant role in phenotypic variance. Broad sense heritability calculations present a robust heritable component to leaf area, leaf mass, and specific leaf area, 0.73, 0.72, 0.60, respectively. Photosynthetic rate (.476) demonstrate moderate heritability, and low heritability is observed in stomatal conductance, WUE_i , and Ci. Given the magnitude of the environmental impact, GWA studies were performed for each year (**Table 2**).

3.2 Population Structure

Genetic relatedness between individuals of the ASDP was calculated utilizing STRUCTURE analysis software. The most probable number of subpopulations was determined by plotting the estimated likelihood value [LnP(D)] obtained from STRUCTURE runs against k. Assessment of plateau determined that 9 subpopulations best described the interrelatedness of these 281-soybean accession, based on the distribution 33,453 SNP loci (**Table 3**, **Figure 2, Figure 3**). All soybean accessions were assigned to a subpopulation based on the correct k, for

which the membership value (Q value) was largest of the subpopulation admixture in each individual. For example, accession FC30265 has Q values for determined subpopulations as follows, 1 =0.396, 2=0, 3=0.022 ,4=0.131, 5=0.001, 6=0, 7=0.299, 8=0.151, and 9=0. As subpopulation 1 comprises the largest component, FC30265 was determined to be in subpopulation 1. Subpopulation 3 is the largest, with a predomination of cultivars from Japan. There were 4 of the 9 subpopulations in which originating from South Korea make up the majority, with subpopulation 5 being entirely composed of Korean accessions. Interestingly, the majority of cultivars collected from outside Eastern Asia are grouped into subpopulation 1.

3.3 Marker Trait Associations

At an established $p < 0.001$, 31 SNP locations were significant using FarmCPU applied across years and phenotypes (**Figure 4, Table 4**). Marker trait associations for stomatal conductance or water use efficiency were not observed, nor were there significant MTAs shared across the years. A single SNP (ss715612385) did associate with leaf mass and specific leaf area in 2021 phenotypes. At a less stringent threshold of $-\log_{10} > 3.5$ ($p \leq 0.000316$), visualized via the dotted line in Manhattan plots, significant MTAs occur for all seven phenotypes in both years (**Figure 4**). There were 155 significant markers found on all chromosomes except, 14. . Markers ss715584424 & ss715584493 on Chromosome 3 are both associated with water use efficiency and were significant in both years of the analysis.

Utilizing 2020 data, 4 SNPs were significant: 1 associated with dried leaf mass (ss715617000, R^2 =3.4%) and 3 (ss715582450, ss715616744, & ss715635823) with photosynthesis. In 2020 markers associations with photosynthesis highlight potential loci on chromosomes 2,13, and 19; markers explain a cumulative 34% to the phenotypic variance.

Twenty-seven SNPs were returned significantly in the 2021 phenotypic data. One SNP (ss715598779, R^2= 28.5%) was associated with intracellular CO_2, 4 with leaf area, 7 with leaf mass, 9 with specific leaf area, and 6 associated with photosynthetic rate. Five of the six SNPs associated with photosynthetic rate are in linkage disequilibrium, spanning a region of 12,278 bp, and will be considered together as a singular potential region. These 5 markers are calculated to cumulatively account for 80% of the phenotypic variance. ss715622987 is not in linkage with the others clustered on chromosome 15, but also contributes nothing to the phenotypic variance. Markers for leaf area and specific leaf area are found exclusively in 2021 data. SNPs associated with leaf area are found on chromosomes 7, 15, and 19, explaining 13.4% of the variance. While specific leaf area has the most denoted markers in a single year, these 9 markers only have a cumulative R^2 of 42.6%, with SNP ss715584902 contributing 11.6% to this culmination. None of the specific leaf area markers are linked, and they are found on chromosomes 1-3,10,12,15, &16. Examining the markers cumulatively, significant hits occur on more than half soybean's 20 chromosomes (Chromosomes 1,2,3,7,10,12,13,15,16,18,19).

Linkage disequilibrium decay suggests using a 250 kb region (~125kb up and downstream) window to survey candidate genes (**Figure 5**). A total of 578 genes were found window (**Supplemental Table 3**). Functional predictions of identified genes, according to Gene Ontology term names and descriptions, include protein binding, chromatin binding, hydrolase activity, relation to membrane-bound organelles, cytosol maintenance, ubiquitination, and growth regulation. Focus was narrowed to putative gene functions related to photosynthetic processes, including genes related to chloroplasts, light signaling pathways, electron transport chain, and NADH dehydrogenase. Through this method, 55 genes of interest, associated with 23

61

of the 31 significant SNPs (**Table 4**), were identified. Candidate gene mining of MTAs

surpassing $-\log_{10} > 3.5$ returned 1210 unique gene stable IDs.

4.   Discussion

4.1 Discussion of Descriptive Statistics

This study aimed to examine endogenous variation in gas exchange capacity as a mechanism to determine genetic factors contributing to photosynthetic efficiency implicitly. Motivation for such an undertaking is driven by the necessity of understanding the genetic reservoirs available to breeders improving yield through photosynthetic optimization and drought resiliency. The application of photosynthetic parameters to drought resistance could be unclear considering that individuals were not grown nor measured in drought conditions; however, the established relationship between gas exchange traits and drought tolerance (Zhang et al. 2022) supports this avenue.

The inherent nature of field studies is uncontrollable environmental conditions. In the 2020 planting at 32.4234° N, 85.88816° W plots experienced an average maximum temperature of 28.03 ℃ and an average low of 16.1 ℃. Cumulatively, these plots also received 98.9 cm of rainfall, with the majority (10.31 cm) of precipitation falling in July. These temperatures equate to 1942 growing degree days (GDD) between planting and sample measurement. Meanwhile, plots planted at 32.4967° N, 85.8905° W in 2021 experienced lower average maximum (27.22 ℃) and minimum (15.7 ℃) temperature, 2056 GDD, with a larger culmination of precipitation (103.6 cm) between planting and sampling (**Figure 6).** Environmental conditions were further exacerbated by the differences in irrigation access in the 2020/2021 growing conditions. The variations in conditions resulted in a strong environmental component in ANOVA analysis and the independent performance and consideration of GWAS.

Examining the results of descriptive statistics for the measured traits, broadly, the gas exchange measurements have a fluctuating variation to those in the literature. The means of

photosynthetic rate were in the range of the measurement from Lu et al. (2018) and Li et al. (2016) (Lü et al. 2018; H. Li et al. 2016). Stomatal conductance measurements were higher than that reported by Lu et al (2018), but dramatically lower than that of Li et al. (2016). Intracellular CO_2 was significantly lower than the means of Lu et al. (2018) and Li et al, (2016) but within the range reported by Yang et al. (Yang et al. 2020). Means for all traits were higher in 2020 measurements, except for WUE_i. As WUE_i is inversely related to stomatal conductance, higher measurements in stomatal conductance will result in lower calculated WUE_i. The calculated heritability of photosynthesis, conductance, and Ci in these experiments is lower than those previously reported (Li et al. 2016; Lü et al. 2018). This is, to some extent, expected given the differences in panel composition, the high variance of error, and the different growing conditions, as the samples here were grown in field conditions and the comparison here had plants grown in greenhouse conditions. Low to moderate heritabilities are the norm when examining gas exchange measurements, as photosynthetic rate is highly sensitive to changes in environmental conditions. Measurements of leaf morphology characteristics demonstrate significantly higher, and stable broad sense heritability. This is expected given the stable genetic impact on leaf morphology and the lesser impact of environment on instantaneous measurements. The moderate heritability of specific leaf area is of note, as specific leaf area has been shown to be negatively correlated with water use efficiency in peanut and amaranth (Songsri et al. 2009; Liu and Stutzel 2004).

4.2 Discussion of Genetic Analysis

The total 281-member population assembled into 9 subpopulations; however, population structure was accounted for in GWAS with a PCA value of 5. Association analysis was also run with other PCA values; however, PCA 5 seemed to best fit the data, as evidenced by the BIC and

eigenvalues, which was surprising given its dramatic variation from STRUCTURE results. Examining the Q matrix, admixture became evident with consistent overlap between subpopulations 2 & 4 and 8 & 9. Furthermore, 4 subpopulations determined by STRUCTURE have less than 20 members, which may have led to a collapsing of subpopulations resulting in the BIC determination of 5. This collapsing of subpopulations is further confused when considering that the subpopulation determination was made in STRUCTURE using 281 individuals but with 261 taxa in BIC determination. Additionally, while this study presents results of FarmCPU modeled-GWAS, a traditional general linear model (GLM), and mixed linear model (MLM) were also performed, as was a multi-locus MLM. The FarmCPU method was chosen due to its statistical power and inherent methods to limit kinship confounding and false positives.

Although identified MTAs did not occur across years at a threshold of -log > 4.54, all presented SNPs have a corresponding value greater than a 0.05 in the alternative year. While no markers are found in this study across years, SNP ss715582171 (Chr. 02, Pos: 37286171), identified at the suggestive threshold $-\log_{10}P > 3.5$ in this study for Leaf Mass in the 2021 population, has been previously categorized as a WUE marker (Kaler et al. 2017). Markers found on Chromosome 15 in this study are of interest due to previous identification of WUE loci on the chromosome (Mian et al. 1998; Kaler et al. 2017). ss715623187, here identified for Leaf Area in 2021 analysis, is at the upper end of the WUE loci denoted by Mian. The qualitative trait loci (QTL) identified here as a cluster of SNPs on chromosome 15 associated with photosynthetic rate in 2021 ranged from Glycine v2 7089421-7133808. This region is on the upper arm of chromosome 15, as is the WUE loci identified by Kaler (2017). However, these loci are at least 600 kb from the cluster of SNPs identified here. The closest of Kaler's loci to this SNP cluster is

65

WUE 2-g34 (Pos. 7742643). Furthermore, Yang 2020 and Montes 2022 both identified regions

of chromosome 19 for photosynthetic and rubisco rate of carboxylation. However, these regions

are at least 10 mB from the SNP ss715635823 identified for photosynthetic rate in 2020.

Differences in loci are unsurprising given that Montes measured RUBISCO efficiency rather

than photosynthetic rate.

Candidate gene mining identified 578 genes in LD with significantly associated SNPs.

Putative gene function classification using Soybase determined 130 genes related to chlorophyll

regulation, chloroplasts structure and organization, photosynthesis, the electron transport chain,

and photosystems. These genes localize to regions on the short arm of chromosomes 1, 2, 7, 15,

16, and 19 and the long arm of chromosomes 2, 10, 16, 18, and 19 (**Figure 7**). While not

denoting the same location, regions of chromosomes 1, 2, 7, 10, 13, 18, and 19 have previously

been identified as QTLs for WUE (Kaler et al. 2017). Genes of great intrigue on the previously

identified chromosomes include, GLYMA_02G047600, GLYMA_10G226300, and

GLYMA_13G068600. Genes not identified on chromosome 2, but with compelling functions

include 2 genes on each chromosome 15 (GLYMA_15G114600 & GLYMA_15G116500) and

chromosome 16 (GLYMA_16G017600 & GLYMA_16G204600). All these genes have

predicted functions in photosynthetic processes. As a ferredoxin--NADP+ reductase,

GLYMA_02G047600 serves as an electron carrier in the electron transport chain and facilitates

the reduction of NADP at photosystem 1. Increased efficiency in NADP reduction during the

light dependent reactions could enable greater "energy currency" be funneled into the Calvin-

Benson cycle, lessening the limitation of biochemical energy on carbon assimilation. Similarly,

GLYMA_13G068600 (gene name:ndhc) encodes for a NAD(P)H-quinone oxidoreductase in the

third subunit of photosystem 1. This protein also aids in the movement of electrons down the

electron transport chain via the electron reduction of quinones (Ma 2021). GLYMA_10G226300

is a protein tyrosine and serine/threonine kinase. Serine/threonine kinases have been shown to

modulate ABA sensitivity during drought conditions. ABA is a stress hormone that causes

stomatal closure, thereby reducing photosynthetic output. Previous research suggests that

CaDIK1, serine/threonine kinase in pepper, is a positive regulator of the ABA-mediated drought-

stress tolerance (L. Yang et al. 2012; Lim, Lim, and Lee 2020). GLYMA_15G114600 encodes

cyctochrome-b, a component of complex III in the electron transport chain. Complex three has

oxidoreductase activity as a mechanism of electron transfer down the chain. Similarly,

GLYMA_15G116500 is an NADH-ubiquinone oxidoreductase in complex I of the electron

transport chain. Selected genes on chromosome 16 have functions in thylakoid protein curvature

(GLYMA_16G017600) and as enolase (GLYMA_16G204600). Thylakoid curvature proteins aid

in the reorgazation of thylakoid predecessors into functional thylakoids, which includes the

assembly of active photosynthetic complexes (Sandoval-Ibáñez et al. 2021). Regarding gene

GLYMA_16G204600, the enolase reaction is a part of the reaction catalysed by photosynthetic

RuBisCO. Enolase catalyzes the conversion of 2-phosphoglycerate (2-PG) to

phosphoenolpyruvate (PEP) (Van der Straeten et al. 1991; Ashida et al. 2008; Furbank and

Leegood 1984; M. Read et al. 1994). While these 7 selected genes have direct function in

photosynthetic processes and immediate implications on yield improvement and/or drought

resiliency, more research is needed to determine the extent of usability. Functional gene

validation could be pursued through gene knockouts, overexpression, or cloning.

5.   Conclusions

GWAS utilizing 33,453 loci of 261 taxa, reveals 31 significant marker-trait associations. Validity of these associations is supported by previously identified QTLs. Identified SNPs can therefore be utilized in markers-assisted selection efforts in breeding programs and used to determine apt lines for hybridization experiments with established cultivars. Disclosed potential candidate genes will need to undergo further research, such as RNA-Seq, fine mapping, and candidate knocking-out or overexpression, for functional validation. However, this project has identified useful markers and individuals to integrate drought resilient characteristics and provided the basis on which further research could build.

Future work on cultivars with extreme and stable photosynthetic rate could include lines FC31952, PI399109, PI82588, PI303652, which have above average photosynthetic rates in at least 3 of the 4 replications across years, PI181547, and PI424417 which both have below average photosynthetic rate in 3 of the 4 replications. All 6 accessions are cultivated and available from the national germplasm collection.

References

Ainsworth, Elizabeth A., Alistair Rogers, Randall Nelson, and S. P. Long. 2004. "Testing the Source-Sink Hypothesis of down-Regulation of Photosynthesis in Elevated [CO_2] in the Field with Single Gene Substitutions in Glycine Max." *Agricultural and Forest Meteorology* 122 (1–2): 85–94.

Alexandratos, Nikos, and Jelle Bruinsma. 2012. "World Agriculture towards 2030/2050: The 2012 Revision." https://ageconsearch.umn.edu/record/288998/.

Allen, D. J., and D. R. Ort. 2001. "Impacts of Chilling Temperatures on Photosynthesis in Warm-Climate Plants." *Trends in Plant Science* 6 (1): 36–42.

America Soybean Association. 2022. "'A Reference Guide to Important Soybean Facts & Figures: SoyStats 2022.'" 2022. https://soygrowers.com/education-resources/publications/soy-stats/.

Araus, J. L., G. A. Slafer, M. P. Reynolds, and C. Royo. 2002. "Plant Breeding and Drought in C3 Cereals: What Should We Breed For?" *Annals of Botany* 89 Spec No (7): 925–40.

Ashida, Hiroki, Yohtaro Saito, Toshihiro Nakano, Nicole Tandeau de Marsac, Agnieszka Sekowska, Antoine Danchin, and Akiho Yokota. 2008. "RuBisCO-like Proteins as the Enolase Enzyme in the Methionine Salvage Pathway: Functional and Evolutionary Relationships between RuBisCO-like Proteins and Photosynthetic RuBisCO." *Journal of Experimental Botany* 59 (7): 1543–54.

Boyer, J. S. 1982. "Plant Productivity and Environment." *Science* 218 (4571): 443–48.

Bradbury, Peter J., Zhiwu Zhang, Dallas E. Kroon, Terry M. Casstevens, Yogesh Ramdoss, and Edward S. Buckler. 2007. "TASSEL: Software for Association Mapping of Complex Traits in Diverse Samples." *Bioinformatics* 23 (19): 2633–35.

Choquette, Nicole E., Funda Ogut, Timothy M. Wertin, Christopher M. Montes, Crystal A. Sorgini, Alison M. Morse, Patrick J. Brown, Andrew D. B. Leakey, Lauren M. McIntyre, and Elizabeth A. Ainsworth. 2019. "Uncovering Hidden Genetic Variation in Photosynthesis of Field-Grown Maize under Ozone Pollution." *Global Change Biology* 25 (12): 4327–38.

Demmig-Adams, B., S. K. Polutchko, M. C. Zenir, P. Fourounjian, J. J. Stewart, M. López-Pozo, and W. W. Iii. 2022. "Intersections: Photosynthesis, Abiotic Stress, and the Plant Microbiome." *Photosynthetica* 60 (SPECIAL2022): 59–69.

Dhanapal, Arun Prabhu, Jeffery D. Ray, Shardendu K. Singh, Valerio Hoyos-Villegas, James R. Smith, Larry C. Purcell, C. Andy King, Perry B. Cregan, Qijian Song, and Felix B. Fritschi. 2015. "Genome-Wide Association Study (GWAS) of Carbon Isotope Ratio (Δ13C) in Diverse Soybean [Glycine Max (L.) Merr.] Genotypes." *TAG. Theoretical and Applied Genetics. Theoretische Und Angewandte Genetik* 128 (1): 73–91.

Du, Tingting, Ping Meng, Jianliang Huang, Shaobing Peng, and Dongliang Xiong. 2020. "Fast Photosynthesis Measurements for Phenotyping Photosynthetic Capacity of Rice." *Plant Methods* 16 (January): 6.

Du, Wenkai, Lihua Ning, Yongshun Liu, Shixi Zhang, Yuming Yang, Qing Wang, Shengqian Chao, et al. 2020. "Identification of Loci and Candidate Gene GmSPX-RING1 Responsible for Phosphorus Efficiency in Soybean via Genome-Wide Association Analysis." *BMC Genomics*. https://doi.org/10.1186/s12864-020-07143-3.

Eberhard, Stephan, Giovanni Finazzi, and Francis-André Wollman. 2008. "The Dynamics of Photosynthesis." *Annual Review of Genetics* 42: 463–515.

Evanno, G., S. Regnaut, and J. Goudet. 2005. "Detecting the Number of Clusters of Individuals Using the Software STRUCTURE: A Simulation Study." *Molecular Ecology* 14 (8): 2611–20.

Evans, L. T. 1996. *Crop Evolution, Adaptation and Yield*. Cambridge University Press.

"Food and Agriculture Organization of the United Nations." 2020. FAOSTAT. 2020. https://www.fao.org/faostat.

Foyer, Christine H., Jenny Neukermans, Guillaume Queval, Graham Noctor, and Jeremy Harbinson. 2012. "Photosynthetic Control of Electron Transport and the Regulation of Gene Expression." *Journal of Experimental Botany* 63 (4): 1637–61.

Furbank, Robert T., and Richard C. Leegood. 1984. "Carbon Metabolism and Gas Exchange in Leaves of Zea Mays L.: Interaction between the C 3 and C 4 Pathways during Photosynthetic Induction." *Planta*, 457–62.

Hay, R. K. M. 1995. "Harvest Index: A Review of Its Use in Plant Breeding and Crop Physiology." *The Annals of Applied Biology* 126 (1): 197–216.

Hubisz, Melissa J., Daniel Falush, Matthew Stephens, and Jonathan K. Pritchard. 2009. "Inferring Weak Population Structure with the Assistance of Sample Group Information." *Molecular Ecology Resources* 9 (5): 1322–32.

Ittersum, M. K. van, and K. G. Cassman. 2013. "Yield Gap Analysis—Rationale, Methods and Applications—Introduction to the Special Issue." *Field Crops Research* 143 (March): 1–3.

Kaler, Avjinder S., Arun P. Dhanapal, Jeffery D. Ray, C. Andy King, Felix B. Fritschi, and Larry C. Purcell. 2017. "Genome-Wide Association Mapping of Carbon Isotope and Oxygen Isotope Ratios in Diverse Soybean Genotypes." *Crop Science* 57 (6): 3085–3100.

Kang, Hyun Min, Noah A. Zaitlen, Claire M. Wade, Andrew Kirby, David Heckerman, Mark J. Daly, and Eleazar Eskin. 2008. "Efficient Control of Population Structure in Model Organism Association Mapping." *Genetics* 178 (3): 1709–23.

Karl, T. R., C. N. Williams Jr, P. J. Young, and W. M. Wendland. 2009. "Global Climate Change Impacts in the United States: A State of Knowledge Report." *Global Climate Change Impacts in the United States: A State of Knowledge Report Number Of*, 196.

Kukal, Meetpal S., and Suat Irmak. 2018. "U.S. Agro-Climate in 20th Century: Growing Degree Days, First and Last Frost, Growing Season Length, and Impacts on Crop Yields." *Scientific Reports* 8 (1): 6977.

Leakey, Andrew D. B., John N. Ferguson, Charles P. Pignon, Alex Wu, Zhenong Jin, Graeme L. Hammer, and David B. Lobell. 2019. "Water Use Efficiency as a Constraint and Target for Improving the Resilience and Productivity of C3 and C4 Crops." *Annual Review of Plant Biology* 70 (1): 781–808.

Li, Hongyan, Yuming Yang, Hengyou Zhang, Shanshan Chu, Xingguo Zhang, Dongmei Yin, Deyue Yu, and Dan Zhang. 2016. "A Genetic Relationship between Phosphorus Efficiency and Photosynthetic Traits in Soybean As Revealed by QTL Analysis Using a High-Density Genetic Map." *Frontiers in Plant Science* 7 (June): 924.

Lim, Junsub, Chae Woo Lim, and Sung Chul Lee. 2020. "Pepper Novel Serine-Threonine Kinase CaDIK1 Regulates Drought Tolerance via Modulating ABA Sensitivity." *Frontiers in Plant Science* 11 (July): 1133.

Liu, Xiaolei, Meng Huang, Bin Fan, Edward S. Buckler, and Zhiwu Zhang. 2016. "Iterative Usage of Fixed and Random Effect Models for Powerful and Efficient Genome-Wide Association Studies." *PLoS Genetics* 12 (2): e1005767.

Long, Stephen P., Xin-Guang Zhu, Shawna L. Naidu, and Donald R. Ort. 2006. "Can Improvement in Photosynthesis Increase Crop Yields?" *Plant, Cell & Environment* 29 (3): 315–30.

Lopez, Miguel Angel, Alencar Xavier, and Katy Martin Rainey. 2019. "Phenotypic Variation and Genetic Architecture for Photosynthesis and Water Use Efficiency in Soybean (Glycine Max L. Merr)." *Frontiers in Plant Science* 10 (May): 680.

Lü, Haiyan, Yuming Yang, Haiwang Li, Qijia Liu, Jianjun Zhang, Junyi Yin, Shanshan Chu, et al. 2018. "Genome-Wide Association Studies of Photosynthetic Traits Related to Phosphorus Efficiency in Soybean." *Frontiers in Plant Science*. https://doi.org/10.3389/fpls.2018.01226.

Makino, Amane. 2011. "Photosynthesis, Grain Yield, and Nitrogen Utilization in Rice and Wheat." *Plant Physiology* 155 (1): 125–29.

Monteith, J. L. 1994. "Validity of the Correlation between Intercepted Radiation and Biomass." *Agricultural and Forest Meteorology* 68 (3): 213–20.

Monteith, J. L., and C. J. Moss. 1977. "Climate and the Efficiency of Crop Production in Britain." *Philosophical Transactions of the Royal Society of London* 281 (980): 277–94.

Montes, Christopher M., Carolyn Fox, Álvaro Sanz-Sáez, Shawn P. Serbin, Etsushi Kumagai, Matheus D. Krause, Alencar Xavier, et al. 2022. "High-Throughput Characterization, Correlation, and Mapping of Leaf Photosynthetic and Functional Traits in the Soybean (Glycine Max) Nested Association Mapping Population." *Genetics* 221 (2). https://doi.org/10.1093/genetics/iyac065.

Mourtzinis, Spyridon, James E. Specht, Laura E. Lindsey, William J. Wiebold, Jeremy Ross, Emerson D. Nafziger, Herman J. Kandel, et al. 2015. "Climate-Induced Reduction in US-Wide Soybean Yields Underpinned by Region- and in-Season-Specific Responses." *Nature Plants*. https://doi.org/10.1038/nplants.2014.26.

Ort, Donald R., Sabeeha S. Merchant, Jean Alric, Alice Barkan, Robert E. Blankenship, Ralph Bock, Roberta Croce, et al. 2015. "Redesigning Photosynthesis to Sustainably Meet Global Food and Bioenergy Demand." *Proceedings of the National Academy of Sciences of the United States of America* 112 (28): 8529–36.

Pearcy, Robert W., John S. Roden, and John A. Gamon. 1990. "Sunfleck Dynamics in Relation to Canopy Structure in a Soybean (Glycine Max (L.) Merr.) Canopy." *Agricultural and Forest Meteorology* 52 (3): 359–72.

Pritchard, J. K., M. Stephens, and P. Donnelly. 2000. "Inference of Population Structure Using Multilocus Genotype Data." *Genetics* 155 (2): 945–59.

R Core Team. 2022. "R: A Language and Environment for Statistical Computing." 2022. https://www.R-project.org/.

Ray, Deepak K., Nathaniel D. Mueller, Paul C. West, and Jonathan A. Foley. 2013. "Yield Trends Are Insufficient to Double Global Crop Production by 2050." *PloS One* 8 (6): e66428.

Read, M., K. E. Hicks, P. F. Sims, and J. E. Hyde. 1994. "Molecular Characterisation of the Enolase Gene from the Human Malaria Parasite Plasmodium Falciparum. Evidence for Ancestry within a Photosynthetic Lineage." *European Journal of Biochemistry / FEBS* 220 (2): 513–20.

Rippey, Bradley R. 2015. "The U.s. Drought of 2012." *Weather and Climate Extremes* 10 (December): 57–64.

Sandoval-Ibáñez, Omar, Anurag Sharma, Michał Bykowski, Guillem Borràs-Gas, James B. Y. H. Behrendorff, Silas Mellor, Klaus Qvortrup, et al. 2021. "Curvature Thylakoid 1 Proteins Modulate Prolamellar Body Morphology and Promote Organized Thylakoid Biogenesis in Arabidopsis Thaliana." *Proceedings of the National Academy of Sciences of the United States of America* 118 (42). https://doi.org/10.1073/pnas.2113934118.

Sanz-Sáez, Álvaro, Gorka Erice, Jone Aguirreolea, Fernando Muñoz, Manuel Sánchez-Díaz, and Juan José Irigoyen. 2012. "Alfalfa Forage Digestibility, Quality and Yield under Future Climate Change Scenarios Vary with Sinorhizobium Meliloti Strain." *Journal of Plant Physiology* 169 (8): 782–88.

Sanz-Sáez, Álvaro, Robert P. Koester, David M. Rosenthal, Christopher M. Montes, Donald R. Ort, and Elizabeth A. Ainsworth. 2017. "Leaf and Canopy Scale Drivers of Genotypic Variation in Soybean Response to Elevated Carbon Dioxide Concentration." *Global Change Biology* 23 (9): 3908–20.

Sharma, Anket, Vinod Kumar, Babar Shahzad, M. Ramakrishnan, Gagan Preet Singh Sidhu, Aditi Shreeya Bali, Neha Handa, et al. 2020. "Photosynthetic Response of Plants under Different Abiotic Stresses: A Review." *Journal of Plant Growth Regulation* 39 (2): 509–31.

Simkin, Andrew J., Patricia E. López-Calcagno, and Christine A. Raines. 2019. "Feeding the World: Improving Photosynthetic Efficiency for Sustainable Crop Production." *Journal of Experimental Botany* 70 (4): 1119–40.

Sinclair, Thomas R., and Thomas W. Rufty. 2012. "Nitrogen and Water Resources Commonly Limit Crop Yield Increases, Not Necessarily Plant Genetics." *Global Food Security* 1 (2): 94–98.

Song, Qijian, David L. Hyten, Gaofeng Jia, Charles V. Quigley, Edward W. Fickus, Randall L. Nelson, and Perry B. Cregan. 2013. "Development and Evaluation of SoySNP50K, a High-Density Genotyping Array for Soybean." *PloS One* 8 (1): e54985.

Tardieu, François, and Roberto Tuberosa. 2010. "Dissection and Modelling of Abiotic Stress Tolerance in Plants." *Current Opinion in Plant Biology* 13 (2): 206–12.

Tilman, David, Christian Balzer, Jason Hill, and Belinda L. Befort. 2011. "Global Food Demand and the Sustainable Intensification of Agriculture." *Proceedings of the National Academy of Sciences of the United States of America* 108 (50): 20260–64.

Van der Straeten, D., R. A. Rodrigues-Pousada, H. M. Goodman, and M. Van Montagu. 1991. "Plant Enolase: Gene Structure, Expression, and Evolution." *The Plant Cell* 3 (7): 719–35.

VanRaden, P. M. 2008. "Efficient Methods to Compute Genomic Predictions." *Journal of Dairy Science* 91 (11): 4414–23.

Wang, Jiabo, and Zhiwu Zhang. 2021. "GAPIT Version 3: Boosting Power and Accuracy for Genomic Association and Prediction." *Genomics, Proteomics & Bioinformatics* 19 (4): 629–40.

Wang, Li, Yuming Yang, Shuyu Zhang, Zhijun Che, Wenjie Yuan, and Deyue Yu. 2020. "GWAS Reveals Two Novel Loci for Photosynthesis-Related Traits in Soybean." *Molecular Genetics and Genomics: MGG* 295 (3): 705–16.

Welikhe, Pauline, Joseph Essamuah-Quansah, Kenneth Boote, Senthold Asseng, and Gamal El Afandi. 2016. "Impact of Climate Change on Corn Yields in Alabama." *Professional Agricultural Workers Journal (PAWJ)* 4 (174-2016–2193): 1–14.

Yang, Jian, Noah A. Zaitlen, Michael E. Goddard, Peter M. Visscher, and Alkes L. Price. 2014. "Advantages and Pitfalls in the Application of Mixed-Model Association Methods." *Nature Genetics* 46 (2): 100–106.

Yang, Liang, Wei Ji, Peng Gao, Yong Li, Hua Cai, Xi Bai, Qin Chen, and Yanming Zhu. 2012. "GsAPK, an ABA-Activated and Calcium-Independent SnRK2-Type Kinase from G. Soja, Mediates the Regulation of Plant Tolerance to Salinity and ABA Stress." *PloS One* 7 (3): e33838.

Yang, Yuming, Li Wang, Dan Zhang, Hao Cheng, Qing Wang, Hui Yang, and Deyue Yu. 2020. "GWAS Identifies Two Novel Loci for Photosynthetic Traits Related to Phosphorus Efficiency in Soybean." *Molecular Breeding: New Strategies in Plant Improvement* 40 (3): 29.

Zhang, Qiong, Phat Dang, Charles Chen, Yucheng Feng, William Batchelor, Marshall Lamb, and Alvaro Sanz-Saez. 2022. "Tolerance to Mid-season Drought in Peanut Can Be Achieved by High Water Use Efficiency or High Efficient Use of Water." *Crop Science* 62 (5): 1948–66.

Zhu, Xin-Guang, Stephen P. Long, and Donald R. Ort. 2010. "Improving Photosynthetic Efficiency for Greater Yield." *Annual Review of Plant Biology* 61: 235–61.
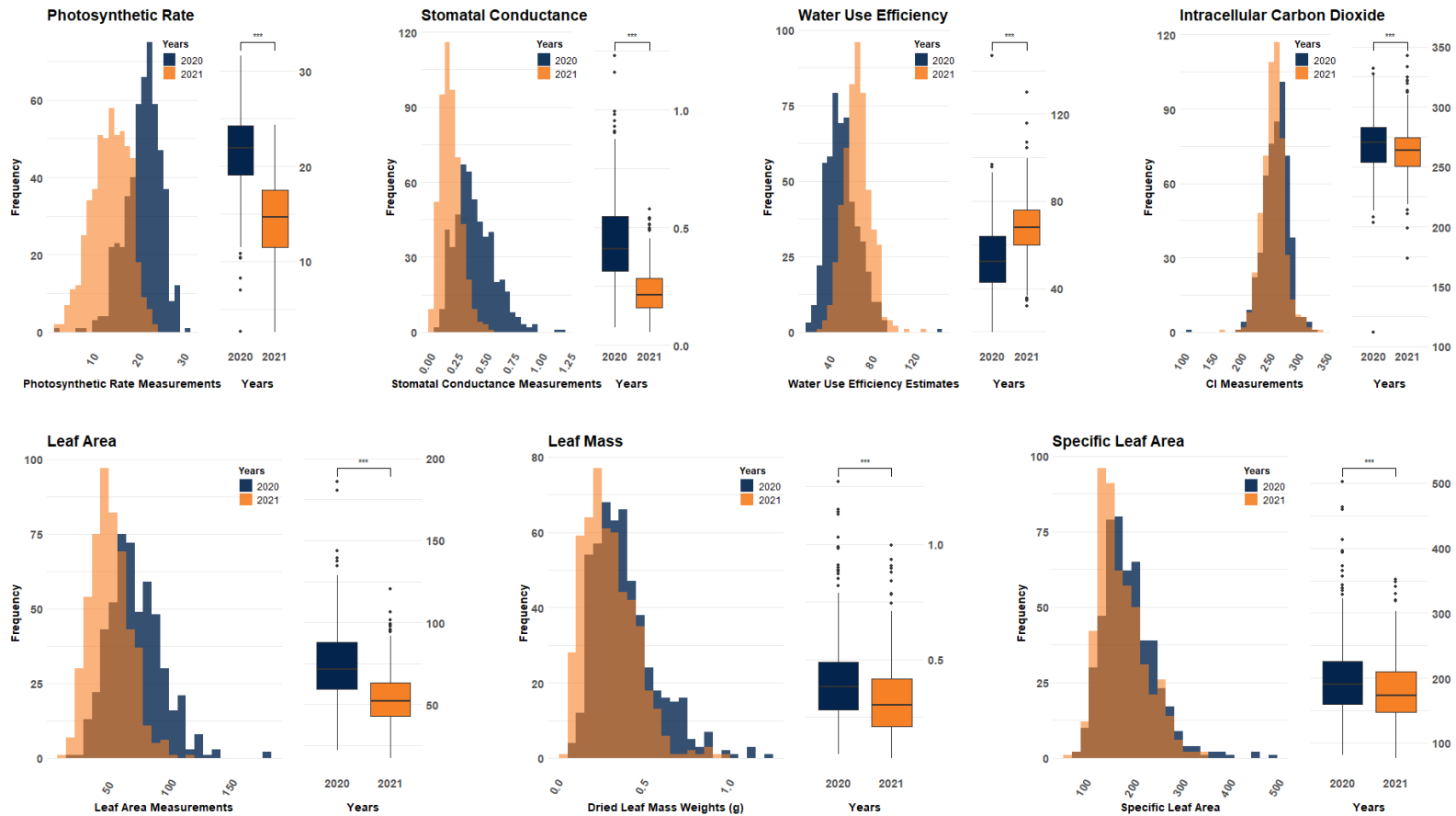
Figure 1: Histograms and boxplots demonstrating and comparing the distribution of gas exchange data (Photosynthetic rate, Stomatal conductance, Water use efficiency, and Intracellular CO_2) and leaf morphology phenotypes across years. Data for the 2020 sampling is denoted in blue, data for 2021 in orange.
N.S. = no significant difference, ** p-value < 0.01, *** p-value < 0.001
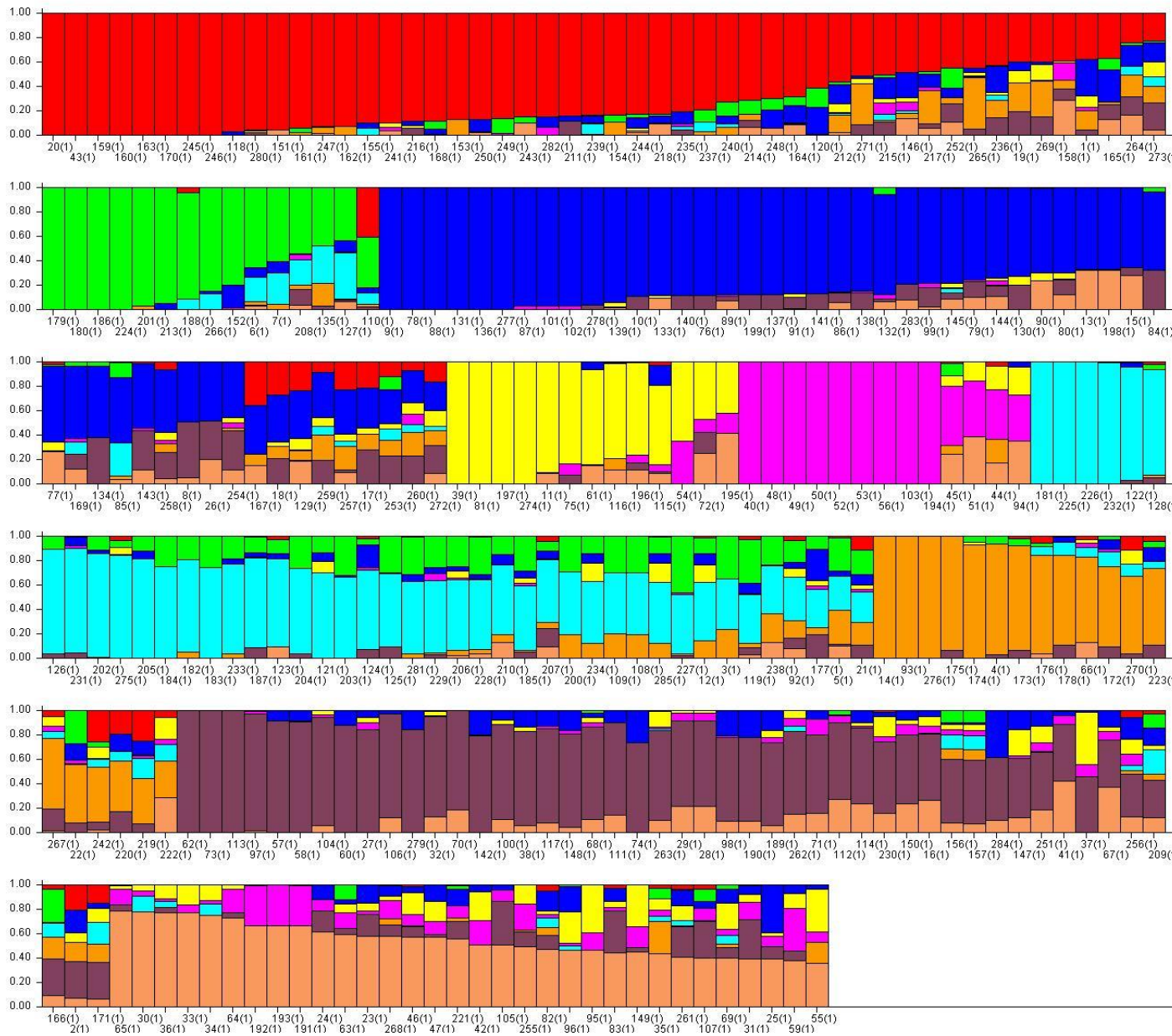
Figure 2: STRUCTURE population output denoting the genetic admixture of individuals. Every vertical bar indicates an individual and each color corresponds to one of the determined 9 subpopulations where: Red: 1, Green: 2, Blue: 3, Yellow: 4, Pink: 5, Teal: 6. Orange: 7, Brown: 8, and Terracotta: 9.

75
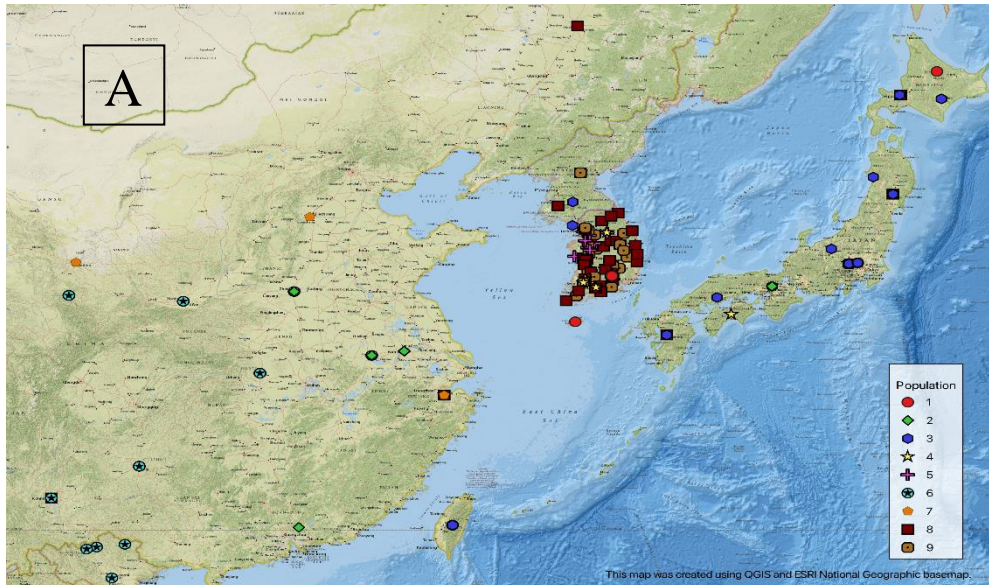
Figure 3:
A) Expansion of STRUCTURE geographic localization centered on the Korean Peninsula, Japan, and China.

B) Global map denoting sampling location of accessions and the subpopulations to which each accession belongs. Subpopulation coloration mirrors the STRUCTURE (Figure 2) where: Red Cicle: 1, Green Diamond: 2, Blue Hexagon: 3, Yellow Star: 4, Pink Cross: 5, Teal Badge: 6. Orange Pentagon: 7, Brown Square: 8, and Terracotta Squircle: 9.
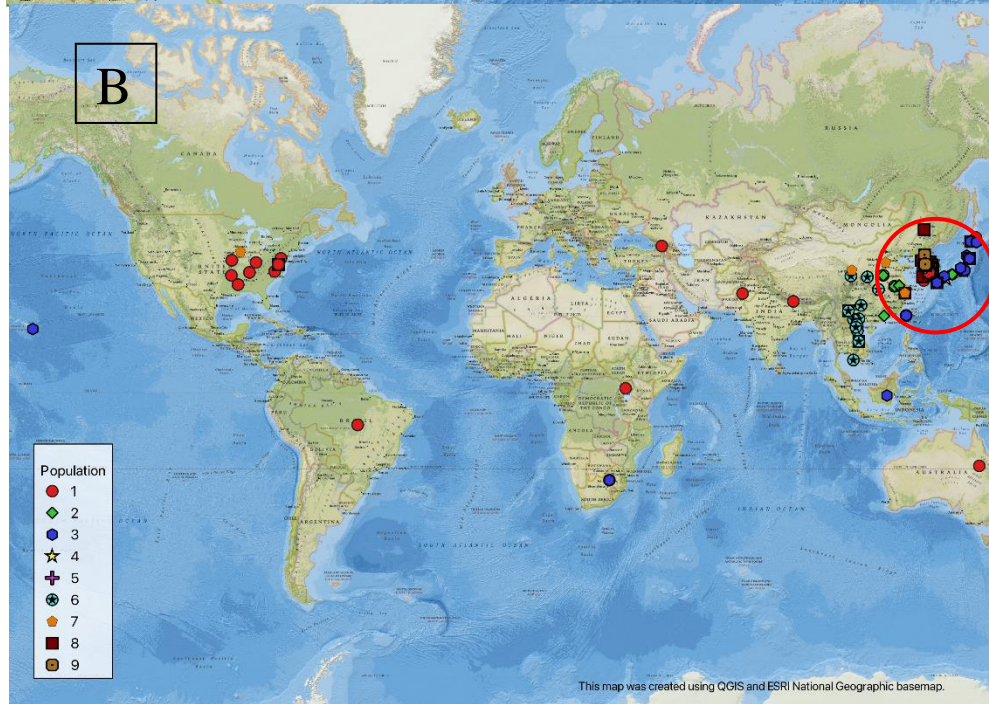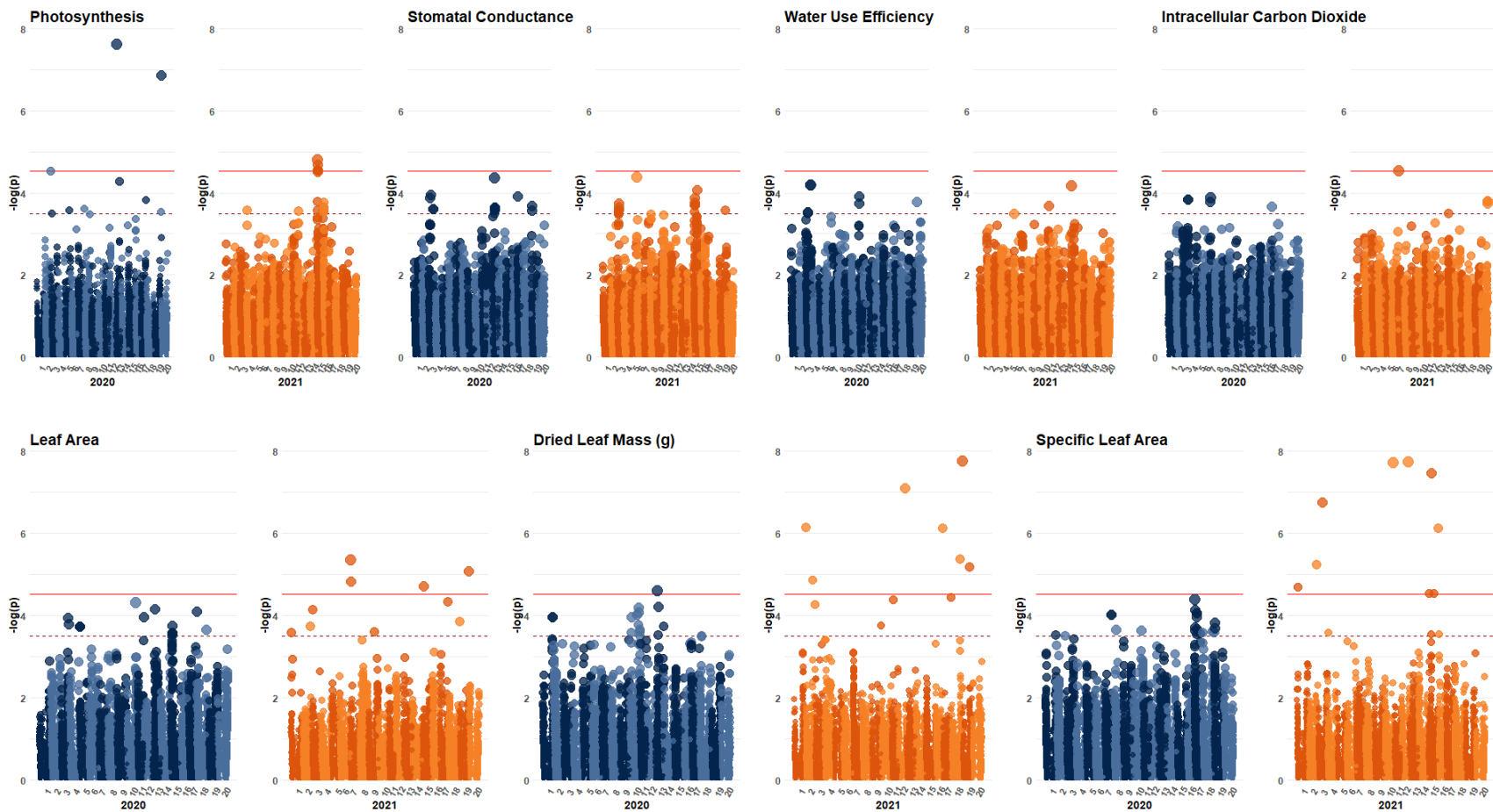
Figure 4: Manhattan plots of FarmCPU genome-wide association study (GWAS) displaying significantly associated SNPs for the seven analyzed above-ground traits with significance threshold ($-\log10 (p) \geq 4.54$), represented by a solid dark red horizontal line. A suggestive threshold of $-\log10 (p) \geq 3.5$ is demonstrated by a dashed red line.
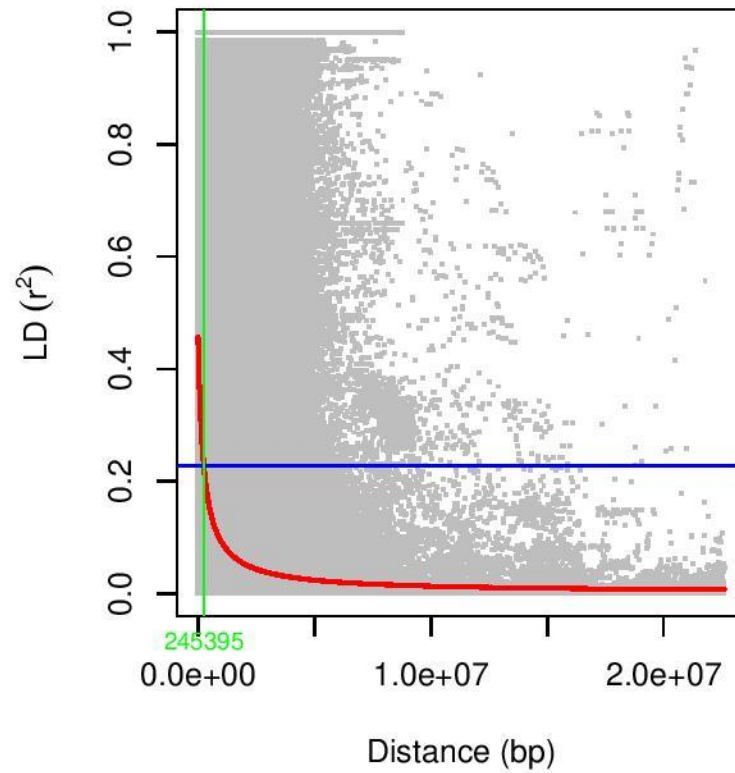
Figure 5: Genome-wide linkage disequilibrium (LD) decay rate estimated in 261 soybean accessions. The value on X- axis represents genetic distance in Kb (killo bases) and Y-axis represents the squared correlation coefficient r^2
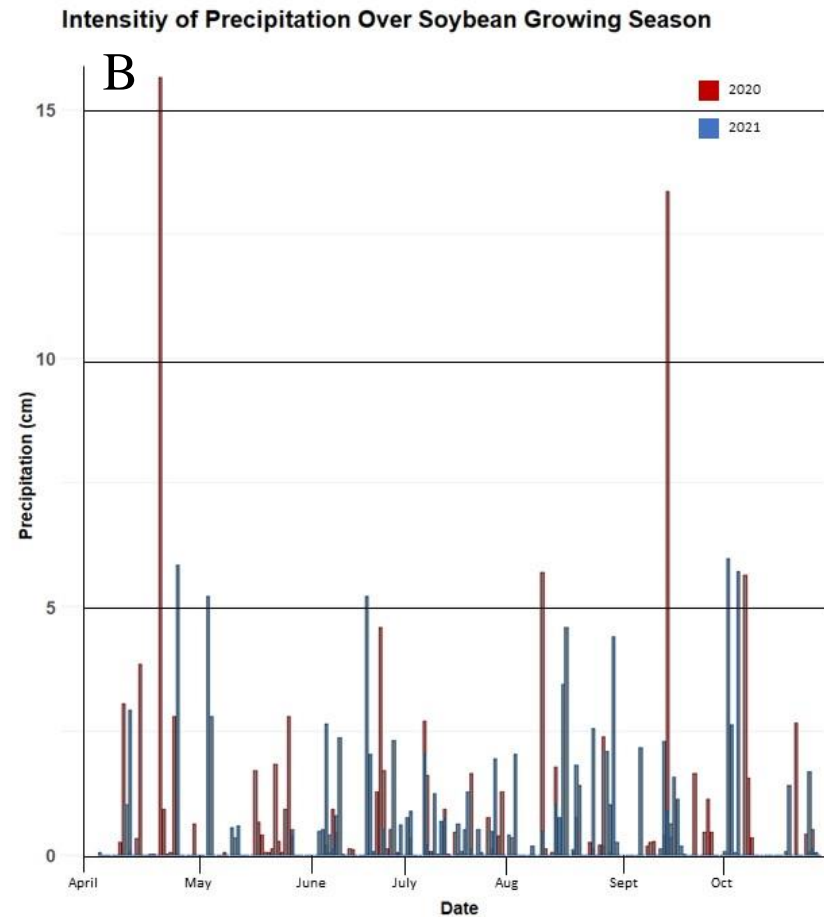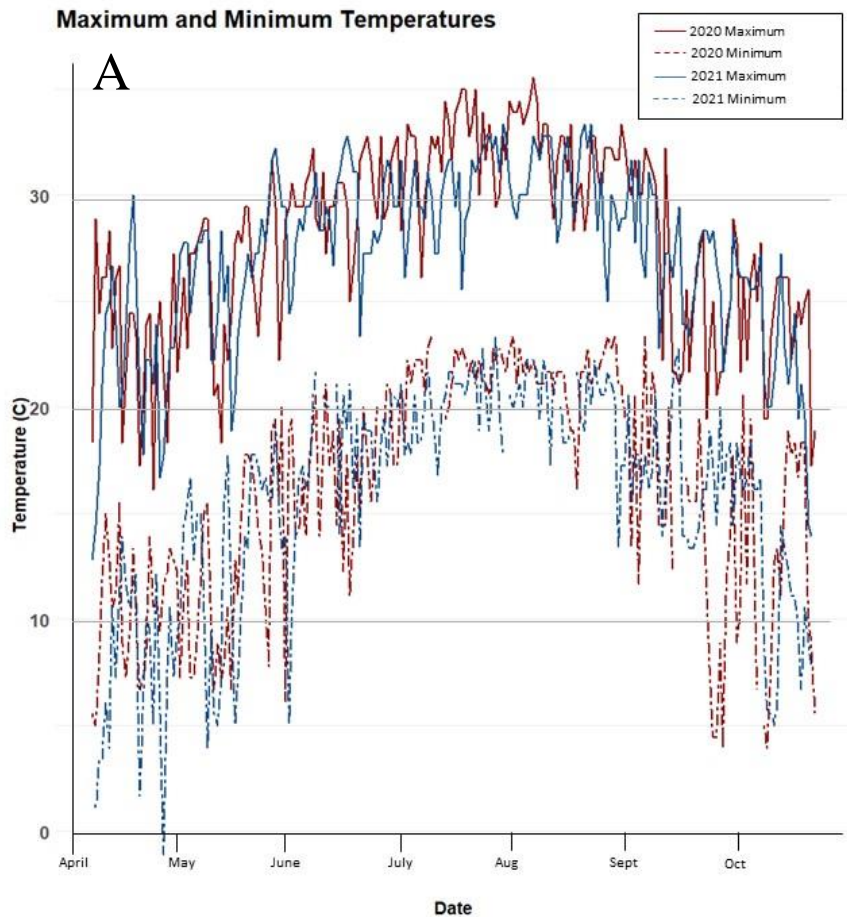
Figure 6: (A) Line graph depicting 2020/2021 growing season maximum and minimum temperatures (°C) with maximum temperature indicated by a solid line, and minimum by a dashed line. (B) Amount (cm) and time of precipitation across the 2020/2021 growing season. For both plots, 2020 data is depicted in red and 2021 in blue

79
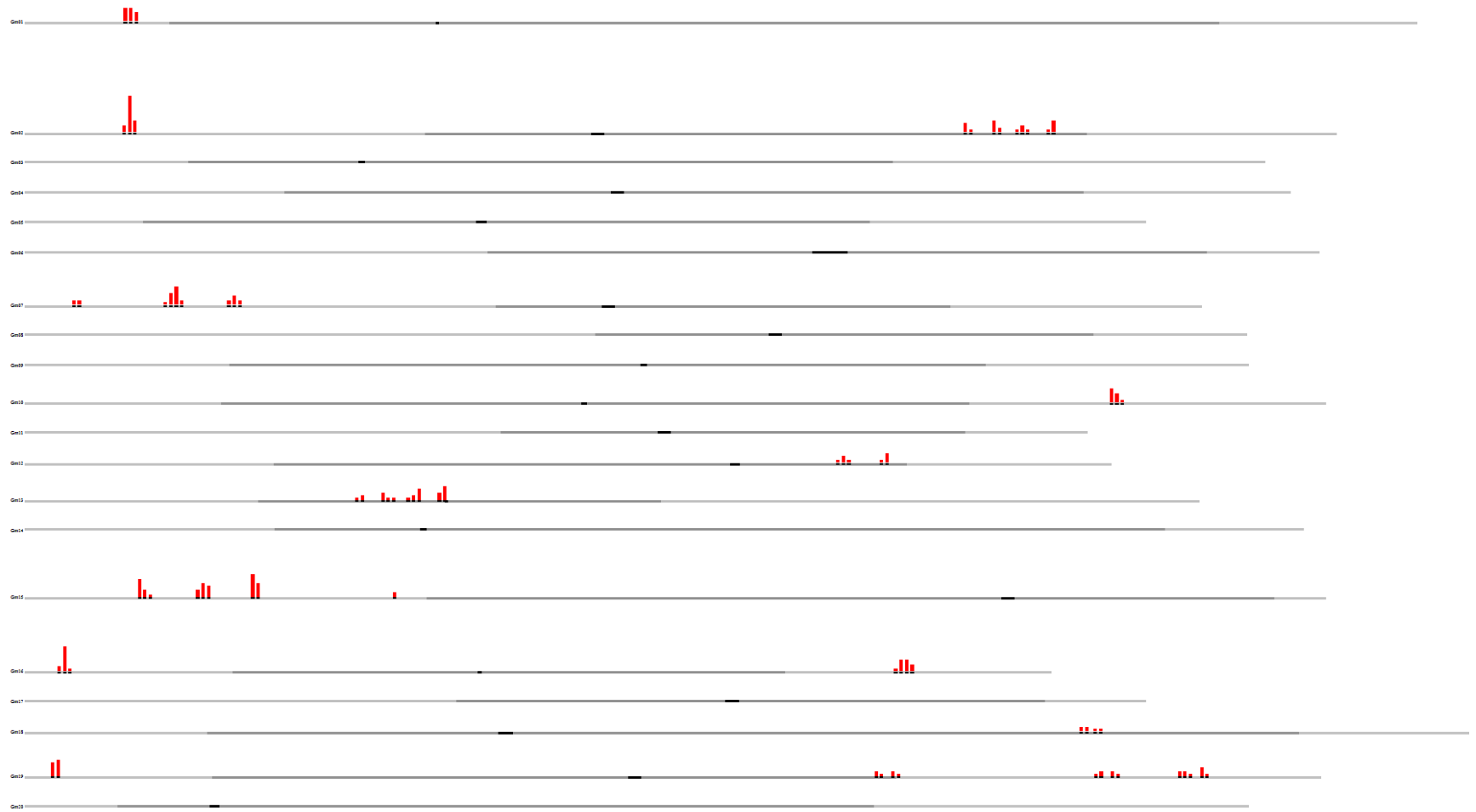
Figure 7: Localization across soybeans 20 chromosomes of determined candidate genes with photosynthetic associated predicted functions. Chromosomes are depicted by labeled horizontal lines. Genes are depicted by red vertical bars; height denotes concentration of genes. Image acquired through Soybase.

TABLE 1: MEANS AND ANOVA TABLE

		Photosynthetic Rate	Stomatal Conductance	Water Use Efficiency	Intracellular Carbon Dioxide (Ci)	Leaf Area	Dried Leaf Mass	Specific Leaf Area
RANGE	2020	2.63 - 31.6	0.075 -1.23	19.8 - 147	112 - 332	22 - 186	0.09 - 1.27	81.1 - 502
	2021	2.56 - 24.4	0.056 - 0.578	31.7 - 130	173 - 333	17.2 - 120	0.072 - 0.997	76.7 - 352
MEAN	2020	21.5	0.439	54.3	268	74.6	0.411	198
	2021	14.3	0.226	68.4	263	53.6	0.523	183
STANDARD DEVIATION	2020	3.92	0.176	15.4	22.2	22.1	0.185	56
	2021	4.144	0.092	12.933	19.714	15.996	4.582	48.022
ANOVA ~ G	Pr(>F)	***	***	***	**	***	***	***
ANOVA ~ E	Pr(>F)	***	***	***	***	***	***	***
ANOVA ~ GXE	Pr(>F)	N.S.	N.S.	N.S.	N.S.	N.S.	N.S.	N.S.

*** < .001　　** < 0.01　　* < .05　　N.S. Non-Significant

Table 2: Broad Sense Heritability

Trait	Variance Components		Heritability (H^2)
	Genotype (V_g)	Residual Error (V_e)	
Photosynthesis	5.95	6.55	0.476
Stomatal Conductance	0.005	0.009	0.361
Water Use Efficiency	38.0	96.0	0.284
Intracellular CO_2	56.15	211.35	0.210
Leaf Area	297.0	107.5	0.734
Dried Leaf Mass	0.022	0.009	0.723
Specific Leaf Area	1471.5	979.0	0.600

Table 3: Subpopulation Composition, as determined by STRUCTURE		
Subpopulation	**Number of Individuals**	**Geographic Composition**
1	48	Africa (2), Australia (1), Brazil (7), China (1), Japan (2), Georgia (1), Pakistan (2), Nepal (2), S. Korea (2), United States (28)
2	15	China (13), Japan (1), Vietnam (1)
3	52	Africa (1), Indonesia (1), Japan (45), N. Korea (1), S. Korea (1), Taiwan (1), US (2)
4	13	Japan (2), S. Korea (11)
5	12	S. Korea
6	43	China (26), Nepal (1), Vietnam (13)
7	18	China (14), Japan (1), N. Korea (1), S. Korea (2), US (1)
8	47	China (3), Japan (4), N. Korea (3), S. Korea (35), US (2), Vietnam (1)
9	33	Japan (2), N. Korea (2), S. Korea (29)

Table 4: *SNPs for which -log(p-value) > 4 .54*

		SNP	Chr	Position	*p-value*	Allele	maf	R^2
Photosynthetic Rate								
	2020	ss715582450	2	39667079	3.00E-05	C/T	0.248	0.043
	2020	ss715616744	13	16757016	2.46E-08	G/A	0.167	0.211
	2020	ss715635823	19	48331053	1.37E-07	C/A	0.369	0.086
	2021	ss715622987	15	7089421	2.07E-05	A/G	0.304	-
	2021	ss715622990	15	7121530	2.79E-05	C/T	0.313	0.061
	2021	ss715622991	15	7125085	1.60E-05	C/T	0.315	0.247
	2021	ss715622992	15	7126448	2.79E-05	T/C	0.313	-
	2021	ss715622993	15	7127877	3.11E-05	C/T	0.315	-
	2021	ss715622995	15	7133808	2.79E-05	G/A	0.313	0.497
	2020	ss715582450	2	39667079	3.00E-05	C/T	0.248	0.043
	2020	ss715616744	13	16757016	2.46E-08	G/A	0.167	0.211
Intracellular CO$_2$								
	2021	ss715598779	7	8237979	2.99E-05	A/G	0.438	0.285
Leaf Area								
	2021	ss715596785	7	2120050	1.51E-05	T/C	0.092	0.032
	2021	ss715598423	7	5999812	4.39E-06	T/C	0.406	0.020
	2021	ss715623187	15	9067087	1.91E-05	A/G	0.321	0.018
	2021	ss715635425	19	45204441	8.39E-06	C/A	0.365	0.064
Leaf Mass								
	2020	ss715617000	13	15059912	2.49E-05	C/T	0.198	0.034
	2021	ss715582534	2	4363973	7.18E-07	T/C	0.087	0.029
	2021	ss715582171	2	37286171	1.35E-05	C/T	0.073	0.032
	2021	ss715612385	12	34187459	7.86E-08	C/T	0.144	0.024
	2021	ss715624847	16	36436443	7.69E-07	A/G	0.485	0.011
	2021	ss715630900	18	44409529	4.33E-06	C/T	0.087	0.126
	2021	ss715633080	19	1232556	1.75E-08	C/T	0.079	0.115
	2021	ss715634448	19	36199222	6.81E-06	A/G	0.135	0.030
Specific Leaf Area								
	2021	ss715579441	1	4312808	2.02E-05	G/A	0.319	0.014
	2021	ss715582633	2	40666705	5.80E-06	A/G	0.106	0.047
	2021	ss715584902	3	23166713	1.77E-07	A/G	0.075	0.116
	2021	ss715607503	10	45615797	1.91E-08	A/G	0.075	0.069
	2021	ss715612385	12	34187459	1.87E-08	C/T	0.144	0.032
	2021	ss715622610	15	4955159	2.85E-05	C/T	0.260	0.044
	2021	ss715620824	15	14739216	3.35E-08	T/C	0.458	0.027
	2021	ss715621745	15	26959702	2.92E-05	C/T	0.173	0.043
	2021	ss715623488	16	1533772	7.46E-07	C/T	0.283	0.034

Year	Trait	SNP	Gene stable ID	Chr	Gene start (bp)	Gene end (bp)	Distance From SNP (bp)	GO term name
			Table 5: Selected Genes Associated with SNPs at -log (*p-value*) > 4.54					
2020	Photosynthesis	ss715582450	GLYMA_02G210800	2	39612143	39619125	-54936	dioxygenase activity
2020	Photosynthesis	ss715582450	GLYMA_02G210900	2	39627059	39627529	-40020	dioxygenase activity
2020	Photosynthesis	ss715582450	GLYMA_02G211300	2	39654528	39661365	-12551	chloroplast
2020	Photosynthesis	ss715616744	GLYMA_13G066500	13	16633758	16638992	-123258	dioxygenase activity
2020	Photosynthesis	ss715616744	GLYMA_13G068500	13	16851649	16854206	94633	oxidoreductase activity, acting on paired donors, with incorporation or reduction of molecular oxygen
2020	Photosynthesis	ss715616744	GLYMA_13G068600	13	16858723	16859438	101707	chloroplast
2020	Photosynthesis	ss715616744	GLYMA_13G068800	13	16864171	16866998	107155	defense response
2020	Photosynthesis	ss715635823	GLYMA_19G233400	19	48321642	48325912	-9411	O-acyltransferase activity
2020	Photosynthesis	ss715635823	GLYMA_19G233900	19	48360813	48367717	29760	oxidoreductase activity, acting on NAD(P)H, oxygen as acceptor
2020	Photosynthesis	ss715635823	GLYMA_19G234600	19	48443273	48450777	112220	chloroplast
2021	Photosynthesis	Photo 15 QTL	GLYMA_15G091200	15	7035032	7038022	-86498	chloroplast
2021	CI	ss715598779	GLYMA_07G089000	7	8296453	8305007	58474	vernalization response
2021	Leaf Area	ss715623187	GLYMA_15G114100	15	8999168	9001915	-67919	electron transfer activity
2021	Leaf Area	ss715623187	GLYMA_15G114600	15	9022570	9023759	-44517	chloroplast
2021	Leaf Area	ss715623187	GLYMA_15G114700	15	9024267	9025694	-42820	O-acyltransferase activity
2021	Leaf Area	ss715635425	GLYMA_19G194800	19	45215929	45223182	11488	chloroplast
2020	Leaf Mass	ss715617000	GLYMA_13G052800	13	15005141	15009623	-54771	dioxygenase activity
2020	Leaf Mass	ss715617000	GLYMA_13G052900	13	15036769	15041148	-23143	oxidoreductase activity, acting on paired donors, with incorporation or reduction of molecular oxygen
2021	Leaf Mass	ss715582534	GLYMA_02G047600	2	4376285	4379912	12312	chloroplast
2021	Leaf Mass	ss715582534	GLYMA_02G048200	2	4419899	4425822	55926	base-excision repair
2021	Leaf Mass	ss715582534	GLYMA_02G048400	2	4440520	4451775	76547	dioxygenase activity
2021	Leaf Mass	ss715582534	GLYMA_02G048600	2	4449030	4451814	85057	dioxygenase activity
2021	Leaf Mass	ss715582534	GLYMA_02G048800	2	4458411	4459296	94438	chloroplast

2021	Leaf Mass	ss715582534	GLYMA_02G049300	2	4486759	4488584	122786	chloroplast
2021	Leaf Mass	ss715630900	GLYMA_18G184000	18	44321857	44323268	-87672	chloroplast thylakoid membrane
2021	Leaf Mass	ss715630900	GLYMA_18G184700	18	44467187	44469616	57658	dioxygenase activity
2021	Leaf Mass	ss715630900	GLYMA_18G185200	18	44491574	44495271	82045	mitochondrion
2021	Leaf Mass	ss715633080	GLYMA_19G012100	19	1155711	1161298	-76845	O-acetyltransferase activity
2021	Leaf Mass	ss715633080	GLYMA_19G014000	19	1316793	1324308	84237	chloroplast
2021	Leaf Mass	ss715633080	GLYMA_19G014100	19	1325913	1333857	93357	chloroplast
2021	Leaf Mass	ss715634448	GLYMA_19G108400	19	36093430	36103823	-105792	water channel activity
2021	Leaf Mass	ss715634448	GLYMA_19G109400	19	36265902	36268445	66680	chloroplast
2021	Specific LA	ss715579441	GLYMA_01G040500	1	4380966	4383169	68158	chloroplast
2021	Specific LA	ss715582633	GLYMA_02G218700	2	40667610	40671395	905	carbohydrate metabolic process
2021	Specific LA	ss715582633	GLYMA_02G218900	2	40692221	40695776	25516	
2021	Specific LA	ss715582633	GLYMA_02G219100	2	40700534	40701497	33829	chloroplast
2021	Specific LA	ss715607503	GLYMA_10G225800	10	45629065	45639027	13268	chloroplast
2021	Specific LA	ss715612385	GLYMA_12G180500	12	34086463	34090398	-100996	chloroplast membrane
2021	Specific LA	ss715612385	GLYMA_12G181800	12	34248924	34251406	61465	chloroplast
2021	Specific LA	ss715622610	GLYMA_15G064300	15	4885565	4887727	-69594	chloroplast
2021	Specific LA	ss715622610	GLYMA_15G064600	15	4911276	4911875	-43883	oxidoreductase activity, acting on NAD(P)H
2021	Specific LA	ss715622610	GLYMA_15G064700	15	4918630	4921488	-36529	oxidoreductase activity, acting on NAD(P)H
2021	Specific LA	ss715623488	GLYMA_16G017500	16	1553689	1556564	19917	dioxygenase activity
2021	Specific LA	ss715623488	GLYMA_16G017600	16	1564173	1566310	30401	chloroplast thylakoid membrane
2021	Specific LA	ss715623488	GLYMA_16G018500	16	1643418	1648032	109646	chloroplast
* "-" denotes that the SNP is located downstream of the gene start								

Chapter 3:
Simply Root-ine: Genome-wide Association Identification of Root System Architecture Traits in soybean *Glycine Max*

Abstract

For plants, roots serve as the connection point between the energy-providing sun and the necessary resources below ground. In soybean, root functions include communication, biological nitrogen fixation, and nutrient and water uptake. Although, given their important functions, roots are an underutilized avenue of research. This is due, in part, to the environmental impact on structure formation and the laborious process of root sampling, particularly in field conditions. This project seeks to progress scientific knowledge pertaining to root system architecture (RSA) through the use of a subset (165 members) of Auburn soybean diversity panel in field conditions. Examination of 12 RSA traits revealed a contribution of both genetic and environmental factors to phenotypic variation, with heritabilities ranging from low to moderate across traits. Genome-wide association (GWA) determined 30 significant SNPs across 5 (number of holes, average hole size, median root diameter, root volume and average root orientation angle) of the 12 measured traits. Candidate gene mining in a 250 kb window surrounding significant markers returned 651 unique genes, including genes with compelling putative functions such as an ethylene-responsive transcription factor, matrix attachment, lateral root development, and response to water deficit.

1.   Introduction

Soybean [*Glycine max* (L.) Merr.] is an important staple crop that provides protein and oil for the food, feed, and fuel powering modern society. It is the second most produced crop globally, with yield and acres planted increasing annually (America Soybean Association 2022). However, the majority of work on soybean utilizes above-ground measurements due to challenges in measuring root phenotypes. Thus, research on below-ground phenotypes lags behind its above-ground counterpart, underutilizes the "hidden half" (Gašparíková, Mistrík, and Čiamporová 2002) of the plant, and leaves a gap in scientific knowledge.

Root type complexity, the difficulty in obtaining such measurements, and the confounding impact of soil environment on root characteristics induce reluctancy in pursuing root analysis. Phenotyping has historically been the limiting factor bottle necking progress in root system architecture (RSA) genetic studies and breeding efforts (Seethepalli et al. 2020). However, recent progress utilizing 2 and 3D imaging and non-destructive techniques have produced mechanisms of high throughput phenotyping. Furthermore, growth conditions in agar, germination plates, cloth bins, "cone-tainers", and "tube systems" have lessened the barrier of discovery for root phenotypes in controlled environments (Seck, Torkamaneh, and Belzile 2020). The harvesting of roots from field conditions is no less labor intensive than it was nearly a century ago when first pioneered by Weaver (J. E. Weaver 1925), but faster phenotyping methods and protocol standardization through the adoption of "shovelomics" enables reproducible methods of root observation (Trachsel et al. 2011; Seethepalli et al. 2020). Shovelomics has provided a high throughput method of field RSA measurement and increased the understanding of root plasticity resulting from environmental factors. These phenotyping improvements are imperative for efficiently screening for improved characteristics and for

unwinding the underlying genetic mechanisms of trait variation. Undertaking root

unsderstanding and improvement is essential, given root functions in biological nitrogen fixation,

nutrient acquisition, and water uptake (J. P. Lynch and Brown 2001; J. Lynch 1995; J. P. Lynch

2013). Therefore, their analysis has multifaceted applications in yield improvement, soil

improvement, and drought resistance.

The soybean root system architecture has three distinct components: the primary root, or

taproot; the lateral roots, or secondary roots; and tertiary growth, growth stemming from

secondary and/or other lateral root structures (Lersten and Carlson 2004). The architecture of the

root structure is modulated via growth inhibition of primary and lateral roots and by the

formation of tertiary structures (Malamy 2005; Waidmann, Sarkel, and Kleine-Vehn 2020;

Hodge et al. 2009). Quantitatively, the RSA is described and considered through the

measurement of root system components' (e.g., length of roots, number of lateral root number,

root diameter, root orientation angle, etc.) size and abundance (Seck, Torkamaneh, and Belzile

2020). In soybean, specific root morphological and anatomical traits have been reported as

adaptive mechanisms that enhance plant performance and productivity under abiotic stress

conditions (L. Song et al. 2016; Prince et al. 2020), implying root topography confers some

drought tolerance through mechanisms of drought avoidance and nutrient foraging characteristics

via root plasticity. Scientific analysis postulates that deep root systems enable soybean to acquire

water for lower soil horizons during extended droughts (C. M. Hudak and Patterson 1995;

Colleen M. Hudak and Patterson 1996), while shallow fibrous roots have been shown to aid in

rapid water absorption during periods of intense precipitation, and increased surface area for

nutrient acquisition (Abdel-Haleem, Lee, and Boerma 2011). Developing varieties with RSA

suitable for the given environment promises to be a sustainable and economical approach to increase crop nutrient efficiency and improve adaptation to stresses.

Considerable progress examining RSA traits and identifying parental types has been made in cereals and legumes. In maize (Tuberosa et al. 2011), wheat (Wasson et al. 2012), and rice (Nguyen, Babu, and Blum 1997; Prince, Beena, et al. 2015), associations of root architecture and drought resistance are well established. QTL mapping in rice has successfully applied markers in assisted breeding programs (Steele et al. 2006; Suji et al. 2012). Similarly, root growth patterns have been studied in other legumes such as common beans (Sponchiado et al. 1989; Battaglia et al. 2014), chickpeas (Manoj Kumar et al. 2019; Hashem et al. 2019), and peanuts (Luo et al. 2022). Root architecture studies in soybean have been conducted through a targeted breeding paradigm. Deep rooting and root elongation (Taylor et al.1978; Kaspar et al.1984, Manavalan et al., 2015) and lateral root production (Read and Bartlett, 1972) studies have determined high-throughput phenotyping techniques and cultivars suited for tailored breeding. The underlying genetic architecture of these traits is still being explored and is imperative in environment-specific breeding efficiency.

Since the turn of the century, QTLs governing root-shoot traits have been identified in soybean populations at various developmental studies in different growing conditions (R. Zhou et al. 2011; Prince et al. 2013; Liang et al. 2014; Manavalan et al. 2010, 2015; Prince, Song, et al. 2015; Chen et al. 2021). However, the majority of the studies identifying markers and loci occur in curated cultivar populations or in recombinant inbred lines with the goal of introgression breeding. Research utilizing diversity populations includes the works of Abdel-Haleem(Abdel-Haleem, Lee, and Boerma 2011), Seck (Seck, Torkamaneh, and Belzile 2020), Mandozai (Mandozai et al. 2021), and Dhanapal (Dhanapal et al. 2020). Leveraging diversity collections is

important in understanding the breadth of variation in root traits. Studies in field conditions are even less numerous due to the practical constraints of root trait selection in uncontrolled conditions. However, the field condition studies are more accurate portrayals of biotic and abiotic stress conditions, providing invaluable information on cultivar performance. The limited work in field studies has, nonetheless, produced alluring QTLs to consider, including 8 loci associated with overall complexity, 3 with taproot definition (Dhanapal et al. 2020), and 5 identified for root score (Abdel-Haleem, Lee, and Boerma 2011). To our knowledge, only Dhanapal et al. (2020) have performed marker-trait associations utilizing a diversity panel in field studies. Dhanapal utilized a 289-member diversity collection of maturity group IV individuals to examine topsoil RSA traits, primarily lateral root density, angle, and number, determining 246 SNPs denoting 67 loci. Identifying adaptive topsoil traits is a vital approach to gleaning insight into the genetic factors contributing to shallow root formation and orientation, as these traits have strong implications in nutrient foraging. This project seeks to address the weakness of limited published research on diverse genotypes in variable conditions through the assessment of RSA in totality by utilizing 165 maturity group V members of the Auburn Soybean Diversity Panel (ASDP) in field conditions. The goal of such a project seeks to improve the understanding of the biological variation of root traits related to water and nutrient uptake as banks of genetic diversity with which breeding programs can expand their genetic reservoirs and provide markers and cultivars with drought tolerance.

2. Materials and Methods

2.1 Plant Material

The ASDP is a 281-member panel of maturity group V soybean cultivars. These lines were selected on several phenotypes, including oleic content, lodging, oil and protein content, growth type, and shattering. Panel composition includes representatives from breeding, landrace, and elite cultivars; it aims to establish a panel through which to explore the genetic diversity of the USDA Soybase germplasm for stakeholder-driven phenotypes. The ASDP was previously utilized in a genome-wide association study examining the endogenous variation and potential markers of traits related to gas exchange and photosynthesis with the dualistic intent of identification of higher-yielding and drought-tolerant tendencies.

During the 2021 and 2022 growing seasons, the ASDP was planted in 2x3m replicate irrigated plots at the plant breeding unit (PBU) of Auburn University, Tallassee, AL. (32.4967° N, 85.8905° W). Plots were planted in May (5-7-2021 & 5-10-2022) and harvested via combine in the following October (10-25-2021, 10-19-2022). Root samples were taken at the R6 growth stage, to maximize root maturity prior to root decomposition, approximately the first week of September in the respective year (August 27-September 6, 2021, September 3-5, 2022). Root harvest occurred in plots where more than 50% of the plot germinated and established; Failure to surpass this check resulted in non-sampling. Root harvesting was performed by "shovelomic" methods (Trachsel, 2011; Seethepalli et al., 2020). Briefly, above-ground biomass was removed to a 10 cm stem. A shovel was inserted into the earth, and a circle was cut in an approximately 14 cm radius around the exposed stem. The shovel was then used as a lever to lift the root from the soil. Loose sand and silt were removed from the sample through vigorous agitation. Samples were placed in appropriately labeled 28.72 cm x 25.4 cm x 2.6 mil sealable clear plastic bags.

These samples were placed in cold storage (4 °C), for a maximum of a week, until image phenotyping could occur. A total of 165 individuals from the ASDP were consistently examined each year for root architecture traits and thus used for further GWAS analysis.

2.2 Phenotyping

Root phenotyping was performed via imaging, as described in Seethepalli et al. (2020). Briefly, a high-contrast imaging lightbox was constructed utilizing a 61 cm × 122 cm LED edge-lit flat panel light (Anten, 40 watts, 6000 K light color) affixed to the back of the imaging box. The backlit design enables near-binary images. In modification to the original Seethepalli hardware construction, five Basler (Basler acA3800-um, Graftek Imaging, Inc., Austin, TX) cameras were arranged along a front cross bar so that 120 degrees of the root was imaged. Cameras were placed 75 cm from the sample and focused on the root crown. To image a root crown, a root was placed into a spring clamp holder, placed inside the imaging box, and imaged using the RhizoVision Imager with gain, gamma, and exposure adjusted appropriately for high-resolution, high-contrast images. Cameras were controlled via a Jupyter command script. Jupyter is a popular web application to create, share, and utilize code.

Quantitative analysis of root images was performed using RhizoVision Explorer v2.0.3 in batch (Seethepalli et al. 2020). Whole roots were measured, and root diameters were categorized into four bins (<2 mm, 2-5 mm, 5-10mm, and >10mm). Irregular edges were smoothed at value = 4, and minimization of non-existent lateral structure was accounted for using root prune = 10. Image alterations are performed based on the Ramer-Douglas-Puecker algorithm, which enables the manual correction of the model to account for different hardware designs. Here that distance measurement was calculated to be 10.9008 pixels per mm.

RhizoVision measures or calculates 27 root phenes, 12 are discussed in this study. The 12 phenotypes discussed were selected for their implication in overall root architecture. The other 15 measurements are either variations on the traits selected here, for example, average root diameter, root width, and/or root depth, or discuss traits in a narrower perspective, for example steep and shallow angle frequency. The median number of root tips is counted within the RhizoVision software via horizontal scans and the binary pixel value transitions. Median number of root tips is indicative of the overall architecture by providing insight to the localization of growth. For example, do tertiary roots grow from a few select lateral roots, or do they disperse across many? The total number of root tips is determined via the counting of each pixel in the skeletonized root image. Total number of roots is descriptive of the complexity of the below-ground biomass. Width-to-Depth ratio provides information on the shallowness and/or depth of the root system and has implications on the ability of an architecture to rapidly absorb nutrients and/or "dig deep" for resources. It is calculated by determining the maximum width and depth of the image. Width-to-depth ratio was selected rather than width or depth individually as a way to estimate the shape of the below ground biomass. Utilization of this metric has the added benefit of being more resilient to hardware limitations, for example, limitations to depth due to imaging box height. Network Area, similar to the total number of root tips, gives insight into the complexity of the root structure and has implications on a plant's ability to forage for nutrients and water. Perimeter provides further information on the overall root network is calculated ad the total Euclidean distance of pixels in the segmented image. The median diameter is calculated by computing the distance between pixels within the skeletonized image and the nearest non-root pixel. Median root diameter assumes a circle, a potential flaw when examining organic structures. Median diameter was selected as a phenotype due to the relationship of vascular

93

thickness and the rapidity of uptake, the reasoning here being that increased median diameter could potentially result in speedier, and thus greater, acquisition (Goss et al. 1993). Both volume and surface area are calculated traits utilizing the determined root diameter. These measurements have connotations on the surface area in which a plant connects with soil, the extent of below-ground biomass, and, in the case of volume, the rapidity of uptake. The number of holes and hole size do not directly characterize the roots, but imply the complexity of the root system. RhizoVision calculates holes and holes size by determining the disconnect between components. The more numerous the holes and smaller the hole size, the more lateral and tertiary structures overlap, indicating root complexity. Lastly, mean root orientation, or the average angle at which roots grow, was selected due to the implications root orientation has on foraging capabilities.

2.4 Phenotypic Statistics

Descriptive statistics, such as mean, median, sample error, and standard deviation, were performed using base R (R Citation) on all 12 measured and calculated phenotypes. Due to strong non normality, data was transformed utilizing a log transformation. Analysis of variance (ANOVA) for genotype, environment, and genotype x environment interaction was performed as a mechanism to analyze the influence of factors on phenotypic expression. Pearson's correlation coefficient within and across years was performed to determine the intrarelationship of traits. Pearson's, as opposed to Spearman's, was utilized as raw values of phenotypic measurement rather than ranked values were better suited to the data. Broad sense heritability was calculated utilizing the equation $H^2=V_g/(V_g+V_e)$, where V_g is the genetic variance and V_e is the variance of error of the residual.

2.4 Genetic Analysis

Genetic data for this project was generated by Song et al. (Q. Song et al. 2013) and is publicly available for download on Soybase (https://www.soybase.org/snps/). For GWAS, principal component analysis (PCA) equals 4 was utilized to account for population structure within the model. PCA level was determined by examining eigenvalue and Bayesian information criterion (BIC) values. Relatedness of individuals within subpopulations is accounted for in GWAS studies using kinship matrices (K), calculated here using the VanRaden method (VanRaden 2008).

Genome association analysis was performed in GAPIT (version 3) (Wang and Zhang 2021) employing the Fixed and Random Circulating (FarmCPU) model (Liu et al. 2016). The mechanism of iterative application of fixed and random cofactors has been determined in previous studies (Jason Gilman) to provide superior statistical power, suppression of confounding errors, and limited false positives. Association significance was determined at an initial threshold of -log10 (p-value) > 3.5 but was adjusted to a more stringent -log10 (p-value) > 4.54, 1/n, where is the number of SNPs used in analysis as reported in Yang 2014 (J. Yang et al. 2014).

Linkage disequilibrium (LD) provides a calculation to estimate the window in which there is a probability of an identified marker segregating with adjacent markers, structural variants, and genes. This estimation was here calculated using TASSEL (Bradbury et al. 2007) and used to determine a window through which to mine candidate genes. Plant Ensembl (https://plants.ensembl.org/biomart/martview/) was used to search for candidate genes in a 250 kb window (125000 bp up and downstream) of significantly determined SNPs. Putative gene function was determined from Soybase.

3.   Results and Discussion

3.1 Descriptive Statistics

Phenotypic information was unbalanced across years, as evident in histograms in which frequency peaks for 2022 data are consistently lower than 2021 **(Figure 1)**. This is due to the maintenance requirement of representation in three of the four plots across years. Field grow outs in 2022 had lower germination rates and less established plots, thus, less sampling. However, even though frequency was lesser, distribution across years was consistent and near normal. Distribution skews in median diameter, volume, and hole size phenotypes are the exception with representation outside the norm. The mirrored distributions of median diameter and volume is unsurprising given the derived nature of volume from median diameter. The skew of hole size is unexpected given the distribution of number of holes across years. Mean values of hole size and hole number indicate that roots in the 2022 season have more numerous, but smaller holes. The right tails of median diameter, volume, and hole size are caused by a few individuals who have larger hole size and median diameters. A noted (unpublished Abendroth, 2022) root-knot nematode infestation could cause these observations; nematode infestation is known to thicken roots and cause a decrease in lateral root formations, resulting in larger diameters and larger hole size (Bridge et al. 1980). The skew of data results in a non-normal distribution of measurements, as demonstrated in Shapiro Wilks normality test. Normality is an assumption of GWA analysis, as deviations from normality increase the amount of type 1 errors (Sitlani et al. 2021). Utilization here of the FarmCPU methodology and consideration of significance at a stringent threshold of - log > 4.54, and alleviate the concern of false positives.

Year effect has significant variation (p <.001), denoted in the respective boxplots for all traits except projected surface area, estimated network area, and width-to-depth ratio **(Figure 1)**.

These three traits are particularly prone to error, with limitations in depth measurement by imaging box height restrictions, and by unintentional destruction lateral root structures in root harvesting. The hypothesis of error resulting in non-significant differences of means for projected surface area, estimated network area, and width-to-depth ratio is supported by ANOVA results in which all phenotypes have significant (p<.05) variation attributed to environment. The contradiction of ANOVA and means variations results in conclusions of error. All twelve traits also had a significant (p<.05) contribution of genotype to variation. This indicates that all twelve of our traits have, to some extent, transference of phenotype across generations. This was calculated through heritability, which ranged from low (16%, average root orientation) to moderately high (78%, median root diameter). The validity of the high heritabilities calculated for median root diameter and volume is questioned based on significant (p < .00001) attribution of genotype by year interaction.

Comparison of measured means and ranges to previously published values, total number of roots and root diameter (Seck et al. 2020), and root surface area and volume (Prince et al. 2020) demonstrate significant difference. However, although these phenotypic measurements are comparable, the growth stage at which they were measured are dramatically different, disabling the ability for direct comparison. Accurate juxtaposition of the root characteristics of the ASDP to other studied populations will require root crown measurements at an earlier growth stage. The most analogous study, in terms of growing conditions, population composition, and growth stage at measurement, with which to compare results of this study would be Dhanapal, however, measurements taken do not offer ready parallels due to Dhanapal's measurement of shallow root traits.

3.2 Marker Trait Associations and Candidate Gene Mining

In the previous analysis using the ASDP, population structure was accounted for in GWAS using PCA=5. Here, Q was accounted for using PCA=4, collapsing population structure. Since population structure is considered dependent on population size, this is unsurprising given there were 89 fewer individuals included in this analysis compared to the previous one. Consequently, the calculated linkage disequilibrium also diminished from 245,395 bp to 215,466 bp. SNPS within 200,000 bp of each other are, thus, in LD and considered as a single locus in this study.

Using FarmCPU, at an established threshold of $p < 0.000029$, 30 unique SNP were significantly associated with different parameters of root architecture (**Figure 3, Table 3**). Examining the 30 returned SNPs in totality, 17 markers were significant in 2021, and 13 occurred in 2022. These markers were found on all but chromosomes 1,6, 11, 14, and 19. Associations at this threshold were only found for 5 phenotypes (hole size, number of holes, median diameter, average root orientation, and volume) of the 12 analyzed. Implications of these phenotypes suggest a markers for root complexity, indicated by hole number and hole size, in the rapidity of uptake, suggested by hits associated with median diameter and volume, and in foraging capabilities as discussed when considering root orientation. There were no significant MTAs shared across the years. This is not unforeseen given the established impact of environment on root architecture and of root plasticity on RSA. The impact of environment is further surmised by the significant impact of environment on variance, as determined by ANOVA. If FarmCPU data is examined for significance using a lower (-log(pvalue) > 3.5 threshold) 212 MTAs are returned. 111 occur in 2021 and 101 occur in 2022. Cumulatively, these markers span all 20 chromosomes, and have returns for all 12 of the analyzed phenotypes as follows: Median number of roots-11, Total number of roots-20, Total root length-6, Width-to-

Depth ratio-15, Network area-16, Median root diameter-18, Root structure perimeter-9, Root volume-23, Projected surface area-17, Number of holes-13, Average hole size-28, Average root orientation angle-36. A number of these SNPs are nonunique and occur associated to multiple phenotypes within a year. For example, ss715594876 (Chr. 6, Pos. 48,364,034) was found to be associated with network area, total number of roots, total root length, and perimeter. Given that total root number is highly correlated with total root length (2021: 0.906, 2022: 0.94), network area (2021: 0.919, 2022: 0.92), and perimeter (2021: 0.943, 2022: 0.937), significant hits associated with all four are unsurprising. This phenomenon of SNP association with multiple phenotypes is also present in literature (Dhanapal et al. 2020). However, even at a laxer threshold, no SNPs are returned as significant across years.

In 2021, the 15 unique markers identified occurred on chromosomes 2,3,4,8,9, 12, 15, 17, 18, and 20. This includes MTAs identified for median root diameter on chromosomes 4, 9,15,17,18 and 20. The total phenotypic variance explained by median root diameter associated markers was 38%, with the largest contributor being the previously discussed marker on chromosome 17. A singular marker for hole size (ss715626472, r2=1.35%) on chromosome 17 was identified in 2021. Three markers for root orientation were also identified, and are in LD with each other, thus considered as a single locus. This locus cumulatively explains 3% of phenotypic variance with markers ss715599977 and ss715599978 contributing nothing to explain the variance. This is perhaps expected given the minor contribution of genotype and the strong attribution of environment on root orientation, as determined by ANOVA. Also identified in 2021 were the only markers associated with volume in this study. There were 6 markers associated with volume across 6 chromosomes, cumulatively these markers explain 62% of the

99

phenotypic variance with ss715611347on chromosome explaining 22% and ss715587929

explaining 18%.

There were 13 unique MTAs determined in 2022. These MTAs are found on

chromosome 4, 5, 7, 8,10,13, 16, 17, and 18. The singular SNP for number of holes identified in

this study was ss715632868, identified on chromosome 7. This SNP contributed 11% to the

phenotypic variance explained but has a maf < 10% making it an in optimal candidate if breeding

for number of holes. This is perhaps not too disappointing given hole size is highly correlated

with other measured phenotypes, and therefore impacted through improvement of alternative

traits. Associations with average hole size occur at two loci on chromosome 5 and 18. Loci on

chromosome 5 are denoted by a cluster of SNPs, ss715589814, ss715589980, ss715589991, &

ss715590011, however these 4 SNPs are calculated to contribute nothing to phenotypic variance

explained and ss715632868 on chromosome 18 contributed less than 1%. Interestingly, analysis

of the phenotypic variance explained by the suggestive threshold (-log(p)>3.5) determined 2

SNPs (ss715606531 & ss715606539) in linkage on chromosome 10 that explain 85% of the

variance. These suggestive SNPs are 4 Mb from a QTL previously determined for total root

length (Seck 2020). Five markers associated with median diameter were found in 2022 data. As

mentioned, one occurred on chromosome 17 in LD with another determined in 2021. The other 4

occurred on chromosomes 4, 8, 10 and 13. A diameter-associated marker on chromosome 4 also

occurred in 2021, however these markers are 32.6 Mb apart and would identify entirely different

loci. The chromosome 4 marker in 2022 explains less than 1% of the phenotypic variance

explained. In fact, all but the marker on chromosome 17 (ss715627617, R^2=6.36%) explain less

than 1%. Finally, there were 2 markers returned for association with root orientation

(ss715601704, Chr. 8 & ss715625429, Chr. 16). As with the cluster of markers identified for root

orientation in 2021, the marker here identified on chromosome 8 has negligible impact on variance; the marker on chromosome 16 explains 3%.

Although no SNP was significant across years, ss715627617 identified for median root diameter in 2022 is in LD (Δ = 105,370 bp) with marker ss715627633 associated with median root diameter in 2021. Chromosome 17 has been previously identified for potential loci pertaining to root retention in soybean sudden death syndrome (Bao 2015a) and has 5 QTLs with this denotation across the chromosome listed on Soybase. QTL "SDS root retention 1-g7" is in the closest proximity to the markers identified here, although still 30 Mb away. Candidate gene mining in the 250 kb surrounding these markers elucidates 30 genes (120 gene ontologies) in linkage. Compelling gene ontologies include those related to lateral root development (GLYMA_17G237500), response to water deprivation (GLYMA_17G238600), water transport and hyperosmotic response (GLYMA_17G239000), and calmodulin binding (GLYMA_17G239200).

GLYMA_17G237500 is a matrix attachment protein that aid in nucleic DNA scaffolding. The regulation of genetic topography is particularly important during rapid cellular replication, like that during lateral root development (Libault 2010, Harder 2000. GLYMA_17G238600 encodes for a dicer-like (DCL) protein, which has general functions in RNA biogenesis. Micro-RNA have regulatory processes in drought stress response (Shanker & Maheswari 2017). GLYMA_17G239000 is a cysteine proteinase, which has previously been determined to be upregulated in drought conditions (Simova 1020, Botha 2017). In soybean cysteine proteases are involved in the regulation nodule bacterial symbiosis and leghemoglobin degradation, resulting in the senescence of soybean root nodules. As such, cysteine proteases are early indicator of drought (Cilliers, van Wyk 2017). Finally, from these selected genes, GLYMA_17G239200

encodes for a WRKY transcription factor. WRKY TFs are the 7th largest class of transcription factors in plants and have been implicated in various biotic/abiotic stress responses (Fei Chen 2018). Another WRKY transcription factor (GmWRKY12) has been demonstrated to confer drought and salt tolerance in soybean (WY Shi et al 2018).

Utilizing the calculated LD decay, candidate genes were mined in a 250 kb window. Genes related to root development were searched around the 30 significantly associated SNP. For SNPs in LD with other markers for the trait, for example the 4 markers on chromosome 5 associated with hole size in 2022, the window was expanded to be 125 kb upstream of the most upstream identified SNP and 125 kb downstream of the furthest SNP. 651 unique gene stable IDs were returned via Plant ensembl Biomart for the 30 SNPs with pvalue<0.000029 **(Supplemental Table).** Gene start and end, gene ontology (GO) accession and description, as a measure of putative function, were then examined. Predicted functions of the 651 genes range from involvement in ATP binding, membrane components, DNA repair regulation, metal ion binding, and photosystem I assembly. Genes with projected functions localized to roots, including nodulation and hydrotropism, are of rapt importance. Following this consideration, 30 candidate genes have been selected for primary consideration (**Table**). Genes in this table are predominately involved in root hair cell differentiations, root development, and root elongation. This table has gene representation from all 5 traits that had significant SNP returns. In this table is GLYMA_17G237500, identified in linkage with a median diameter marker, whose role in matrix attachment has already been discussed. Similarly, GLYMA_16G074200, linked to root orientation associated SNP ss715625429, has a role in chromosomal condensation, an important genetic function of root development. Included is gene, GLYMA_07G086000, on chromosome 7, identified in LD with hole associated SNP ss715598725. Prince 2020 also found a compelling

QTLs, relating to root surface area, on chromosome 7. However, these loci are 7 Mb from the gene proposed here. There are two genes, GLYMA_05G037800 & GLYMA_05G038300 in this candidate gene table associated with the cluster of SNPs associated with hole size. GLYMA_05G037800 encodes for a DOF zinc finger protein, while GLYMA_05G038300 is annotated as a integral membrane inorganic anion protein. In sweet potatoes, DOF zinc finger transcription factors are preferentially expressed in storage roots. The implication of this function on root radial pattern formation, as suggested by gene ontology, is unclear. The role of an integral membrane inorganic anion protein is clearer given the role of roots to transport nutrient ions from the soil solution to the xylem vessels. There could be implications of this protein in the foraging mechanisms of root development (Tanaka et al. 2009).

4. Conclusions

The mirror distributions and correlations for measured traits and the significant contribution of genotype to phenotypic variance are promising evidence to utilize RSA as a breeding target. The calculated moderate heritabilities further support this conclusion. The identification of numerous MTAs provide the foundation for marker assisted selection. A total of 30 high confidence SNPs were associated with 5 RSA traits. Candidate gene and predicted function mining results in several compelling genes to be used in future work. The identification of genetic markers associated with root trait performance in distinct environments will be critical to strategically target and exploit root characteristics to increase crop yields and ensure cropping system sustainability

References

Abdel-Haleem, Hussein, Geung-Joo Lee, and Roger H. Boerma. 2011. "Identification of QTL for Increased Fibrous Roots in Soybean." *TAG. Theoretical and Applied Genetics. Theoretische Und Angewandte Genetik* 122 (5): 935–46.

America Soybean Association. 2022. "'A Reference Guide to Important Soybean Facts & Figures: SoyStats 2022.'" 2022. https://soygrowers.com/education-resources/publications/soy-stats/.

Bao, Yong, James E. Kurle, Grace Anderson, and Nevin D. Young. 2015. "Association Mapping and Genomic Prediction for Resistance to Sudden Death Syndrome in Early Maturing Soybean Germplasm." *Molecular Breeding: New Strategies in Plant Improvement* 35 (6): 128.

Battaglia, Marina, Carolina Rípodas, Joaquín Clúa, Maël Baudin, O. Mario Aguilar, Andreas Niebel, María Eugenia Zanetti, and Flavio Antonio Blanco. 2014. "A Nuclear Factor Y Interacting Protein of the GRAS Family Is Required for Nodule Organogenesis, Infection Thread Progression, and Lateral Root Growth." *Plant Physiology* 164 (3): 1430–42.

Botha, Anna-Maria, Karl J. Kunert, and Christopher A. Cullis. 2017. "Cysteine Proteases and Wheat (Triticum Aestivum L) under Drought: A Still Greatly Unexplored Association." *Plant, Cell & Environment* 40 (9): 1679–90.

Bradbury, Peter J., Zhiwu Zhang, Dallas E. Kroon, Terry M. Casstevens, Yogesh Ramdoss, and Edward S. Buckler. 2007. "TASSEL: Software for Association Mapping of Complex Traits in Diverse Samples." *Bioinformatics* 23 (19): 2633–35.

Bridge, J., and S. L. J. Page. 1980. "Estimation of Root-Knot Nematode Infestation Levels on Roots Using a Rating Chart." *Tropical Pest Management* 26 (3): 296–98.

Brown, E. A., C. E. Caviness, and D. A. Brown. 1985. "Response of Selected Soybean Cultivars to Soil Moisture Deficit [1]." *Agronomy Journal* 77 (2): 274–78.

Chen, Huatao, Giriraj Kumawat, Yongliang Yan, Baojie Fan, and Donghe Xu. 2021. "Mapping and Validation of a Major QTL for Primary Root Length of Soybean Seedlings Grown in Hydroponic Conditions." *BMC Genomics* 22 (1): 132.

Cilliers, Magdeleen, Stefan George van Wyk, Philippus Daniel Riekert van Heerden, Karl Josef Kunert, and Barend Juan Vorster. 2018. "Identification and Changes of the Drought-Induced Cysteine Protease Transcriptome in Soybean (Glycine Max) Root Nodules." *Environmental and Experimental Botany* 148 (April): 59–69.

Dhanapal, Arun Prabhu, Larry M. York, Kasey A. Hames, and Felix B. Fritschi. 2020. "Genome-Wide Association Study of Topsoil Root System Architecture in Field-Grown Soybean [Glycine Max (L.) Merr.]." *Frontiers in Plant Science* 11: 590179.

Gašparíková, Otília, Igor Mistrík, and Milada Čiamporová. 2002. "Waisel, Y., Eshel, A., Kafkafi, U., Eds. Plant Roots – the Hidden Half." *Annals of Botany* 90 (6): 775–76.

Harder, P. A., R. A. Silverstein, and I. Meier. 2000. "Conservation of Matrix Attachment Region-Binding Filament-like Protein 1 among Higher Plants." *Plant Physiology* 122 (1): 225–34.

Hashem, Abeer, Ashwani Kumar, Abeer M. Al-Dbass, Abdulaziz A. Alqarawi, Al-Bandari Fahad Al-Arjani, Garima Singh, Muhammad Farooq, and Elsayed Fathi Abd Allah. 2019. "Arbuscular Mycorrhizal Fungi and Biochar Improves Drought Tolerance in Chickpea." *Saudi Journal of Biological Sciences* 26 (3): 614–24.

Hodge, Angela, Graziella Berta, Claude Doussan, Francisco Merchan, and Martin Crespi. 2009. "Plant Root Growth, Architecture and Function." *Plant and Soil* 321 (1–2): 153–87.

Hudak, C. M., and R. P. Patterson. 1995. "Vegetative Growth Analysis of a Drought-Resistant Soybean Plant Introduction." *Crop Science* 35 (2): 464.

Hudak, Colleen M., and Robert P. Patterson. 1996. "Root Distribution and Soil Moisture Depletion Pattern of a Drought-resistant Soybean Plant Introduction." *Agronomy Journal* 88 (3): 478–85.

Kaler, Avjinder S., Jason D. Gillman, Timothy Beissinger, and Larry C. Purcell. 2019. "Comparing Different Statistical Models and Multiple Testing Corrections for Association Mapping in Soybean and Maize." *Frontiers in Plant Science* 10: 1794.

Kaspar, T. C., H. M. Taylor, and R. M. Shibles. 1984. "Taproot-elongation Rates of Soybean Cultivars in the Glasshouse and Their Relation to Field Rooting Depth 1." *Crop Science* 24 (5): 916–20.

Kumar, Manoj, Mohd Aslam Yusuf, Pooja Yadav, Shiv Narayan, and Manoj Kumar. 2019. "Overexpression of Chickpea Defensin Gene Confers Tolerance to Water-Deficit Stress in Arabidopsis Thaliana." *Frontiers in Plant Science* 10 (March): 290.

Lersten, Nels R., and John B. Carlson. 2016. "Vegetative Morphology." In *Agronomy Monographs*, 15–57. Madison, WI, USA: American Society of Agronomy, Crop Science Society of America, and Soil Science Society of America.

Liang, Huizhen, Yongliang Yu, Hongqi Yang, Lanjie Xu, Wei Dong, Hua Du, Weiwen Cui, and Haiyang Zhang. 2014. "Inheritance and QTL Mapping of Related Root Traits in Soybean at the Seedling Stage." *TAG. Theoretical and Applied Genetics. Theoretische Und Angewandte Genetik* 127 (10): 2127–37.

Libault, Marc, Andrew Farmer, Laurent Brechenmacher, Jenny Drnevich, Raymond J. Langley, Damla D. Bilgin, Osman Radwan, et al. 2010. "Complete Transcriptome of the Soybean Root Hair Cell, a Single-Cell Model, and Its Alteration in Response to Bradyrhizobium Japonicum Infection." *Plant Physiology* 152 (2): 541–52.

Liu, Xiaolei, Meng Huang, Bin Fan, Edward S. Buckler, and Zhiwu Zhang. 2016. "Iterative Usage of Fixed and Random Effect Models for Powerful and Efficient Genome-Wide Association Studies." *PLoS Genetics* 12 (2): e1005767.

Lynch, J. 1995. "Root Architecture and Plant Productivity." *Plant Physiology* 109 (1): 7–13.

Lynch, Jonathan P. 2013. "Steep, Cheap and Deep: An Ideotype to Optimize Water and N Acquisition by Maize Root Systems." *Annals of Botany* 112 (2): 347–57.

Lynch, Jonathan P., and Kathleen M. Brown. 2001. "Topsoil Foraging–an Architectural Adaptation of Plants to Low Phosphorus Availability." *Plant and Soil* 237 (2): 225–37.

Malamy, J. E. 2005. "Intrinsic and Environmental Response Pathways That Regulate Root System Architecture." *Plant, Cell & Environment* 28 (1): 67–77.

Manavalan, Lakshmi P., Satish K. Guttikonda, Vinh T. Nguyen, J. Grover Shannon, and Henry T. Nguyen. 2010. "Evaluation of Diverse Soybean Germplasm for Root Growth and Architecture." *Plant and Soil* 330 (1): 503–14.

Manavalan, Lakshmi P., Silvas J. Prince, Theresa A. Musket, Julian Chaky, Rupesh Deshmukh, Tri D. Vuong, Li Song, et al. 2015. "Identification of Novel QTL Governing Root Architectural Traits in an Interspecific Soybean Population." *PloS One* 10 (3): e0120490.

Mandozai, Ajmal, Abdourazak Alio Moussa, Qi Zhang, Jing Qu, Yeyao Du, Gulaqa Anwari, Noor Al Amin, and Piwu Wang. 2021. "Genome-Wide Association Study of Root and Shoot Related Traits in Spring Soybean (Glycine Max L.) at Seedling Stages Using SLAF-Seq." *Frontiers in Plant Science* 12 (July): 568995.

Nguyen, H. T., R. C. Babu, and A. Blum. 1997. "Breeding for Drought Resistance in Rice: Physiology and Molecular Genetics Considerations." *Crop Science*. https://doi.org/10.2135/cropsci1997.0011183X003700050002x.

Prince, Silvas J., Raymond N. Mutava, Camila Pegoraro, Antonio Costa de Oliveira, and Henry T. Nguyen. 2013. "Root Characters." In *Genomics and Breeding for Climate-Resilient Crops: Vol. 2 Target Traits*, edited by Chittaranjan Kole, 67–131. Berlin, Heidelberg: Springer Berlin Heidelberg.

Prince, Silvas J., Li Song, Dan Qiu, Joao V. Maldonado Dos Santos, Chenglin Chai, Trupti Joshi, Gunvant Patil, et al. 2015. "Genetic Variants in Root Architecture-Related Genes in a Glycine Soja Accession, a Potential Resource to Improve Cultivated Soybean." *BMC Genomics* 16 (1): 132.

Prince, Silvas J., Tri D. Vuong, Xiaolei Wu, Yonghe Bai, Fang Lu, Siva P. Kumpatla, Babu Valliyodan, J. Grover Shannon, and Henry T. Nguyen. 2020. "Mapping Quantitative Trait Loci for Soybean Seedling Shoot and Root Architecture Traits in an Inter-Specific Genetic Population." *Frontiers in Plant Science* 11 (August): 1284.

R Core Team. 2022. "R: A Language and Environment for Statistical Computing." 2022. https://www.R-project.org/.

Read, D. J., and E. M. Bartlett. 1972. "The Psychology of Drought Resistance in the Soy-Bean Plant (Glycine Max). I. The Relationship Between Dought Resistance and Growth." *The Journal of Applied Ecology* 9 (2): 487–99.

Rippey, Bradley R. 2015. "The U.s. Drought of 2012." *Weather and Climate Extremes* 10 (December): 57–64.

Seck, Waldiodio, Davoud Torkamaneh, and François Belzile. 2020. "Comprehensive Genome-Wide Association Analysis Reveals the Genetic Basis of Root System Architecture in Soybean." *Frontiers in Plant Science* 11 (December): 590740.

Seethepalli, Anand, Kundan Dhakal, Marcus Griffiths, Haichao Guo, Gregoire T. Freschet, and Larry M. York. 2021. "RhizoVision Explorer: Open-Source Software for Root Image Analysis and Measurement Standardization." *AoB Plants* 13 (6): lab056.

Seethepalli, Anand, Haichao Guo, Xiuwei Liu, Marcus Griffiths, Hussien Almtarfi, Zenglu Li, Shuyu Liu, et al. 2020. "RhizoVision Crown: An Integrated Hardware and Software Platform for Root Crown Phenotyping." *Plant Phenomics (Washington, D.C.)* 2020 (February): 3074916.

Shanker, Arun K., and M. Maheswari. 2017. "Small RNA and Drought Tolerance in Crop Plants." *Indian Journal of Plant Physiology* 22 (4): 422–33.

Shi, Wen-Yan, Yong-Tao Du, Jian Ma, Dong-Hong Min, Long-Guo Jin, Jun Chen, Ming Chen, et al. 2018. "The WRKY Transcription Factor GmWRKY12 Confers Drought and Salt Tolerance in Soybean." *International Journal of Molecular Sciences* 19 (12). https://doi.org/10.3390/ijms19124087.

Simova-Stoilova, Lyudmila, Irina Vaseva, Biliana Grigorova, Klimentina Demirevska, and Urs Feller. 2010. "Proteolytic Activity and Cysteine Protease Expression in Wheat Leaves under Severe Soil Drought and Recovery." *Plant Physiology and Biochemistry: PPB / Societe Francaise de Physiologie Vegetale* 48 (2–3): 200–206.

Song, Li, Silvas Prince, Babu Valliyodan, Trupti Joshi, Joao V. Maldonado dos Santos, Jiaojiao Wang, Li Lin, et al. 2016. "Genome-Wide Transcriptome Analysis of Soybean Primary Root under Varying Water-Deficit Conditions." *BMC Genomics* 17 (January): 57.

Song, Qijian, David L. Hyten, Gaofeng Jia, Charles V. Quigley, Edward W. Fickus, Randall L. Nelson, and Perry B. Cregan. 2013. "Development and Evaluation of SoySNP50K, a High-Density Genotyping Array for Soybean." *PloS One* 8 (1): e54985.

Sponchiado, B. N., J. W. White, J. A. Castillo, and P. G. Jones. 1989. "Root Growth of Four Common Bean Cultivars in Relation to Drought Tolerance in Environments with Contrasting Soil Types." *Experimental Agriculture* 25 (2): 249–57.

Steele, K. A., A. H. Price, H. E. Shashidhar, and J. R. Witcombe. 2006. "Marker-Assisted Selection to Introgress Rice QTLs Controlling Root Traits into an Indian Upland Rice Variety." *Theoretical and Applied Genetics* 112 (2): 208–21.

Suji, K. K., K. Silvas Jebakumar Prince, P. Sumeet Mankhar, P. Kanagaraj, R. Poornima, K. Amutha, S. Kavitha, K. R. Biji, S. Michael Gomez, and R. Chandra Babu. 2012. "Evaluation of Rice (Oryza Sativa L.) near Iso-Genic Lines with Root QTLs for Plant Production and Root Traits in Rainfed Target Populations of Environment." *Field Crops Research* 137 (October): 89–96.

Tanaka, Masaru, Yasuhiro Takahata, Hiroki Nakayama, Makoto Nakatani, and Makoto Tahara. 2009. "Altered Carbohydrate Metabolism in the Storage Roots of Sweetpotato Plants Overexpressing the SRF1 Gene, Which Encodes a Dof Zinc Finger Transcription Factor." *Planta* 230 (4): 737–46.

Trachsel, Samuel, Shawn M. Kaeppler, Kathleen M. Brown, and Jonathan P. Lynch. 2011. "Shovelomics: High Throughput Phenotyping of Maize (Zea Mays L.) Root Architecture in the Field." *Plant and Soil* 341 (1–2): 75–87.

Tuberosa, Roberto, Silvio Salvi, Silvia Giuliani, Maria Corinna Sanguineti, Elisabetta Frascaroli, Sergio Conti, and Pierangelo Landi. 2011. "Genomics of Root Architecture and Functions in Maize." In *Root Genomics*, edited by Antonio Costa de Oliveira and Rajeev K. Varshney, 179–204. Berlin, Heidelberg: Springer Berlin Heidelberg.

Valliyodan, Babu, Tara T. Van Toai, Jose Donizeti Alves, Patricia de Fátima P Goulart, Jeong Dong Lee, Felix B. Fritschi, Mohammed Atiqur Rahman, Rafiq Islam, J. Grover Shannon, and Henry T. Nguyen. 2014. "Expression of Root-Related Transcription Factors Associated with Flooding Tolerance of Soybean (Glycine Max)." *International Journal of Molecular Sciences* 15 (10): 17622–43.

VanRaden, P. M. 2008. "Efficient Methods to Compute Genomic Predictions." *Journal of Dairy Science* 91 (11): 4414–23.

Waidmann, Sascha, Elizabeth Sarkel, and Jürgen Kleine-Vehn. 2020. "Same Same, but Different: Growth Responses of Primary and Lateral Roots." *Journal of Experimental Botany* 71 (8): 2397–2411.

Wang, Jiabo, and Zhiwu Zhang. 2021. "GAPIT Version 3: Boosting Power and Accuracy for Genomic Association and Prediction." *Genomics, Proteomics & Bioinformatics* 19 (4): 629–40.

Wasson, A. P., R. A. Richards, R. Chatrath, S. C. Misra, S. V. Sai Prasad, G. J. Rebetzke, J. A. Kirkegaard, J. Christopher, and M. Watt. 2012. "Traits and Selection Strategies to Improve Root Systems and Water Uptake in Water-Limited Wheat Crops." *Journal of Experimental Botany* 63 (9): 3485–98.

Weaver, J. E. 1925. "Investigations on the Root Habits of Plants." *American Journal of Botany* 12 (8): 502–9.

Weaver, John Ernest. 1926. *Root Development of Field Crops*. McGraw-Hill Book Company.

Yang, Jian, Noah A. Zaitlen, Michael E. Goddard, Peter M. Visscher, and Alkes L. Price. 2014. "Advantages and Pitfalls in the Application of Mixed-Model Association Methods." *Nature Genetics* 46 (2): 100–106.

Zhou, Rong, Hai-Feng Chen, Xian-Zhi Wang, Bao-Duo Wu, Shui-Lian Chen, Xiao-Juan Zhang, Xue-Jun Wu, et al. 2011. "Analysis of QTLs for Root Traits at Seedling Stage in Soybean." *Acta Agronomica Sinica* 37 (7): 1151–58.
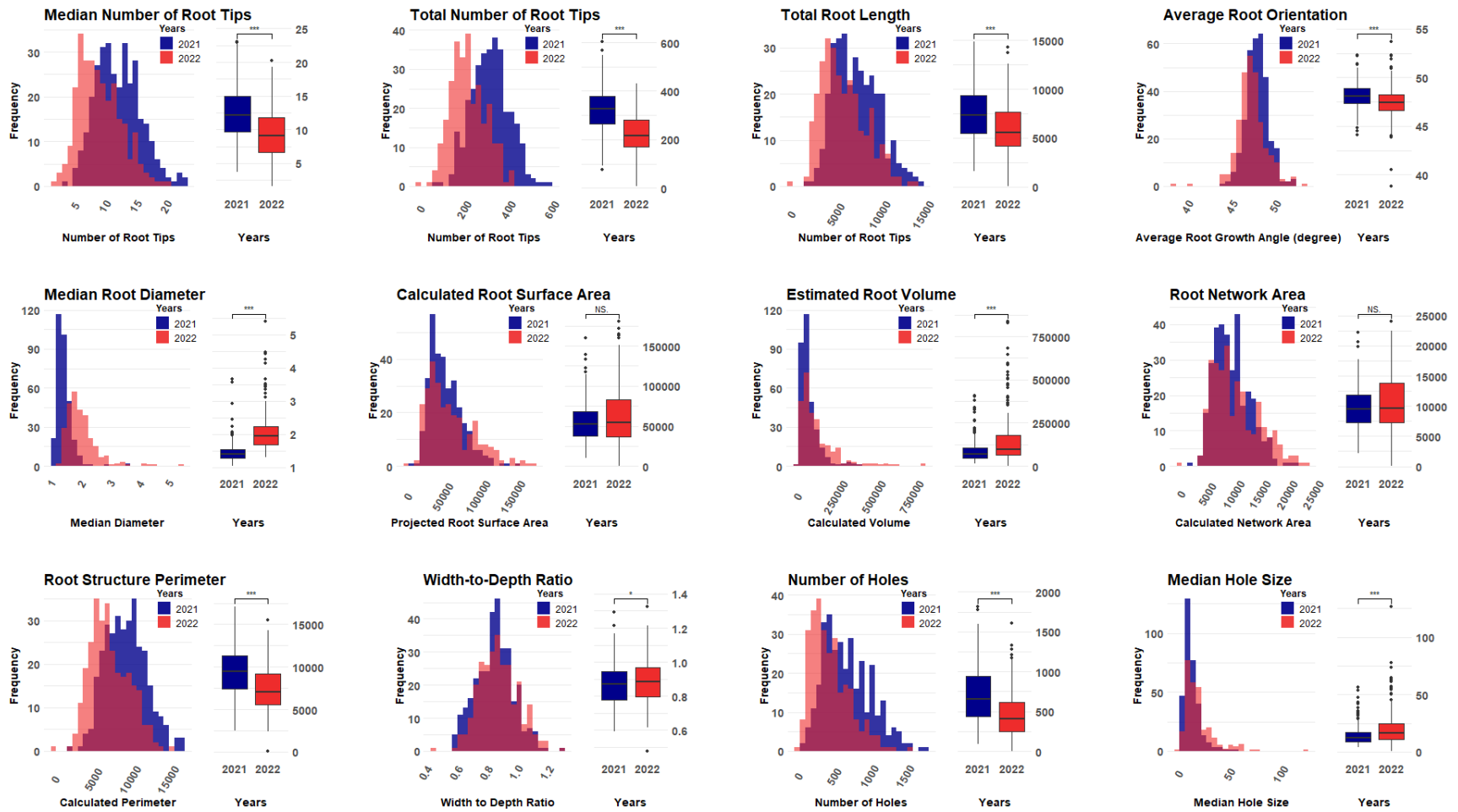
Figure 1: Histograms and boxplots demonstrating and comparing the distribution of root system architecture traits across years. Data for the 2021 sampling is denoted in blue, data for 2022 in red.
N.S. = no significant difference, ** *p*-value < 0.01, *** *p*-value < 0.001

Figure 2: Manhattan plots of FarmCPU genome-wide association study (GWAS) displaying significantly associated SNPs for twelve root system architecture. Significance threshold ($-\log 10\ (p) \geq 4.54$), represented by a solid dark red horizontal line. A suggestive threshold of $-\log 10\ (p) \geq 3.5$ is demonstrated by a dashed red line.

Table 1: Descriptive Statistics, Analysis of Variance, and Heritability for 12 Root Architecture Traits

		Median Number of Root Tips	Total Number Root Tips	Total Root Length (mm)	Width-to-Depth Ratio	Network Area (mm2)	Median Diameter (mm)	Perimeter (mm)	Volume (mm3)	Surface Area (mm2)	Number of Holes	Average Hole Size (mm2)	Average Root Orientation (deg)
Min	**2021**	2021	3.75	77.2	1577	0.59	2222	1.04	2465	15332	10527	88.6	4.24
	2022	2022	1.60	7.6	52	0.48	62.1	1.31	94.1	123	240	1.80	0.63
Max	**2021**	2021	23.1	605	14901	1.29	22251	3.66	17131	406317	159863	1819	56.5
	2022	2022	20.3	432	14337	1.33	24086	5.40	15522	838297	180996	1609	127
Mean	**2021**	2021	12.4	325	7545	0.87	9908	1.45	9521	87638	56075	708	14.4
	2022	2022	9.37	225	6075	0.89	10673	2.04	7419	142482	62851	464	21
Standard Deviation	**2021**	2021	3.67	85.9	2510	0.12	3295	0.28	2653	61740	23524	335	7.88
	2022	2022	3.46	78.5	2510	0.13	4395	0.54	2541	129723	33733	274	14.8
ANOVA	Gen	**	***	***	*	***	***	***	***	***	***	***	N.S.
	Year	***	***	***	*	**	***	***	***	***	***	***	***
	GxY	N.S.	N.S.	N.S.	N.S.	*	***	N.S.	***	**	N.S.	**	N.S.
Heritability (H2)		0.333	0.440	0.456	0.222	0.567	0.781	0.348	0.736	0.642	0.472	0.701	0.167

Table 2: Pearson's Correlation Coefficient for Root Architecture Traits in the ASDP 2021 grow out

	Median Number of Root Tips	Total Number Root Tips	Total Root Length (mm)	Width-to-Depth Ratio	Network Area (mm2)	Median Diameter (mm)	Perimeter (mm)	Volume (mm3)	Surface Area (mm2)	Number of Holes	Average Hole Size (mm2)	Average Root Orientation (deg)
Median Number of Root Tips	1.000	**0.906**	**0.948**	0.202	0.825	-0.013	**0.974**	0.586	0.779	**0.913**	-0.495	0.006
Total Number Root Tips		1.000	0.906	0.276	0.781	-0.019	**0.943**	0.558	0.737	0.857	-0.481	-0.121
Total Root Length			1.000	0.181	**0.919**	0.129	**0.966**	0.729	0.898	**0.970**	-0.639	-0.116
Width-to-Depth Ratio				1.000	0.209	0.004	0.251	0.210	0.173	0.097	0.088	-0.452
Network Area					1.000	0.414	0.838	**0.903**	**0.989**	0.834	-0.575	-0.145
Median Diameter						1.000	-0.034	0.539	0.445	0.028	-0.169	-0.133
Perimeter							1.000	0.602	0.790	0.927	-0.500	-0.061
Volume								1.000	**0.936**	0.645	-0.509	-0.240
Surface Area									1.000	0.827	-0.628	-0.172
Number of Holes										1.000	-0.728	-0.129
Average Hole Size											1.000	0.184
Average Root Orientation												1.000

Table 3: Pearson's Correlation Coefficient for Root Architecture Traits in the ASDP 2022 grow out

	Median Number of Root Tips	Total Number Root Tips	Total Root Length (mm)	Width-to-Depth Ratio	Network Area (mm2)	Median Diameter (mm)	Perimeter (mm)	Volume (mm3)	Surface Area (mm2)	Number of Holes	Average Hole Size (mm2)	Average Root Orientation (deg)
Median Number of Root Tips	1.000	0.896	**0.910**	0.291	0.731	-0.073	**0.960**	0.437	0.651	0.891	-0.292	0.217
Total Number Root Tips		1.000	**0.940**	0.257	0.814	0.066	**0.937**	0.576	0.759	**0.909**	-0.431	0.077
Total Root Length			1.000	0.224	**0.920**	0.195	**0.950**	0.707	0.873	**0.968**	-0.505	0.051
Width-to-Depth Ratio				1.000	0.185	-0.009	0.281	0.085	0.134	0.173	0.035	-0.329
Network Area					1.000	0.507	0.788	0.898	**0.983**	0.840	-0.557	-0.069
Median Diameter						1.000	-0.052	0.717	0.588	0.124	-0.471	-0.362
Perimeter							1.000	0.493	0.700	**0.915**	-0.294	0.161
Volume								1.000	**0.951**	0.648	-0.658	-0.226
Surface Area									1.000	0.811	-0.646	-0.125
Number of Holes										1.000	-0.576	0.041
Average Hole Size											1.000	0.248
Average Root Orientation												1.000

Table 4: *RSA Associated SNPs for which -log(p-value) > 4 .54*

	SNP	Chr	Position	*p-value*	Allele	maf	R^2
Average Hole Size							
2021	ss715626472	17	23469087	1.97E-05	G/A	0.197	0.0135
2022	ss715589814	5	2804036	1.84E-05	A/G	0.133	--
2022	ss715589980	5	3236161	9.48E-06	G/T	0.103	--
2022	ss715589991	5	3261123	4.51E-06	C/T	0.100	--
2022	ss715590011	5	3308357	8.49E-06	G/A	0.097	--
2022	ss715632868	18	9159569	1.15E-05	C/T	0.115	0.0096
Number of Holes							
2022	ss715598725	7	7989492	2.48E-05	G/A	0.082	0.1166
Median Root Diameter							
2021	ss715587921	4	42194415	5.02E-08	T/G	0.115	0.0367
2021	ss715604810	9	47548832	2.30E-05	T/C	0.061	0.0348
2021	ss715623302	15	9957356	1.38E-05	C/T	0.161	0.0196
2021	ss715622445	15	49164769	8.53E-06	G/A	0.155	0.0212
2021	ss715627633	17	39481935	2.36E-10	A/C	0.055	0.2181
2021	ss715631582	18	50344707	8.88E-06	A/G	0.079	0.0322
2021	ss715637437	20	34414971	1.27E-10	C/T	0.442	0.0182
2022	ss715589687	4	9581724	2.13E-06	C/T	0.100	0.0082
2022	ss715600757	8	21813168	2.34E-05	G/A	0.215	0.0077
2022	ss715607495	10	45463820	2.39E-06	G/A	0.245	0.0085
2022	ss715613717	13	11706814	2.66E-05	A/C	0.458	0.0066
2022	ss715627617	17	39376565	5.57E-08	G/A	0.067	0.0636
Average Root Orientation							
2021	ss715599977	8	17801521	3.80E-06	T/C	0.227	--

115

2021	ss715599978	8	17801693	5.87E-06	T/C	0.221	--
2021	ss715599979	8	17803816	3.80E-06	A/C	0.227	0.0346
2022	ss715601704	8	40235461	2.56E-05	T/C	0.112	--
2022	ss715625429	16	7411543	2.77E-05	C/A	0.091	0.0367

Volume

2021	ss715582616	2	4420727	3.67E-07	A/C	0.052	0.0924
2021	ss715585103	3	307872	2.30E-05	A/G	0.400	0.0188
2021	ss715587929	4	42461950	6.27E-06	G/A	0.061	0.1821
2021	ss715604909	9	48665322	1.01E-05	A/C	0.106	0.0829
2021	ss715611347	12	1036614	1.90E-05	C/A	0.055	0.2258
2021	ss715621455	15	2740735	1.08E-05	C/T	0.339	0.0191

Table 5: Selected Genes *Associated with SNPs for which -log(p-value) > 4 .54*

Year	Trait	SNP	Gene stable ID	Chr	Gene start (bp)	Gene end (bp)	Distance From SNP (bp)	GO term name
2021	Hole Size	ss715626472	GLYMA_17G185200	17	23552065	23557873	82978	root hair elongation
2022	Hole Size	Chr 5 Cluster	GLYMA_05G037800	5	3361590	3364100	53233	root radial pattern formation;
2022	Hole Size	Chr 5 Cluster	GLYMA_05G038300	5	3401960	3408039	93603	root development;
2022	Holes	ss715598725	GLYMA_07G086000	7	7942077	7944540	-47415	lateral root formation
2021	Median Root Tip	ss715623302	GLYMA_15G126100	15	9986010	9986372	28654	integral component of membrane
2021	Median Diameter	ss715604810	GLYMA_09G255400	9	47475550	47482896	-73282	root hair cell differentiation
2021	Median Diameter	ss715623302	GLYMA_15G124600	15	9894533	9898193	-62823	root hair cell differentiation
2021	Median Diameter	ss715631582	GLYMA_18G215800	18	50287921	50291401	-56786	root hair elongation
2022	Median Diameter	ss715600757	GLYMA_08G249200	8	21727446	21730345	-85722	root hair elongation
2022	Median Diameter	ss715600757	GLYMA_08G249400	8	21748017	21750483	-65151	root hair elongation
2022	Median Diameter	ss715600757	GLYMA_08G249700	8	21802765	21806491	-10403	root morphogenesis
2022	Median Diameter	ss715604811	GLYMA_09G268300	9	48581218	48593414	1032385	root development
2022	Median Diameter	ss715607495	GLYMA_10G223500	10	45444200	45451455	-19620	root hair elongation
2022	Median Diameter	ss715613717	GLYMA_13G037800	13	11749903	11750913	43089	root hair elongation
2022	Median Diameter	ss715627617	GLYMA_17G237500	17	39275410	39276430	-101155	lateral root development
2023	Median Diameter	ss715604812	GLYMA_09G268700	9	48615020	48619110	1066186	lateral root formation
2024	Median Diameter	ss715604813	GLYMA_09G270000	9	48704737	48708820	1155902	root development
2022	Root Orientation	ss715625429	GLYMA_16G074200	16	7465834	7473801	54291	root development
2021	Volume	ss715582616	GLYMA_02G046900	2	4314354	4319916	-106373	post-embryonic root development
2021	Volume	ss715621455	GLYMA_15G033600	15	2675618	2678073	-65117	primary root development;
2021	Volume	ss715621455	GLYMA_15G034600	15	2765299	2770528	24564	root hair

Supplemental Material

Supplemental Table 2.1: Analysis of Variance for Above Ground Traits

	df	Sum Squares	Mean Squares	F value	Pr(>F)	Significance
Photosynthesis						
Genotype	260	6497.3	25.0	1.90	3.585×10^{-10}	***
Year	1	13421.7	13421.7	1021.74	2.2×10^{-16}	***
Genotype: Year	259	3582.0	13.8	1.05	0.316	
Residuals	519	6817.7	13.1			
Stomatal Conductance						
Genotype	260	7.398	0.029	1.56	1.11×10^{-05}	***
Year	1	11.758	11.758	644.90	2.2×10^{-16}	***
Genotype: Year	259	3.553	0.014	0.75	0.995	
Residuals	519	9.462	0.018			
Water Use Efficiency						
Genotype	260	69771.0	268.0	1.35	8.08×10^{-04}	***
Year	1	51773.0	51773.0	268.96	2.2×10^{-16}	***
Genotype: Year	259	40285.0	156.0	0.81	0.974	
Residuals	519	99903.0	192.0			
Intracellular CO_2						
Genotype	260	139112.0	535.0	1.27	0.013	*
Year	1	6363.0	6363.0	15.05	1.17×10^{-04}	***
Genotype: Year	259	98188.0	379.1	0.90	0.839	
Residuals	519	219360.0	422.7			
Leaf Area						
Genotype	260	210396.0	809.0	3.76	2.2×10^{-16}	***
Year	1	115157.0	115157.0	535.66	2.2×10^{-16}	***
Genotype: Year	259	63282.0	244.0	1.14	0.114	
Residuals	517	111145.0	215.0			
Leaf Mass						
Genotype	260	16.097	0.062	3.61	2.2×10^{-16}	***
Year	1	2.028	2.028	118.31	2.2×10^{-16}	***
Genotype: Year	259	4.842	0.019	1.09	0.206	
Residuals	517	8.861	0.017			
Specific Leaf Area						
Genotype	260	1274147.0	4901.0	2.50	2.2×10^{-16}	***
Year	1	59500.0	59500.0	30.40	5.58×10^{-08}	***
Genotype: Year	259	533054.0	2058.0	1.05	0.316	
Residuals	517	1008121.0	1958.0			

Significance codes: 0 '***'   0.001 '**'   0.01 '*'   0.05 '.'   0.1 ' '   1

Supplemental Table 2.2: Expanded Statistics For Above-Ground Traits

	2020		2021	
	3000	**4000**	**7000**	**8000**
Photosynthesis				
Min	2.63	6.99	3.07	2.56
Max	31.60	29.60	23.80	24.35
Median	21.30	22.75	13.47	15.51
Mean	20.87	22.14	13.52	15.12
Sample Variance	16.28	13.73	14.83	18.31
St. Deviation	4.04	3.71	3.85	4.28
Skew	-0.54	-0.76	-0.14	-0.49
Stomatal Conductance				
Min	0.07	0.09	0.07	0.06
Max	1.00	1.23	0.58	0.54
Median	0.36	0.48	0.20	0.23
Mean	0.38	0.50	0.22	0.24
Sample Variance	0.02	0.04	0.01	0.01
St. Deviation	0.14	0.19	0.09	0.09
Skew	0.74	0.51	0.83	0.54
Water Use Efficiency				
Min	24.17	19.83	34.63	31.65
Max	96.84	146.70	130.04	115.67
Median	58.04	46.49	67.28	68.95
Mean	59.00	49.59	67.50	69.32
Sample Variance	178.65	252.38	170.48	163.04
St. Deviation	13.37	15.89	13.06	12.77
Skew	0.25	1.57	0.40	0.24
CI				
Min	208.00	112.00	173.52	198.64
Max	332.00	326.00	333.23	342.39
Median	262.00	277.00	266.13	259.75
Mean	261.75	274.38	265.52	260.71
Sample Variance	365.54	538.83	396.88	370.29
St. Deviation	19.12	23.21	19.92	19.24
Skew	0.20	-1.73	-0.08	0.45
Leaf Area				
Min	30.85	21.95	17.23	20.22
Max	180.65	185.70	106.30	120.35
Median	73.42	69.99	52.91	50.92
Mean	77.20	72.10	54.30	52.86

Sample Variance	476.36	486.53	249.97	261.67
St. Deviation	21.83	22.06	15.81	16.18
Skew	0.76	0.86	0.36	0.62
Dried Leaf Mass (g)				
Min	0.09	0.09	0.08	0.07
Max	1.27	1.13	0.91	1.00
Median	0.36	0.39	0.31	0.29
Mean	0.40	0.42	0.73	0.31
Sample Variance	0.04	0.03	41.87	0.02
St. Deviation	0.19	0.18	6.47	0.14
Skew	1.59	0.88	16.11	1.11
Specific Leaf Area				
Min	81.08	98.40	97.20	76.70
Max	463.26	501.89	352.42	347.71
Median	206.41	175.08	168.19	175.46
Mean	213.25	183.23	180.28	185.83
Sample Variance	3518.74	2318.99	2325.08	2280.72
St. Deviation	59.32	48.16	48.22	47.76
Skew	1.01	1.74	0.76	0.82

Supplemental Table 2.3: Gas Exchange and Leaf Morphology Associated SNPs for which -log(*p-value*) > 3.5

Year	Trait	SNP	Chr	Pos	P.value	Neg. Log	MAF
2020	Intracellular CO_2	ss715585481	3	34587344	0.000148638	3.83E+00	0.273
2020	Intracellular CO_2	ss715585482	3	34588195	0.000148638	3.83E+00	0.273
2020	Intracellular CO_2	ss715598498	7	6559823	0.000165249	3.78E+00	0.288
2020	Intracellular CO_2	ss715598682	7	7782025	0.000130474	3.88E+00	0.156
2020	Intracellular CO_2	ss715624546	16	32777894	0.000215814	3.67E+00	0.388
2021	Intracellular CO_2	ss715598779	7	8237979	2.99E-05	4.52E+00	0.438
2021	Intracellular CO_2	ss715638195	20	41786051	0.000157025	3.80E+00	0.369
2021	Intracellular CO_2	ss715638198	20	41797319	0.000157025	3.80E+00	0.369
2021	Intracellular CO_2	ss715638199	20	41798239	0.000185292	3.73E+00	0.356
2020	Leaf Area	ss715585855	3	37779807	0.000115284	3.94E+00	0.208
2020	Leaf Area	ss715586165	3	40583852	0.000163526	3.79E+00	0.125
2020	Leaf Area	ss715592558	5	469490	0.000183388	3.74E+00	0.121
2020	Leaf Area	ss715592554	5	477177	0.000183388	3.74E+00	0.121
2020	Leaf Area	ss715592553	5	484990	0.000183388	3.74E+00	0.121
2020	Leaf Area	ss715607308	10	43757485	4.81E-05	4.32E+00	0.185
2020	Leaf Area	ss715610566	11	34070012	0.000111395	3.95E+00	0.262
2020	Leaf Area	ss715617000	13	15059912	6.93E-05	4.16E+00	0.198
2020	Leaf Area	ss715623191	15	9085052	0.000177514	3.75E+00	0.258
2020	Leaf Area	ss715623192	15	9087229	0.000271321	3.57E+00	0.256
2020	Leaf Area	ss715623212	15	9209919	0.000263576	3.58E+00	0.262
2020	Leaf Area	ss715623215	15	9216048	0.00028181	3.55E+00	0.265
2020	Leaf Area	ss715627776	17	40705987	8.15E-05	4.09E+00	0.100
2020	Leaf Area	ss715631546	18	49972102	0.00022576	3.65E+00	0.092
2021	Leaf Area	ss715578509	1	1423756	0.000267404	3.57E+00	0.450
2021	Leaf Area	ss715582422	2	39545696	0.000188964	3.72E+00	0.162
2021	Leaf Area	ss715586730	3	4939933	7.30E-05	4.14E+00	0.337
2021	Leaf Area	ss715596785	7	2120050	1.51E-05	4.82E+00	0.092
2021	Leaf Area	ss715598423	7	5999812	4.39E-06	5.36E+00	0.406
2021	Leaf Area	ss715603533	9	32620539	0.000256793	3.59E+00	0.404
2021	Leaf Area	ss715623187	15	9067087	1.91E-05	4.72E+00	0.321
2021	Leaf Area	ss715627597	17	39262513	4.80E-05	4.32E+00	0.169
2021	Leaf Area	ss715632478	18	57549280	0.000140425	3.85E+00	0.229
2021	Leaf Area	ss715635425	19	45204441	8.39E-06	5.08E+00	0.365
2020	Leaf Mass	ss715579677	1	48105796	0.000107017	3.97E+00	0.094
2020	Leaf Mass	ss715579684	1	48123227	0.000107017	3.97E+00	0.094
2020	Leaf Mass	ss715608459	10	6726554	0.000108741	3.96E+00	0.135
2020	Leaf Mass	ss715608461	10	6756941	0.000263105	3.58E+00	0.154
2020	Leaf Mass	ss715606557	10	37916823	9.68E-05	4.01E+00	0.121

Year	Trait	Marker	Chr	Position	p-value	-log10(p)	R²
2020	Leaf Mass	ss715607316	10	43782999	0.000171087	3.77E+00	0.098
2020	Leaf Mass	ss715607318	10	43783975	8.26E-05	4.08E+00	0.094
2020	Leaf Mass	ss715607320	10	43785260	6.30E-05	4.20E+00	0.098
2020	Leaf Mass	ss715608129	10	50442406	0.000316662	3.50E+00	0.167
2020	Leaf Mass	ss715608130	10	50450778	0.000250228	3.60E+00	0.169
2020	Leaf Mass	ss715608133	10	50462248	0.000226247	3.65E+00	0.167
2020	Leaf Mass	ss715617000	13	15059912	2.49E-05	4.60E+00	0.198
2020	Leaf Mass	ss715616744	13	16757016	6.17E-05	4.21E+00	0.167
2020	Leaf Mass	ss715616737	13	16796464	0.000298196	3.53E+00	0.438
2020	Leaf Mass	ss715616437	13	43326463	0.000183286	3.74E+00	0.213
2020	Leaf Mass	ss715632859	18	9114287	0.000309164	3.51E+00	0.460
2021	Leaf Mass	ss715582534	2	4363973	7.18E-07	6.14E+00	0.087
2021	Leaf Mass	ss715582171	2	37286171	1.35E-05	4.87E+00	0.073
2021	Leaf Mass	ss715583480	2	47942834	5.46E-05	4.26E+00	0.108
2021	Leaf Mass	ss715604829	9	47851315	0.000180905	3.74E+00	0.323
2021	Leaf Mass	ss715611318	11	9695622	4.20E-05	4.38E+00	0.150
2021	Leaf Mass	ss715612385	12	34187459	7.86E-08	7.10E+00	0.144
2021	Leaf Mass	ss715624847	16	36436443	7.69E-07	6.11E+00	0.485
2021	Leaf Mass	ss715627571	17	39123666	3.65E-05	4.44E+00	0.271
2021	Leaf Mass	ss715630900	18	44409529	4.33E-06	5.36E+00	0.087
2021	Leaf Mass	ss715633080	19	1232556	1.75E-08	7.76E+00	0.079
2021	Leaf Mass	ss715634448	19	36199222	6.81E-06	5.17E+00	0.135
2020	Photosynthesis	ss715582450	2	39667079	3.00E-05	4.52E+00	0.248
2020	Photosynthesis	ss715586846	3	5389967	0.000319274	3.50E+00	0.269
2020	Photosynthesis	ss715590926	5	33926353	0.000267049	3.57E+00	0.460
2020	Photosynthesis	ss715602611	8	5821229	0.000249467	3.60E+00	0.081
2020	Photosynthesis	ss715616744	13	16757016	2.46E-08	7.61E+00	0.167
2020	Photosynthesis	ss715615064	13	30937609	5.15E-05	4.29E+00	0.250
2020	Photosynthesis	ss715627649	17	39615478	0.000155259	3.81E+00	0.123
2020	Photosynthesis	ss715635823	19	48331053	1.37E-07	6.86E+00	0.369
2020	Photosynthesis	ss715637218	20	294010	0.00029635	3.53E+00	0.460
2021	Photosynthesis	ss715589353	4	8121697	0.000267488	3.57E+00	0.169
2021	Photosynthesis	ss715611849	12	2390147	0.000284349	3.55E+00	0.158
2021	Photosynthesis	ss715622987	15	7089421	2.07E-05	4.68E+00	0.304
2021	Photosynthesis	ss715622988	15	7094505	0.000267945	3.57E+00	0.479
2021	Photosynthesis	ss715622990	15	7121530	2.79E-05	4.55E+00	0.313
2021	Photosynthesis	ss715622991	15	7125085	1.60E-05	4.80E+00	0.315
2021	Photosynthesis	ss715622992	15	7126448	2.79E-05	4.55E+00	0.313
2021	Photosynthesis	ss715622993	15	7127877	3.11E-05	4.51E+00	0.315
2021	Photosynthesis	ss715622995	15	7133808	2.79E-05	4.55E+00	0.313
2021	Photosynthesis	ss715623086	15	7892897	0.000169247	3.77E+00	0.212

Year	Trait	Marker	Chr	Position	P-value	LOD	R²
2021	Photosynthesis	ss715622616	15	50194648	0.00026606	3.58E+00	0.175
2021	Photosynthesis	ss715623457	16	1430399	0.000224697	3.65E+00	0.475
2021	Photosynthesis	ss715623458	16	1431551	0.000173917	3.76E+00	0.473
2021	Photosynthesis	ss715623462	16	1451244	0.000298353	3.53E+00	0.469
2021	Photosynthesis	ss715625036	16	3871263	0.000229297	3.64E+00	0.356
2021	Photosynthesis	ss715625041	16	3905889	0.000275172	3.56E+00	0.358
2020	Specific Leaf Area	ss715579917	1	49888773	0.00030776	3.51E+00	0.058
2020	Specific Leaf Area	ss715583067	2	44037267	0.000316096	3.50E+00	0.212
2020	Specific Leaf Area	ss715597355	7	35782527	9.59E-05	4.02E+00	0.433
2020	Specific Leaf Area	ss715597356	7	35784231	9.48E-05	4.02E+00	0.431
2020	Specific Leaf Area	ss715599630	8	14807467	0.000219912	3.66E+00	0.137
2020	Specific Leaf Area	ss715607302	10	43698485	0.000228464	3.64E+00	0.073
2020	Specific Leaf Area	ss715626515	17	2492277	0.000231826	3.63E+00	0.288
2020	Specific Leaf Area	ss715626516	17	2492594	0.000198273	3.70E+00	0.296
2020	Specific Leaf Area	ss715626600	17	2757522	4.06E-05	4.39E+00	0.225
2020	Specific Leaf Area	ss715626612	17	2800784	7.22E-05	4.14E+00	0.231
2020	Specific Leaf Area	ss715625885	17	12491227	0.000213623	3.67E+00	0.352
2020	Specific Leaf Area	ss715625886	17	12503786	0.000283224	3.55E+00	0.352
2020	Specific Leaf Area	ss715625909	17	12649595	8.77E-05	4.06E+00	0.231
2020	Specific Leaf Area	ss715625910	17	12651804	0.000109743	3.96E+00	0.223
2020	Specific Leaf Area	ss715625911	17	12653658	8.77E-05	4.06E+00	0.231
2020	Specific Leaf Area	ss715626739	17	32189445	0.000276895	3.56E+00	0.285
2020	Specific Leaf Area	ss715630931	18	488756	0.000266687	3.57E+00	0.408
2020	Specific Leaf Area	ss715631360	18	48309457	0.000243831	3.61E+00	0.433
2020	Specific Leaf Area	ss715632495	18	57724502	0.000249614	3.60E+00	0.419
2020	Specific Leaf Area	ss715633134	19	1368196	0.000202099	3.69E+00	0.437
2020	Specific Leaf Area	ss715633135	19	1370347	0.000145905	3.84E+00	0.435
2021	Specific Leaf Area	ss715579441	1	4312808	2.02E-05	4.70E+00	0.319
2021	Specific Leaf Area	ss715582633	2	40666705	5.80E-06	5.24E+00	0.106
2021	Specific Leaf Area	ss715584902	3	23166713	1.77E-07	6.75E+00	0.075
2021	Specific Leaf Area	ss715589653	4	9416865	0.000270152	3.57E+00	0.208
2021	Specific Leaf Area	ss715607503	10	45615797	1.91E-08	7.72E+00	0.075
2021	Specific Leaf Area	ss715612385	12	34187459	1.87E-08	7.73E+00	0.144
2021	Specific Leaf Area	ss715622610	15	4955159	2.85E-05	4.54E+00	0.260
2021	Specific Leaf Area	ss715620824	15	14739216	3.35E-08	7.47E+00	0.458
2021	Specific Leaf Area	ss715620916	15	15190979	0.000292107	3.53E+00	0.460
2021	Specific Leaf Area	ss715621745	15	26959702	2.92E-05	4.53E+00	0.173
2021	Specific Leaf Area	ss715623488	16	1533772	7.46E-07	6.13E+00	0.283
2021	Specific Leaf Area	ss715624023	16	2897268	0.000292975	3.53E+00	0.100
2020	Stomatal Conductance	ss715584424	3	12040444	0.000134562	3.87E+00	0.063

Year	Trait	Marker	Chr	Position	p-value	-log10(p)	R2
2020	Stomatal Conductance	ss715584493	3	14064971	0.000109511	3.96E+00	0.063
2020	Stomatal Conductance	ss715585481	3	34587344	0.000248393	3.60E+00	0.273
2020	Stomatal Conductance	ss715585482	3	34588195	0.000248393	3.60E+00	0.273
2020	Stomatal Conductance	ss715616744	13	16757016	0.000241986	3.62E+00	0.167
2020	Stomatal Conductance	ss715616734	13	16804858	0.000253893	3.60E+00	0.429
2020	Stomatal Conductance	ss715616733	13	16811968	0.000233359	3.63E+00	0.413
2020	Stomatal Conductance	ss715616732	13	16812499	0.000228354	3.64E+00	0.412
2020	Stomatal Conductance	ss715616731	13	16816882	4.49E-05	4.35E+00	0.435
2020	Stomatal Conductance	ss715626598	17	2753360	0.000122332	3.91E+00	0.083
2020	Stomatal Conductance	ss715634629	19	3788771	0.000207864	3.68E+00	0.331
2020	Stomatal Conductance	ss715634667	19	3807639	0.000270397	3.57E+00	0.327
2021	Stomatal Conductance	ss715587015	3	9084340	0.000269352	3.57E+00	0.088
2021	Stomatal Conductance	ss715584422	3	11997372	0.000227989	3.64E+00	0.058
2021	Stomatal Conductance	ss715584424	3	12040444	0.000292808	3.53E+00	0.063
2021	Stomatal Conductance	ss715584433	3	12293511	0.000179779	3.75E+00	0.062
2021	Stomatal Conductance	ss715584821	3	13131970	0.00026697	3.57E+00	0.062
2021	Stomatal Conductance	ss715584493	3	14064971	0.000315349	3.50E+00	0.063
2021	Stomatal Conductance	ss715584808	3	16235737	0.00026697	3.57E+00	0.062
2021	Stomatal Conductance	ss715594164	6	3279594	4.21E-05	4.38E+00	0.121
2021	Stomatal Conductance	ss715622987	15	7089421	0.000292052	3.53E+00	0.304
2021	Stomatal Conductance	ss715622990	15	7121530	0.000195052	3.71E+00	0.313
2021	Stomatal Conductance	ss715622991	15	7125085	0.000132053	3.88E+00	0.315
2021	Stomatal Conductance	ss715622992	15	7126448	0.000195052	3.71E+00	0.313

Year	Trait	SNP	Chr	Position	P-value		MAF
2021	Stomatal Conductance	ss715622993	15	7127877	0.000177601	3.75E+00	0.315
2021	Stomatal Conductance	ss715622995	15	7133808	0.000195052	3.71E+00	0.313
2021	Stomatal Conductance	ss715621332	15	23457107	8.69E-05	4.06E+00	0.369
2021	Stomatal Conductance	ss715635148	19	42039925	0.00027295	3.56E+00	0.146
2020	Water Use Efficiency	ss715584424	3	12040444	0.000298451	3.53E+00	0.063
2020	Water Use Efficiency	ss715584493	3	14064971	0.000303997	3.52E+00	0.063
2020	Water Use Efficiency	ss715585481	3	34587344	6.43E-05	4.19E+00	0.273
2020	Water Use Efficiency	ss715585482	3	34588195	6.43E-05	4.19E+00	0.273
2020	Water Use Efficiency	ss715608989	11	1332612	0.000179439	3.75E+00	0.062
2020	Water Use Efficiency	ss715609554	11	1828355	0.00012439	3.91E+00	0.060
2020	Water Use Efficiency	ss715636683	20	10209786	0.00016787	3.78E+00	0.185
2021	Water Use Efficiency	ss715611263	11	8748512	0.000203957	3.69E+00	0.150
2021	Water Use Efficiency	ss715621402	15	2565284	6.95E-05	4.16E+00	0.135

Supplemental Table 2.4: Complete List of Genes in Linkage with Significant SNPs Associated with Above-Ground Traits

Gene stable ID	Chromosome	Gene start (bp)	Gene end (bp)	GO term name
GLYMA_01G039000	1	4212429	4221344	ADP binding
GLYMA_01G039100	1	4235182	4237298	integral component of membrane
GLYMA_01G039200	1	4239455	4243315	DNA-binding transcription factor activity
GLYMA_01G039300	1	4256747	4258161	auxin-activated signaling pathway
GLYMA_01G039400	1	4270598	4275060	
GLYMA_01G039500	1	4289457	4295700	
GLYMA_01G039600	1	4300332	4302844	kinase activity
GLYMA_01G039700	1	4304713	4310259	cellular anatomical entity
GLYMA_01G039800	1	4316464	4321369	carbohydrate binding
GLYMA_01G039900	1	4324079	4325876	integral component of membrane
GLYMA_01G040000	1	4336374	4338196	cytoplasm
GLYMA_01G040100	1	4341457	4342817	cytoplasm
GLYMA_01G040200	1	4345723	4347332	cytoplasm
GLYMA_01G040300	1	4353053	4358969	protein binding
GLYMA_01G040400	1	4369831	4378842	
GLYMA_01G040500	1	4380966	4383169	chloroplast
GLYMA_01G040600	1	4389420	4392033	chaperone binding
GLYMA_01G040700	1	4392159	4393458	cell redox homeostasis
GLYMA_01G040800	1	4395069	4395257	
GLYMA_01G040900	1	4396965	4402461	ATP binding
GLYMA_01G041000	1	4397506	4397703	
GLYMA_01G041100	1	4403613	4404643	cell redox homeostasis
GLYMA_01G041200	1	4420529	4421978	cell redox homeostasis
GLYMA_01G041300	1	4428651	4434734	
GLYMA_02G046100	2	4242678	4246278	actin cytoskeleton organization
GLYMA_02G046200	2	4249191	4251536	nucleus
GLYMA_02G046300	2	4253322	4256284	

ENSRNA049760345	2	4256137	4256210	
GLYMA_02G046400	2	4256614	4260141	cytoplasm
GLYMA_02G046500	2	4266744	4269200	extracellular region
GLYMA_02G046600	2	4276605	4283705	anatomical structure development
GLYMA_02G046700	2	4297419	4301373	plasma membrane
GLYMA_02G046800	2	4302936	4312761	alpha-mannosidase activity
GLYMA_02G046900	2	4314354	4319916	cytosol
GLYMA_02G047000	2	4322834	4324959	catalytic activity
GLYMA_02G047100	2	4329417	4333528	methylation
GLYMA_02G047200	2	4337518	4343470	integral component of membrane
GLYMA_02G047300	2	4344431	4351294	calmodulin-lysine N-methyltransferase activity
GLYMA_02G047400	2	4356203	4358686	defense response
GLYMA_02G047500	2	4373609	4374901	DNA binding
GLYMA_02G047600	2	4376285	4379912	chloroplast
GLYMA_02G047700	2	4384491	4386890	cell surface receptor signaling pathway
GLYMA_02G047800	2	4396176	4398689	cytosolic small ribosomal subunit
GLYMA_02G047900	2	4402299	4403204	
GLYMA_02G048000	2	4407580	4408194	
GLYMA_02G048100	2	4412271	4418176	chromatin binding
GLYMA_02G048200	2	4419899	4425822	base-excision repair
GLYMA_02G048300	2	4426937	4434315	abscisic acid-activated signaling pathway
GLYMA_02G048400	2	4440520	4451775	dioxygenase activity
GLYMA_02G048500	2	4447769	4448744	
GLYMA_02G048600	2	4449030	4451814	dioxygenase activity
GLYMA_02G048700	2	4456124	4457800	
GLYMA_02G048800	2	4458411	4459296	chloroplast
GLYMA_02G048900	2	4459650	4462929	cytoplasm
GLYMA_02G049000	2	4464177	4467693	carbohydrate metabolic process
GLYMA_02G049100	2	4469856	4474398	negative gravitropism

GLYMA_02G049200	2	4479569	4480377	auxin-activated signaling pathway
GLYMA_02G049300	2	4486759	4488584	chloroplast
GLYMA_02G196200	2	37187941	37188366	protein ubiquitination
GLYMA_02G196300	2	37188414	37189447	protein ubiquitination
GLYMA_02G196400	2	37235650	37236219	
GLYMA_02G196500	2	37250175	37255107	DNA binding
GLYMA_02G196600	2	37319294	37319584	cytoplasm
GLYMA_02G196700	2	37329955	37332768	DNA binding
GLYMA_02G196800	2	37333447	37336731	
GLYMA_02G196900	2	37350433	37353304	maturation of 5.8S rRNA
GLYMA_02G210300	2	39541304	39543047	
GLYMA_02G210400	2	39548347	39550424	integral component of membrane
GLYMA_02G210500	2	39558785	39562318	DNA-binding transcription factor activity, RNA polymerase II-specific
GLYMA_02G210600	2	39584498	39586513	integral component of membrane
GLYMA_02G210700	2	39599283	39601285	integral component of membrane
GLYMA_02G210800	2	39612143	39619125	dioxygenase activity
GLYMA_02G210900	2	39627059	39627529	dioxygenase activity
GLYMA_02G211000	2	39634165	39636520	integral component of membrane
GLYMA_02G211100	2	39637131	39637337	
GLYMA_02G211200	2	39637739	39651535	ATP binding
GLYMA_02G211300	2	39654528	39661365	chloroplast
GLYMA_02G211400	2	39675173	39678485	ATP binding
GLYMA_02G211500	2	39679465	39682574	Golgi apparatus
GLYMA_02G211600	2	39684359	39689079	cytoplasm
GLYMA_02G211700	2	39685671	39693704	fumarate transport
GLYMA_02G211800	2	39709361	39712971	protein binding
GLYMA_02G211900	2	39734578	39737341	DNA binding
GLYMA_02G212000	2	39751967	39753877	ATP binding

GLYMA_02G212100	2	39761722	39763140	metal ion binding
GLYMA_02G212200	2	39777091	39780933	
GLYMA_02G212300	2	39779313	39779618	
GLYMA_02G218100	2	40542301	40547137	auxin-activated signaling pathway
GLYMA_02G218200	2	40564224	40566636	
GLYMA_02G218300	2	40588552	40592354	glutamyl-tRNA reductase activity
GLYMA_02G218400	2	40642050	40644285	antiporter activity
GLYMA_02G218500	2	40651541	40652473	
GLYMA_02G218600	2	40652986	40658669	integral component of plasma membrane
GLYMA_02G218700	2	40667610	40671395	carbohydrate metabolic process
GLYMA_02G218800	2	40681436	40684690	cation transport
GLYMA_02G218900	2	40692221	40695776	
GLYMA_02G219000	2	40696384	40700339	intracellular membrane-bounded organelle
GLYMA_02G219100	2	40700534	40701497	chloroplast
GLYMA_02G219200	2	40702208	40716518	ATP binding
GLYMA_02G219300	2	40719112	40728068	lipid homeostasis
GLYMA_02G219400	2	40730226	40735968	regulation of defense response to fungus
GLYMA_02G219500	2	40746990	40747379	
GLYMA_02G219600	2	40747324	40759797	
GLYMA_02G219700	2	40757222	40761117	jasmonic acid metabolic process
GLYMA_02G219800	2	40783290	40787658	ATP binding
GLYMA_03G083100	3	23042135	23096359	carbohydrate metabolic process
GLYMA_03G083200	3	23140219	23143908	hydrolase activity
GLYMA_03G083300	3	23214945	23217446	DNA binding
GLYMA_03G083400	3	23219238	23225184	ATP binding
GLYMA_03G083500	3	23230441	23235871	
GLYMA_03G083600	3	23289648	23291767	
GLYMA_07G025500	7	1994659	1997431	
GLYMA_07G025600	7	1999918	2002329	deubiquitinase activity

GLYMA_07G025700	7	2006893	2011646	cullin family protein binding
GLYMA_07G025800	7	2020503	2021932	DNA binding
GLYMA_07G025900	7	2034307	2040659	ATP binding
GLYMA_07G026000	7	2042360	2043520	
GLYMA_07G026100	7	2047119	2049504	alpha-tubulin binding
GLYMA_07G026200	7	2051841	2054034	protein binding
GLYMA_07G026300	7	2055072	2058068	obsolete coenzyme binding
GLYMA_07G026400	7	2060055	2062749	cytoplasm
GLYMA_07G026500	7	2071932	2081979	
GLYMA_07G026600	7	2088004	2091019	aspartyl esterase activity
GLYMA_07G026700	7	2094012	2094242	
GLYMA_07G026800	7	2100016	2104324	calcium ion transmembrane transport
GLYMA_07G026900	7	2108335	2110582	channel activity
GLYMA_07G027000	7	2119435	2120329	DNA binding
GLYMA_07G027100	7	2131942	2134796	nucleus
GLYMA_07G027200	7	2143712	2147133	nucleus
GLYMA_07G027300	7	2156201	2160044	nucleus
GLYMA_07G027400	7	2170765	2175801	nucleus
GLYMA_07G027500	7	2185500	2187191	integral component of membrane
GLYMA_07G027600	7	2190907	2192553	integral component of membrane
GLYMA_07G027700	7	2195890	2197352	
GLYMA_07G027800	7	2201136	2220876	chromatin DNA binding
GLYMA_07G027900	7	2225560	2227182	
GLYMA_07G065500	7	5850775	5875209	ADP binding
GLYMA_07G065600	7	5878703	5899005	ADP binding
GLYMA_07G065700	7	5923612	5927198	biosynthetic process
GLYMA_07G065800	7	5937301	5941192	metal ion binding
GLYMA_07G065900	7	5946716	5947413	integral component of membrane
GLYMA_07G066000	7	5953957	5957348	integral component of membrane

GLYMA_07G066100	7	5960745	5967003	DNA binding
GLYMA_07G066200	7	5967723	5968271	integral component of membrane
GLYMA_07G066300	7	5978659	5981481	integral component of membrane
GLYMA_07G066400	7	5985880	5986044	mitochondrial inner membrane
GLYMA_07G066500	7	5987261	5990684	root development
GLYMA_07G066600	7	6000626	6003834	ATP binding
GLYMA_07G066700	7	6011344	6014687	extrinsic component of mitochondrial inner membrane
GLYMA_07G066800	7	6018022	6023893	ATP binding
GLYMA_07G066900	7	6023894	6029346	carbohydrate metabolic process
GLYMA_07G067000	7	6032415	6036498	carbohydrate metabolic process
GLYMA_07G067100	7	6047501	6052182	methyltransferase activity
GLYMA_07G067200	7	6056575	6058569	glycosyltransferase activity
GLYMA_07G067300	7	6062592	6073333	glycosyltransferase activity
GLYMA_07G067400	7	6074564	6078985	integral component of membrane
GLYMA_07G067500	7	6085336	6090387	acetylglucosaminyltransferase activity
GLYMA_07G067600	7	6091311	6093654	
GLYMA_07G067700	7	6098621	6103054	ferric-chelate reductase activity
GLYMA_07G067800	7	6103673	6104951	defense response
GLYMA_07G067900	7	6106491	6110846	ADP binding
GLYMA_07G087700	7	8111751	8121053	ATP binding
GLYMA_07G087800	7	8125996	8135514	cytosol
GLYMA_07G087900	7	8139156	8142798	GO_0044212
GLYMA_07G088000	7	8148873	8150072	
GLYMA_07G088100	7	8155777	8157594	cytosolic small ribosomal subunit
GLYMA_07G088200	7	8183002	8188290	integral component of membrane
GLYMA_07G088300	7	8226178	8228486	
GLYMA_07G088400	7	8242895	8249911	integral component of membrane
GLYMA_07G088500	7	8251132	8259419	cytoplasm
GLYMA_07G088600	7	8266336	8267985	metal ion binding

GLYMA_07G088700	7	8270116	8275026	integral component of membrane
GLYMA_07G088800	7	8270319	8271130	
GLYMA_07G088900	7	8285431	8289641	
GLYMA_07G089000	7	8296453	8305007	vernalization response
GLYMA_07G089100	7	8306577	8310277	integral component of membrane
GLYMA_07G089200	7	8312557	8324908	4 iron, 4 sulfur cluster binding
GLYMA_07G089300	7	8340065	8344088	
GLYMA_07G089400	7	8354495	8360682	cellular lipid metabolic process
GLYMA_10G224000	10	45479863	45493565	carbohydrate metabolic process
GLYMA_10G224100	10	45494198	45496872	cell redox homeostasis
GLYMA_10G224200	10	45498206	45500186	cytosol
GLYMA_10G224300	10	45503642	45505214	
GLYMA_10G224400	10	45509340	45510452	integral component of membrane
GLYMA_10G224500	10	45514702	45516815	integral component of membrane
GLYMA_10G224600	10	45526661	45531424	
GLYMA_10G224700	10	45534516	45534867	
GLYMA_10G224800	10	45537703	45537876	
GLYMA_10G224900	10	45540859	45544972	phosphatidylinositol binding
GLYMA_10G225000	10	45549152	45550892	
GLYMA_10G225100	10	45561745	45564354	
GLYMA_10G225200	10	45579021	45582548	DNA-binding transcription factor activity
GLYMA_10G225300	10	45598119	45603561	
GLYMA_10G225400	10	45605390	45609815	carbohydrate metabolic process
GLYMA_10G225500	10	45612670	45623310	cysteine-type deubiquitinase activity
GLYMA_10G225600	10	45616985	45617457	
GLYMA_10G225700	10	45624809	45626702	RNA binding
GLYMA_10G225800	10	45629065	45639027	chloroplast
GLYMA_10G225900	10	45640990	45641657	cellular manganese ion homeostasis
GLYMA_10G226000	10	45653088	45657459	DNA-binding transcription factor activity

GLYMA_10G226100	10	45658317	45660220	carbon-carbon lyase activity
GLYMA_10G226200	10	45666030	45668827	carbon-carbon lyase activity
GLYMA_10G226300	10	45674356	45684646	ATP binding
GLYMA_10G226400	10	45682181	45682976	ATPase binding
GLYMA_10G226500	10	45706001	45707052	
GLYMA_10G226600	10	45710673	45716672	integral component of membrane
GLYMA_10G226700	10	45718946	45725503	mRNA binding
GLYMA_10G226800	10	45729028	45730338	extracellular space
GLYMA_10G226900	10	45733893	45742369	metal ion binding
GLYMA_12G180200	12	34061073	34062960	hydrolase activity, acting on ester bonds
GLYMA_12G180300	12	34067346	34070546	carboxy-lyase activity
GLYMA_12G180400	12	34076999	34081142	protein ubiquitination
GLYMA_12G180500	12	34086463	34090398	chloroplast membrane
GLYMA_12G180600	12	34098277	34110951	AP-2 adaptor complex
GLYMA_12G180700	12	34111598	34119168	chromatin
GLYMA_12G180800	12	34134888	34144510	ATP binding
GLYMA_12G180900	12	34148236	34151052	amino acid transmembrane transport
GLYMA_12G181000	12	34152310	34159417	amino acid transmembrane transport
GLYMA_12G181100	12	34162280	34167387	amino acid transmembrane transport
GLYMA_12G181200	12	34172329	34184694	
ENSRNA049760075	12	34182634	34182716	
GLYMA_12G181300	12	34187891	34191566	metal ion binding
GLYMA_12G181400	12	34193664	34197110	negative regulation of DNA-templated transcription
GLYMA_12G181500	12	34198074	34199528	
GLYMA_12G181600	12	34216382	34222864	membrane
GLYMA_12G181700	12	34238057	34239400	cell differentiation
ENSRNA049760065	12	34245540	34245620	
GLYMA_12G181800	12	34248924	34251406	chloroplast
GLYMA_12G181900	12	34268545	34275215	adenine import across plasma membrane

GLYMA_12G182000	12	34287952	34289818	assembly of large subunit precursor of preribosome
GLYMA_12G182100	12	34299658	34301166	
GLYMA_13G052200	13	14934398	14936703	
GLYMA_13G052300	13	14939773	14940715	
GLYMA_13G052400	13	14945122	14946581	
GLYMA_13G052500	13	14946865	14947805	
GLYMA_13G052600	13	14947806	14950192	
GLYMA_13G052700	13	14956158	14962088	DNA binding
ENSRNA049760535	13	14993004	14993077	
GLYMA_13G052800	13	15005141	15009623	dioxygenase activity
GLYMA_13G052900	13	15036769	15041148	oxidoreductase activity, acting on paired donors, with incorporation or reduction of molecular oxygen
GLYMA_13G053000	13	15046821	15050021	cell wall organization
GLYMA_13G053100	13	15052712	15060153	integral component of membrane
GLYMA_13G053200	13	15063244	15063878	anchored component of membrane
GLYMA_13G053300	13	15064460	15069264	anchored component of membrane
GLYMA_13G053400	13	15070294	15076224	integral component of membrane
GLYMA_13G053500	13	15076805	15079309	
GLYMA_13G053600	13	15088943	15092606	ATP binding
GLYMA_13G053700	13	15096852	15099898	ATP binding
GLYMA_13G053800	13	15110071	15112808	ATP binding
GLYMA_13G053900	13	15125067	15126092	ATP binding
GLYMA_13G054000	13	15126544	15128286	acyltransferase activity, transferring groups other than amino-acyl groups
GLYMA_13G054100	13	15138725	15138925	
GLYMA_13G054200	13	15144990	15148021	ATP binding
GLYMA_13G054300	13	15153615	15156149	ATP binding
GLYMA_13G054400	13	15164832	15168321	ATP binding
GLYMA_13G054500	13	15173682	15182007	integrator complex

GLYMA_13G066500	13	16633758	16638992	dioxygenase activity
GLYMA_13G066600	13	16641083	16643176	DNA binding
GLYMA_13G066700	13	16644061	16646454	
GLYMA_13G066800	13	16646920	16651317	
GLYMA_13G066900	13	16662928	16667207	
GLYMA_13G067000	13	16671710	16673786	cell-cell signaling involved in cell fate commitment
GLYMA_13G067100	13	16679231	16680442	membrane
GLYMA_13G067200	13	16688567	16689544	protein binding
GLYMA_13G067300	13	16695633	16700683	
GLYMA_13G067400	13	16704086	16704947	integral component of membrane
GLYMA_13G067500	13	16729033	16733978	catalytic activity
GLYMA_13G067600	13	16747744	16749376	chromatin
GLYMA_13G067700	13	16753333	16759339	core mediator complex
GLYMA_13G067800	13	16765722	16775985	chromatin
GLYMA_13G067900	13	16787469	16789119	glycosyltransferase activity
GLYMA_13G068000	13	16791059	16795343	
GLYMA_13G068100	13	16805832	16813055	alpha-mannosidase activity
GLYMA_13G068200	13	16825383	16836935	integral component of membrane
GLYMA_13G068300	13	16825585	16825785	
GLYMA_13G068400	13	16842894	16857764	
GLYMA_13G068500	13	16851649	16854206	oxidoreductase activity, acting on paired donors, with incorporation or reduction of molecular oxygen
GLYMA_13G068600	13	16858723	16859438	chloroplast
GLYMA_13G068700	13	16862241	16863536	
GLYMA_13G068800	13	16864171	16866998	defense response to other organism
GLYMA_13G068900	13	16875941	16876821	
GLYMA_13G069000	13	16881996	16885400	carboxylic ester hydrolase activity
GLYMA_15G063100	15	4829928	4832753	cell redox homeostasis
GLYMA_15G063200	15	4834356	4840906	ATP binding

GLYMA_15G063300	15	4844062	4846067	nucleus
GLYMA_15G063400	15	4847887	4849531	4-hydroxy-4-methyl-2-oxoglutarate aldolase activity
GLYMA_15G063500	15	4851531	4853186	integral component of membrane
GLYMA_15G063600	15	4856453	4858921	
GLYMA_15G063700	15	4860570	4862419	integral component of membrane
GLYMA_15G063800	15	4865547	4868230	protein ubiquitination
GLYMA_15G063900	15	4872268	4873131	DNA-binding transcription factor activity
GLYMA_15G064000	15	4875731	4877163	DNA-binding transcription factor activity
GLYMA_15G064100	15	4877866	4879175	
GLYMA_15G064200	15	4881333	4882827	phosphatidic acid binding
GLYMA_15G064300	15	4885565	4887727	chloroplast
GLYMA_15G064400	15	4887887	4888175	
GLYMA_15G064500	15	4900235	4903742	DNA-binding transcription activator activity, RNA polymerase II-specific
GLYMA_15G064600	15	4911276	4911875	oxidoreductase activity, acting on NAD(P)H
GLYMA_15G064700	15	4918630	4921488	oxidoreductase activity, acting on NAD(P)H
GLYMA_15G064800	15	4930588	4932450	cytoplasm
GLYMA_15G064900	15	4941726	4945663	ATP binding
GLYMA_15G065000	15	4947661	4949230	ATP binding
GLYMA_15G065100	15	4949613	4956189	ATP binding
GLYMA_15G065200	15	4960133	4964112	ATP binding
GLYMA_15G065300	15	4968841	4969328	ATP binding
GLYMA_15G065400	15	4971607	4972756	anchored component of plasma membrane
GLYMA_15G065500	15	4976617	4979221	ATP binding
GLYMA_15G065600	15	4981427	4985949	beta-amyrin synthase activity
GLYMA_15G065700	15	4999673	5000833	calcium ion binding
GLYMA_15G065800	15	5002340	5006288	cysteine-type deubiquitinase activity
GLYMA_15G065900	15	5011484	5012449	intracellular anatomical structure
GLYMA_15G066000	15	5014939	5017695	metal ion binding

GLYMA_15G066100	15	5020169	5023571	integral component of membrane
GLYMA_15G066200	15	5040782	5043187	cell cycle
GLYMA_15G066300	15	5045441	5048956	cation transport
GLYMA_15G066400	15	5054526	5057612	integral component of membrane
GLYMA_15G066500	15	5062061	5065754	integral component of membrane
GLYMA_15G066600	15	5071113	5076886	chromatin
GLYMA_15G066700	15	5077630	5082260	integral component of membrane
GLYMA_15G090500	15	6964803	6967999	
GLYMA_15G090600	15	6966380	6967073	
GLYMA_15G090700	15	6969340	6972077	mitochondrion
GLYMA_15G090800	15	6973952	6975439	cytosolic large ribosomal subunit
GLYMA_15G090900	15	6974908	6975245	
GLYMA_15G091000	15	6983384	6990249	auxin-activated signaling pathway
GLYMA_15G091100	15	7012077	7013118	
GLYMA_15G091200	15	7035032	7038022	chloroplast
GLYMA_15G091300	15	7040509	7043103	protein ubiquitination
GLYMA_15G091400	15	7042610	7044237	cytoplasm
GLYMA_15G091500	15	7047753	7054541	carbohydrate binding
GLYMA_15G091600	15	7061732	7066615	calcium activated cation channel activity
GLYMA_15G091700	15	7066675	7068841	mitochondrion
GLYMA_15G091800	15	7069801	7074975	integral component of membrane
GLYMA_15G091900	15	7077782	7081975	adenyl-nucleotide exchange factor activity
GLYMA_15G092000	15	7085612	7094574	BRCA1-A complex
GLYMA_15G092100	15	7095267	7096838	
GLYMA_15G092200	15	7099027	7102226	protein binding
GLYMA_15G092300	15	7102873	7104042	protein binding
GLYMA_15G092400	15	7119377	7140583	ABC-type transporter activity
GLYMA_15G092500	15	7156448	7167239	DNA binding
GLYMA_15G092600	15	7177044	7180068	protein binding

GLYMA_15G092700	15	7187504	7190396	GPI anchor biosynthetic process
GLYMA_15G092800	15	7192682	7197207	intracellular membrane-bounded organelle
GLYMA_15G092900	15	7199767	7200772	integral component of membrane
GLYMA_15G093000	15	7208720	7210848	integral component of membrane
GLYMA_15G093100	15	7225813	7228753	nucleus
GLYMA_15G093200	15	7234291	7238709	integral component of membrane
GLYMA_15G093300	15	7239966	7242365	protein binding
GLYMA_15G093400	15	7242698	7242853	
GLYMA_15G093500	15	7245007	7245776	integral component of membrane
GLYMA_15G093600	15	7246404	7258440	Cul4-RING E3 ubiquitin ligase complex
GLYMA_15G113500	15	8945664	8951383	ATP binding
GLYMA_15G113600	15	8959813	8962275	protein binding
GLYMA_15G113700	15	8967440	8968561	
GLYMA_15G113800	15	8976993	8978992	integral component of mitochondrial inner membrane
GLYMA_15G113900	15	8979921	8984053	
ENSRNA050000318	15	8985364	8985468	
GLYMA_15G114000	15	8990054	8991982	
GLYMA_15G114100	15	8999168	9001915	electron transfer activity
GLYMA_15G114200	15	9001382	9007144	DNA binding
GLYMA_15G114300	15	9010977	9018699	aromatic amino acid family metabolic process
GLYMA_15G114400	15	9018700	9021429	chaperone binding
GLYMA_15G114500	15	9019321	9021429	
GLYMA_15G114600	15	9022570	9023759	chloroplast
GLYMA_15G114700	15	9024267	9025694	O-acyltransferase activity
GLYMA_15G114800	15	9027896	9030669	cytoplasm
GLYMA_15G114900	15	9031222	9033306	integral component of membrane
GLYMA_15G115000	15	9045318	9047577	
GLYMA_15G115100	15	9053766	9056711	protein binding
GLYMA_15G115200	15	9069783	9074529	anion transmembrane transport

GLYMA_15G115300	15	9076848	9077830	cysteine-type endopeptidase inhibitor activity
GLYMA_15G115400	15	9081677	9086514	GO_0023014
GLYMA_15G115500	15	9087902	9093221	hydrolase activity
GLYMA_15G115600	15	9093454	9096411	integral component of membrane
GLYMA_15G115700	15	9108067	9108546	
GLYMA_15G115800	15	9118834	9121579	cytoplasm
GLYMA_15G115900	15	9121807	9128839	integral component of membrane
ENSRNA049760167	15	9130155	9130235	
GLYMA_15G116000	15	9130584	9134253	ATP binding
ENSRNA050000324	15	9135168	9135272	
GLYMA_15G116100	15	9135197	9135487	
GLYMA_15G116200	15	9136796	9139582	
GLYMA_15G116300	15	9141617	9145667	DNA-binding transcription factor activity
GLYMA_15G116400	15	9144027	9144278	
GLYMA_15G116500	15	9160515	9161398	integral component of membrane
GLYMA_15G116600	15	9163979	9164630	
GLYMA_15G116700	15	9176466	9176887	
GLYMA_15G116800	15	9183826	9186787	4 iron, 4 sulfur cluster binding
GLYMA_15G116900	15	9190898	9193445	endoplasmic reticulum
GLYMA_15G167000	15	14653629	14658354	protein metabolic process
GLYMA_15G167100	15	14666790	14686181	endolysosome membrane
GLYMA_15G167200	15	14687797	14693252	ATP binding
GLYMA_15G167300	15	14730333	14731295	
GLYMA_15G167400	15	14778654	14781422	cytosolic large ribosomal subunit
GLYMA_15G167500	15	14807357	14837243	ATP binding
GLYMA_15G167600	15	14838173	14845754	fucose metabolic process
GLYMA_15G204300	15	26953824	26957140	DNA-templated transcription
GLYMA_16G016200	16	1409241	1413726	maturation of 5.8S rRNA
GLYMA_16G016300	16	1422046	1426370	3'-5'-exoribonuclease activity

GLYMA_16G016400	16	1431637	1433520	DNA binding
GLYMA_16G016500	16	1440846	1441640	
GLYMA_16G016600	16	1450709	1455979	DNA binding
GLYMA_16G016700	16	1460102	1463552	DNA binding
GLYMA_16G016800	16	1467805	1469620	
GLYMA_16G016900	16	1481288	1483272	
GLYMA_16G017000	16	1483461	1483663	integral component of membrane
GLYMA_16G017100	16	1483694	1486538	DNA binding
GLYMA_16G017200	16	1512023	1514299	cytoplasm
GLYMA_16G017300	16	1519674	1525290	ATP binding
GLYMA_16G017400	16	1526133	1539596	DNA binding
GLYMA_16G017500	16	1553689	1556564	dioxygenase activity
GLYMA_16G017600	16	1564173	1566310	chloroplast thylakoid membrane
GLYMA_16G017700	16	1576687	1580079	DNA-binding transcription factor activity, RNA polymerase II-specific
GLYMA_16G017800	16	1586339	1591621	cation transmembrane transport
GLYMA_16G017900	16	1596871	1597614	anchored component of plasma membrane
GLYMA_16G018000	16	1601748	1607341	cytokinin-activated signaling pathway
GLYMA_16G018100	16	1612068	1614560	
GLYMA_16G018200	16	1617162	1618781	cytoplasm
GLYMA_16G018300	16	1619151	1623559	acetyl-CoA biosynthetic process from pyruvate
GLYMA_16G018400	16	1625609	1638381	endosomal vesicle fusion
GLYMA_16G018500	16	1643418	1648032	chloroplast
GLYMA_16G018600	16	1648737	1651614	cell differentiation
GLYMA_16G018700	16	1658687	1660150	double-strand break repair via homologous recombination
GLYMA_16G201500	16	36309502	36312180	ATP binding
GLYMA_16G201600	16	36319636	36324825	glycosyltransferase activity
GLYMA_16G201700	16	36328017	36330362	hydrolase activity

GLYMA_16G201800	16	36334150	36337319	acyltransferase activity, transferring groups other than amino-acyl groups
GLYMA_16G201900	16	36341171	36346160	integral component of membrane
GLYMA_16G202000	16	36346588	36347952	cytoplasm
GLYMA_16G202100	16	36350016	36351422	
GLYMA_16G202200	16	36360357	36365645	ATP binding
GLYMA_16G202300	16	36371066	36375227	acyltransferase activity, transferring groups other than amino-acyl groups
GLYMA_16G202400	16	36383751	36388542	ATP binding
GLYMA_16G202500	16	36388841	36390938	cytoplasm
GLYMA_16G202600	16	36394360	36395478	protein binding
GLYMA_16G202700	16	36400757	36403044	maturation of SSU-rRNA from tricistronic rRNA transcript (SSU-rRNA, 5.8S rRNA, LSU-rRNA)
GLYMA_16G202800	16	36404765	36405844	protein binding
GLYMA_16G202900	16	36409506	36410606	protein binding
GLYMA_16G203000	16	36412774	36413868	protein binding
GLYMA_16G203100	16	36416105	36417800	2 iron, 2 sulfur cluster binding
GLYMA_16G203200	16	36419277	36431786	cation transport
GLYMA_16G203300	16	36437330	36445131	ATP binding
GLYMA_16G203400	16	36449021	36451535	box C/D snoRNP assembly
ENSRNA049760089	16	36452769	36452839	
GLYMA_16G203500	16	36455086	36456623	integral component of membrane
GLYMA_16G203600	16	36457598	36461359	aromatic-amino-acid:2-oxoglutarate aminotransferase activity
GLYMA_16G203700	16	36464668	36465760	cellular amino acid metabolic process
GLYMA_16G203800	16	36470848	36472257	positive regulation of growth
GLYMA_16G203900	16	36485467	36506395	mRNA polyadenylation
GLYMA_16G204000	16	36507514	36511554	protein metabolic process
GLYMA_16G204100	16	36513142	36517351	protein metabolic process
GLYMA_16G204200	16	36519694	36524106	DNA binding

GLYMA_16G204300	16	36527485	36532808	cytoplasm
GLYMA_16G204400	16	36534047	36539263	DNA binding
GLYMA_16G204500	16	36543873	36545291	integral component of membrane
GLYMA_16G204600	16	36552157	36556546	glycolytic process
GLYMA_18G183800	18	44296869	44302459	amino acid transmembrane transport
GLYMA_18G183900	18	44311932	44316813	mRNA processing
GLYMA_18G184000	18	44321857	44323268	chloroplast thylakoid membrane
GLYMA_18G184100	18	44361532	44362540	
GLYMA_18G184200	18	44364673	44366631	cytoplasm
GLYMA_18G184300	18	44398974	44400996	cell wall
GLYMA_18G184400	18	44401734	44407633	Cul4A-RING E3 ubiquitin ligase complex
GLYMA_18G184500	18	44451085	44457655	auxin-activated signaling pathway
GLYMA_18G184600	18	44459335	44461314	metal ion binding
GLYMA_18G184700	18	44467187	44469616	dioxygenase activity
GLYMA_18G184800	18	44469990	44478649	metal ion binding
GLYMA_18G184900	18	44479759	44482896	metal ion binding
GLYMA_18G185000	18	44483394	44484541	protein dimerization activity
GLYMA_18G185100	18	44485609	44486232	defense response
GLYMA_18G185200	18	44491574	44495271	mitochondrion
GLYMA_19G011600	19	1111789	1116419	integral component of membrane
GLYMA_19G011700	19	1123637	1130946	cellular oxidant detoxification
GLYMA_19G011800	19	1134716	1143232	cellular oxidant detoxification
GLYMA_19G011900	19	1148510	1149495	
GLYMA_19G012000	19	1152228	1154655	
GLYMA_19G012100	19	1155711	1161298	O-acetyltransferase activity
GLYMA_19G012200	19	1163379	1164570	
GLYMA_19G012300	19	1165111	1173031	chromatin binding
GLYMA_19G012400	19	1191668	1194091	
GLYMA_19G012500	19	1196510	1201064	integral component of membrane

GLYMA_19G012600	19	1198067	1198635	integral component of membrane
GLYMA_19G012700	19	1216285	1219961	glycosyltransferase activity
GLYMA_19G012800	19	1222154	1227306	nucleic acid binding
GLYMA_19G012900	19	1228610	1232288	
GLYMA_19G013000	19	1245134	1247617	
GLYMA_19G013100	19	1252613	1253131	carboxylic ester hydrolase activity
GLYMA_19G013200	19	1255021	1262058	carboxylic ester hydrolase activity
GLYMA_19G013300	19	1266757	1267629	carboxylic ester hydrolase activity
GLYMA_19G013400	19	1267841	1269313	cellular oxidant detoxification
GLYMA_19G013500	19	1275080	1277652	cytoplasm
GLYMA_19G013600	19	1281754	1282986	nucleic acid binding
GLYMA_19G013700	19	1290717	1293481	cytoplasm
GLYMA_19G013800	19	1293458	1297881	4 iron, 4 sulfur cluster binding
GLYMA_19G013900	19	1308096	1308515	integral component of membrane
GLYMA_19G014000	19	1316793	1324308	chloroplast
GLYMA_19G014100	19	1325913	1333857	chloroplast
GLYMA_19G014200	19	1345795	1347011	collagen catabolic process
GLYMA_19G014300	19	1350880	1351779	collagen catabolic process
GLYMA_19G108300	19	36079585	36083553	calcium channel activity
GLYMA_19G108400	19	36093430	36103823	water channel activity
GLYMA_19G108500	19	36108880	36123356	ATP binding
GLYMA_19G108600	19	36124686	36127281	mitochondrion
GLYMA_19G108700	19	36132590	36133705	DNA binding
GLYMA_19G108800	19	36152702	36154505	DNA binding
GLYMA_19G108900	19	36163835	36164863	
GLYMA_19G109000	19	36170931	36174540	
GLYMA_19G109100	19	36236790	36239152	DNA binding
GLYMA_19G109200	19	36245338	36253058	mRNA splicing, via spliceosome
GLYMA_19G109300	19	36255414	36258883	ADP binding

GLYMA_19G109400	19	36265902	36268445	chloroplast
GLYMA_19G109500	19	36312452	36331944	CCR4-NOT core complex
GLYMA_19G193000	19	45083416	45083784	
GLYMA_19G193100	19	45084723	45089886	ATP binding
GLYMA_19G193200	19	45098812	45101623	cytoplasmic translational elongation
GLYMA_19G193300	19	45103820	45107114	nucleus
GLYMA_19G193400	19	45110924	45116012	DNA-binding transcription factor activity
GLYMA_19G193500	19	45118043	45121712	hydrolase activity, acting on ester bonds
GLYMA_19G193600	19	45125361	45126227	
GLYMA_19G193700	19	45128512	45131581	cytosol
GLYMA_19G193800	19	45141719	45143222	DNA binding
GLYMA_19G193900	19	45144855	45148565	acid phosphatase activity
GLYMA_19G194000	19	45151880	45155271	acid phosphatase activity
GLYMA_19G194100	19	45162928	45164877	
GLYMA_19G194200	19	45170699	45172441	endoplasmic reticulum to Golgi vesicle-mediated transport
GLYMA_19G194300	19	45183357	45185175	cytoplasm
GLYMA_19G194400	19	45195804	45200599	
GLYMA_19G194500	19	45201612	45206816	DNA-binding transcription factor activity
GLYMA_19G194600	19	45207593	45209670	protein binding
GLYMA_19G194700	19	45210818	45215315	2 iron, 2 sulfur cluster binding
GLYMA_19G194800	19	45215929	45223182	chloroplast
GLYMA_19G194900	19	45227431	45228555	blue light signaling pathway
GLYMA_19G195000	19	45240022	45240691	
GLYMA_19G195100	19	45246104	45247508	catalytic step 2 spliceosome
GLYMA_19G195200	19	45249420	45250751	auxin-activated signaling pathway
GLYMA_19G195300	19	45253254	45259742	ATP binding
GLYMA_19G195400	19	45262941	45267834	carbohydrate metabolic process
GLYMA_19G195500	19	45269604	45270824	cytoplasm
GLYMA_19G195600	19	45273343	45277374	

GLYMA_19G195700	19	45278065	45279422	
ENSRNA050030486	19	45283719	45283819	
GLYMA_19G195800	19	45294380	45296644	DNA binding
GLYMA_19G195900	19	45304487	45307515	endosome
GLYMA_19G196000	19	45316499	45334008	gibberellic acid mediated signaling pathway
GLYMA_19G231500	19	48206422	48209353	aspartyl esterase activity
GLYMA_19G231600	19	48211413	48214156	integral component of membrane
GLYMA_19G231700	19	48219220	48221865	catalytic activity
GLYMA_19G231800	19	48224250	48225913	catalytic activity
GLYMA_19G231900	19	48228664	48230383	catalytic activity
GLYMA_19G232000	19	48237680	48239239	catalytic activity
GLYMA_19G232100	19	48242546	48244493	cytosolic large ribosomal subunit
GLYMA_19G232200	19	48245375	48248932	carbohydrate transmembrane transport
GLYMA_19G232300	19	48249933	48253371	cytoplasm
GLYMA_19G232400	19	48255346	48257445	
GLYMA_19G232500	19	48265550	48271467	maturation of 5.8S rRNA from tricistronic rRNA transcript (SSU-rRNA, 5.8S rRNA, LSU-rRNA)
ENSRNA050030479	19	48279155	48279245	
GLYMA_19G232600	19	48283860	48285872	catalytic activity
GLYMA_19G232700	19	48285828	48287134	cytoplasmic translation
GLYMA_19G232800	19	48288544	48294901	protein ubiquitination
GLYMA_19G232900	19	48296415	48299266	ATP binding
GLYMA_19G233000	19	48299541	48304769	acyltransferase activity
GLYMA_19G233100	19	48306057	48313443	integral component of membrane
GLYMA_19G233200	19	48315208	48316230	
GLYMA_19G233300	19	48317190	48320962	actin binding
GLYMA_19G233400	19	48321642	48325912	O-acyltransferase activity
GLYMA_19G233500	19	48326072	48330318	
GLYMA_19G233600	19	48330596	48334879	ATPase binding

GLYMA_19G233700	19	48341606	48342474	calcium-mediated signaling
GLYMA_19G233800	19	48353015	48356793	cellular response to ionizing radiation
GLYMA_19G233900	19	48360813	48367717	oxidoreductase activity, acting on NAD(P)H, oxygen as acceptor
GLYMA_19G234000	19	48377054	48380675	actin binding
GLYMA_19G234100	19	48382565	48383761	chromatin binding
GLYMA_19G234200	19	48388585	48393447	hydrolase activity
GLYMA_19G234300	19	48397238	48402182	
GLYMA_19G234400	19	48403334	48414011	cytosol
GLYMA_19G234500	19	48415851	48420752	DNA-binding transcription factor activity
GLYMA_19G234600	19	48443273	48450777	chloroplast
GLYMA_19G234700	19	48451297	48453777	DNA binding

Supplemental Table 3.1: Descriptive Statistics, Analysis of Variance, and Heritability for 12 Root Architecture Traits

		Median Number of Root Tips	Total Number Root Tips	Total Root Length (mm)	Width-to-Depth Ratio	Network Area (mm2)	Median Diameter (mm)	Perimeter (mm)	Volume (mm3)	Surface Area (mm2)	Number of Holes	Average Hole Size (mm2)	Average Root Orientation (deg)
Min	2021	3.75	77.20	1577.14	0.59	2221.70	1.04	2465.53	15332.18	10526.70	88.60	4.24	44.12
	2022	1.60	7.60	52.01	0.48	62.14	1.31	94.13	122.90	239.78	1.80	0.63	38.81
Max	2021	23.10	604.85	14901.46	1.29	22250.58	3.66	17131.65	406316.89	159862.70	1819.15	56.46	52.33
	2022	20.27	432.27	14337.31	1.33	24085.87	5.40	15522.40	838296.61	180995.90	1609.27	126.88	53.73
Median	2021	12.15	325.08	7306.09	0.87	9445.25	1.39	9474.28	69639.98	52196.88	658.10	12.33	48.08
	2022	9.13	217.40	5580.88	0.88	9579.72	1.94	7078.48	97679.05	54664.00	409.40	16.73	47.41
Mean	2021	12.41	324.88	7545.42	0.87	9908.24	1.45	9521.83	87638.23	56075.19	708.01	14.42	48.11
	2022	9.37	225.35	6075.46	0.89	10673.11	2.04	7419.55	142481.67	62851.19	463.71	21.03	47.51
Sample Error	2021	0.20	4.79	139.88	0.01	183.64	0.02	147.89	3440.62	1310.96	18.67	0.44	0.07
	2022	0.21	4.68	149.79	0.01	262.22	0.03	151.60	7738.63	2012.35	16.32	0.88	0.10
Standard Deviation	2021	3.67	85.90	2510.11	0.12	3295.26	0.28	2653.76	61739.70	23524.36	334.97	7.88	1.28
	2022	3.46	78.48	2510.91	0.13	4395.61	0.54	2541.23	129723.11	33733.06	273.62	14.78	1.68
Skew	2021	0.41	0.14	0.41	0.14	0.61	3.62	0.31	2.44	1.01	0.62	1.94	0.18
	2022	0.51	0.31	0.60	0.25	0.69	2.28	0.41	2.46	1.00	1.00	2.53	-0.10
Kurtosis	2021	-0.06	-0.03	-0.36	-0.02	0.20	22.56	-0.14	7.78	1.26	-0.07	5.61	0.69
	2022	-0.17	-0.34	-0.11	0.13	-0.16	8.31	-0.20	7.66	0.61	0.94	10.51	3.87
ANOVA	Gen	0.0016	1.2×10^{-05}	4.4×10^{-06}	0.057	4.5×10^{-10}	2.2×10^{-16}	0.0009386	2.2×10^{-16}	2.77×10^{-14}	1.5×10^{-06}	2.2×10^{-16}	0.092
	Year	2.2×10^{-16}	2.2×10^{-16}	2.2×10^{-16}	0.01711	0.004	2.2×10^{-16}	2.2×10^{-16}	2.2×10^{-16}	0.0002936	2.2×10^{-16}	2.2×10^{-16}	8.664×10^{-07}
	GxY	0.626	0.437	0.373	0.377	0.041	1.5×10^{-06}	0.472	1.06×10^{-12}	0.0025155	0.3523	0.0106	0.792
Heritability (H2)		0.333	0.440	0.456	0.222	0.567	0.781	0.348	0.736	0.642	0.472	0.701	0.167

Supplemental Table 3.2: Analysis of Variance for RSA Traits

	df	Sum Squares	Mean Squares	F value	Pr(>F)	Significance
Median Number of Root Tips						
Genotype	164	2799.2	17.07	1.8	0.0016	**
Year	1	1380.9	1380.94	121.28	2.2×10^{-16}	***
Genotype: Year	164	1782.3	10.87	0.95	0.626	
Residuals	273	3108.5	11.39			
Total Number of Root Tips						
Genotype	164	1639798	9999	1.78	1.18×10^{-05}	***
Year	1	1486446	1486446	265.35	2.2×10^{-16}	***
Genotype: Year	164	937928	5719	1.021	0.437	***
Residuals	273	1529319	5602			
Total Root Length						
Genotype	164	1536315200	9367776	1.84	4.43×10^{-06}	***
Year	1	324234615	324234615	63.63	2.2×10^{-16}	***
Genotype: Year	164	872968489	5322979	1.04	0.373	
Residuals	273	1391144304	5095767			
Width-to-Depth Ratio						
Genotype	164	3	0.018	1.24	0.057	.
Year	1	0.085	0.085	5.75	0.01711	*
Genotype: Year	164	2.52	0.015	1.04	0.377	
Residuals	273	4.02	0.014			
Network Area						
Genotype	164	3932171695	23976657	2.31	4.49×10^{-10}	***
Year	1	87786134	87786134	8.4623	0.004	**
Genotype: Year	164	2161617646	13180595	1.27	0.041	*
Residuals	273	2832040524	10373775			
Median Diameter						
Genotype	164	61.457	0.375	4.58	2.2×10^{-16}	***
Year	1	53.18	53.18	650.25	2.2×10^{-16}	***
Genotype: Year	164	25.44	0.155	1.89	1.49×10^{-06}	***
Residuals	273	22.33	0.082			
Perimeter						
Genotype	164	1487960948	9072933	1.53	0.0009386	***

	Df	Sum Sq	Mean Sq	F value	Pr(>F)	
Year	1	663173933	663173933	112.04	2.2×10^{-16}	***
Genotype: Year	164	978513837	5966548	1.0081	0.472	
Residuals	273	1615834128	5918806			

Volume

	Df	Sum Sq	Mean Sq	F value	Pr(>F)	
Genotype	164	2.80E+12	1.71E+10	3.7887	2.2×10^{-16}	***
Year	1	4.15E+11	4.15E+11	100.2424	2.2×10^{-16}	***
Genotype: Year	164	1.29E+12	1.18E+10	2.613	1.058×10^{-12}	***
Residuals	273	1.229 e +12	4.50E+09			

Surface Area

	Df	Sum Sq	Mean Sq	F value	Pr(>F)	
Genotype	164	2.34 e +11	1431002572	2.795	2.77×10^{-14}	***
Year	1	6.889 e +09	6889559078	13.4558	0.0002936	***
Genotype: Year	164	1.234 E+11	752953213	1.4706	0.0025155	**
Residuals	273	1.40E+11	512014510			

Holes

	Df	Sum Sq	Mean Sq	F value	Pr(>F)	
Genotype	164	23488998	143226	1.8952	1.526×10^{-06}	***
Year	1	8955834	8955834	118.505	2.2×10^{-16}	***
Genotype: Year	164	13046210	79550	1.0526	0.3523	
Residuals	273	20631506	75573			

Size of Hole

	Df	Sum Sq	Mean Sq	F value	Pr(>F)	
Genotype	164	42637	260	3.345	2.2×10^{-16}	***
Year	1	6567	6567.3	84.5116	2.2×10^{-16}	***
Genotype: Year	164	17500	106.7	1.373	0.0106	*
Residuals	273	21214	77.7			

Root Orientation

	Df	Sum Sq	Mean Sq	F value	Pr(>F)	
Genotype	164	421.1	2.568	1.2	0.092	.
Year	1	54.22	54.22	25.358	8.664×10^{-07}	***
Genotype: Year	164	31221	1.9	89	0.792	
Residuals	273	583.75	2.138			

Significance codes: 0 '***' 0.001 '**' 0.01 '*' 0.05 '.' 0.1 ' ' 1

Supplemental Table 3.3: SNPs significant at threshold -log > 3.5

Year	Trait	SNP	Chr	Pos	Neg Log (*p*)	MAF
2021	Average Root Orientation	ss715601650	8	39883389	4.097	0.121
2021	Average Root Orientation	ss715601651	8	39889128	3.771	0.127
2021	Average Root Orientation	ss715601653	8	39894181	3.569	0.124
2021	Average Root Orientation	ss715601655	8	39895283	3.771	0.127
2021	Average Root Orientation	ss715601671	8	39996936	3.964	0.142
2021	Average Root Orientation	ss715601674	8	40012317	3.689	0.142
2021	Average Root Orientation	ss715601683	8	40087882	3.776	0.100
2021	Average Root Orientation	ss715601688	8	40151052	3.706	0.115
2021	Average Root Orientation	ss715601689	8	40152462	3.655	0.121
2021	Average Root Orientation	ss715601692	8	40174127	3.818	0.152
2021	Average Root Orientation	ss715601693	8	40177924	3.767	0.124
2021	Average Root Orientation	ss715601694	8	40181980	4.094	0.109
2021	Average Root Orientation	ss715601697	8	40186293	4.140	0.118
2022	Average Root Orientation	ss715582823	2	41873746	3.955	0.094
2022	Average Root Orientation	ss715594602	6	46884182	3.714	0.091
2022	Average Root Orientation	ss715599973	8	17754828	4.390	0.379
2022	Average Root Orientation	ss715599977	8	17801521	5.420	0.227
2022	Average Root Orientation	ss715599978	8	17801693	5.232	0.221
2022	Average Root Orientation	ss715599979	8	17803816	5.420	0.227
2022	Average Root Orientation	ss715599980	8	17824366	3.643	0.252
2022	Average Root Orientation	ss715601634	8	39694930	4.453	0.127
2022	Average Root Orientation	ss715601635	8	39695136	4.391	0.124
2022	Average Root Orientation	ss715601636	8	39709156	4.167	0.127
2022	Average Root Orientation	ss715601637	8	39714639	3.876	0.094
2022	Average Root Orientation	ss715601640	8	39776648	4.455	0.121
2022	Average Root Orientation	ss715601646	8	39864704	4.097	0.121
2022	Average Root Orientation	ss715601647	8	39868750	4.169	0.115
2022	Average Root Orientation	ss715601648	8	39869850	4.097	0.121
2022	Average Root Orientation	ss715601649	8	39876133	4.169	0.115
2022	Average Root Orientation	ss715601675	8	40012567	3.653	0.152
2022	Average Root Orientation	ss715601676	8	40013536	3.895	0.145
2022	Average Root Orientation	ss715601678	8	40066757	3.691	0.103
2022	Average Root Orientation	ss715601681	8	40083423	3.691	0.103
2022	Average Root Orientation	ss715601682	8	40086074	3.773	0.106
2022	Average Root Orientation	ss715601704	8	40235461	4.592	0.112
2022	Average Root Orientation	ss715625429	16	7411543	4.558	0.091
2021	Hole Size	ss715588357	4	4401469	4.301	0.136
2021	Hole Size	ss715592607	5	209284	4.044	0.133
2021	Hole Size	ss715592625	5	2581248	4.005	0.118
2021	Hole Size	ss715592636	5	2594262	3.634	0.106
2021	Hole Size	ss715592650	5	2635309	3.913	0.100
2021	Hole Size	ss715589814	5	2804036	4.735	0.133
2021	Hole Size	ss715589830	5	2849405	4.352	0.097

2021	Hole Size	ss715589980	5	3236161	5.023	0.103
2021	Hole Size	ss715589991	5	3261123	5.346	0.100
2021	Hole Size	ss715590011	5	3308357	5.071	0.097
2021	Hole Size	ss715590094	5	3594614	4.377	0.082
2021	Hole Size	ss715602780	8	8613083	4.369	0.061
2021	Hole Size	ss715602170	8	44120395	4.040	0.115
2021	Hole Size	ss715602969	9	1128733	3.950	0.073
2021	Hole Size	ss715606496	10	37530875	3.827	0.064
2021	Hole Size	ss715606531	10	37673933	3.732	0.064
2021	Hole Size	ss715632688	18	7816342	3.959	0.088
2021	Hole Size	ss715632868	18	9159569	4.939	0.115
2021	Hole Size	ss715635850	19	48577554	3.630	0.194
2022	Hole Size	ss715606539	10	37686422	4.324	0.055
2022	Hole Size	ss715607749	10	48012886	3.729	0.448
2022	Hole Size	ss715612183	12	32539490	4.491	0.079
2022	Hole Size	ss715618877	14	43248107	4.040	0.070
2022	Hole Size	ss715622589	15	50044525	4.076	0.161
2022	Hole Size	ss715622679	15	50728936	3.688	0.197
2022	Hole Size	ss715625781	17	11383688	3.617	0.233
2022	Hole Size	ss715626472	17	23469087	4.705	0.197
2022	Hole Size	ss715630470	18	3947639	4.076	0.242
2021	Holes	ss715598725	7	7989492	4.605	0.082
2021	Holes	ss715596521	7	16172077	4.040	0.464
2021	Holes	ss715599497	8	13934839	3.956	0.394
2021	Holes	ss715608596	10	828695	3.769	0.055
2022	Holes	ss715584235	2	9675440	3.575	0.452
2022	Holes	ss715595487	6	7265304	4.000	0.312
2022	Holes	ss715596504	7	16111431	3.897	0.370
2022	Holes	ss715604792	9	47332269	3.526	0.255
2022	Holes	ss715610894	11	5747839	4.150	0.303
2022	Holes	ss715610895	11	5747930	4.085	0.312
2022	Holes	ss715610899	11	5782132	3.901	0.303
2022	Holes	ss715610902	11	5801255	4.125	0.291
2022	Holes	ss715620046	14	8743445	4.129	0.461
2021	Median Diameter	ss715582823	2	41873746	4.204	0.094
2021	Median Diameter	ss715589687	4	9581724	5.673	0.100
2021	Median Diameter	ss715587921	4	42194415	7.300	0.115
2021	Median Diameter	ss715592047	5	39435793	3.682	0.173
2021	Median Diameter	ss715600757	8	21813168	4.632	0.215
2021	Median Diameter	ss715600852	8	22270529	3.893	0.073
2021	Median Diameter	ss715604810	9	47548832	4.639	0.061
2021	Median Diameter	ss715607495	10	45463820	5.622	0.245
2021	Median Diameter	ss715613179	12	5486355	4.393	0.376
2021	Median Diameter	ss715613717	13	11706814	4.576	0.458
2021	Median Diameter	ss715614603	13	28326564	4.274	0.482

2021	Median Diameter	ss715620061	14	8897988	3.997	0.058
2021	Median Diameter	ss715623302	15	9957356	4.861	0.161
2021	Median Diameter	ss715622445	15	49164769	5.069	0.155
2022	Median Diameter	ss715627617	17	39376565	7.254	0.067
2022	Median Diameter	ss715627633	17	39481935	9.626	0.055
2022	Median Diameter	ss715631582	18	50344707	5.052	0.079
2022	Median Diameter	ss715637437	20	34414971	9.897	0.442
2021	Median Number of Root Tips	ss715595487	6	7265304	3.909	0.312
2021	Median Number of Root Tips	ss715620046	14	8743445	3.948	0.461
2021	Median Number of Root Tips	ss715624160	16	2949920	4.441	0.148
2021	Median Number of Root Tips	ss715629431	18	18199541	3.526	0.097
2021	Median Number of Root Tips	ss715629445	18	18283444	3.724	0.103
2021	Median Number of Root Tips	ss715629450	18	18333296	3.724	0.103
2021	Median Number of Root Tips	ss715629452	18	18356060	3.608	0.091
2021	Median Number of Root Tips	ss715629457	18	18383144	3.608	0.091
2021	Median Number of Root Tips	ss715629458	18	18386311	3.608	0.091
2021	Median Number of Root Tips	ss715629464	18	18402884	3.608	0.091
2022	Median Number of Root Tips	ss715584235	2	9675440	3.610	0.452
2021	Network Area	ss715579825	1	49176585	3.754	0.118
2021	Network Area	ss715580039	1	50700924	3.645	0.488
2021	Network Area	ss715592820	6	11812926	3.679	0.152
2021	Network Area	ss715594876	6	48364034	3.585	0.212
2021	Network Area	ss715594878	6	48379671	3.786	0.361
2021	Network Area	ss715594883	6	48394685	3.517	0.336
2021	Network Area	ss715600371	8	19775377	3.564	0.430
2021	Network Area	ss715600376	8	19788540	3.539	0.482
2021	Network Area	ss715600383	8	19796815	3.665	0.476
2021	Network Area	ss715604909	9	48665322	3.856	0.106
2021	Network Area	ss715604910	9	48668504	3.517	0.106
2021	Network Area	ss715604912	9	48714806	3.838	0.324
2021	Network Area	ss715604913	9	48729435	3.772	0.118
2021	Network Area	ss715604915	9	48750636	3.994	0.124
2022	Network Area	ss715580930	2	10618540	3.594	0.400
2022	Network Area	ss715600379	8	19788939	3.760	0.473

2021	Perimeter	ss715582527	2	40018672	3.995	0.097
2021	Perimeter	ss715604792	9	47332269	3.856	0.255
2021	Perimeter	ss715624160	16	2949920	3.910	0.148
2021	Perimeter	ss715629445	18	18283444	3.613	0.103
2021	Perimeter	ss715629450	18	18333296	3.613	0.103
2022	Perimeter	ss715595487	6	7265304	4.049	0.312
2022	Perimeter	ss715594876	6	48364034	3.637	0.212
2022	Perimeter	ss715594878	6	48379671	3.629	0.361
2022	Perimeter	ss715620046	14	8743445	3.851	0.461
2021	Surface Area	ss715579825	1	49176585	4.123	0.118
2021	Surface Area	ss715582616	2	4420727	3.589	0.052
2022	Surface Area	ss715592820	6	11812926	3.617	0.152
2022	Surface Area	ss715600371	8	19775377	3.645	0.430
2022	Surface Area	ss715600379	8	19788939	3.693	0.473
2022	Surface Area	ss715600383	8	19796815	3.600	0.476
2022	Surface Area	ss715604887	9	48445356	3.519	0.130
2022	Surface Area	ss715604909	9	48665322	4.409	0.106
2022	Surface Area	ss715604910	9	48668504	3.921	0.106
2022	Surface Area	ss715604912	9	48714806	3.723	0.324
2022	Surface Area	ss715604913	9	48729435	3.650	0.118
2022	Surface Area	ss715604915	9	48750636	3.853	0.124
2022	Surface Area	ss715607770	10	48127921	3.568	0.270
2022	Surface Area	ss715607774	10	48152278	3.568	0.270
2022	Surface Area	ss715607778	10	48170699	3.623	0.270
2022	Surface Area	ss715607784	10	48181565	3.813	0.267
2022	Surface Area	ss715623521	16	1621536	3.676	0.091
2021	Total Number of Root Tips	ss715582527	2	40018672	3.640	0.097
2021	Total Number of Root Tips	ss715594592	6	46854506	3.671	0.091
2021	Total Number of Root Tips	ss715594596	6	46856883	4.051	0.073
2021	Total Number of Root Tips	ss715605657	10	1522807	3.603	0.124
2021	Total Number of Root Tips	ss715624154	16	2947272	3.523	0.142
2021	Total Number of Root Tips	ss715627650	17	39617509	3.614	0.067
2021	Total Number of Root Tips	ss715629458	18	18386311	4.019	0.091
2022	Total Number of Root Tips	ss715582031	2	3742486	3.594	0.261
2022	Total Number of Root Tips	ss715586200	3	41162031	3.558	0.203
2022	Total Number of Root Tips	ss715594876	6	48364034	3.668	0.212
2022	Total Number of Root Tips	ss715594883	6	48394685	3.567	0.336
2022	Total Number of Root Tips	ss715594885	6	48396005	3.545	0.321
2022	Total Number of Root Tips	ss715598775	7	8215952	3.510	0.261
2022	Total Number of Root Tips	ss715624160	16	2949920	4.127	0.148
2022	Total Number of Root Tips	ss715629431	18	18199541	3.643	0.097
2022	Total Number of Root Tips	ss715629445	18	18283444	3.608	0.103
2022	Total Number of Root Tips	ss715629450	18	18333296	3.608	0.103
2022	Total Number of Root Tips	ss715629452	18	18356060	4.019	0.091
2022	Total Number of Root Tips	ss715629457	18	18383144	4.019	0.091

2022	Total Number of Root Tips	ss715629464	18	18402884	4.019	0.091
2021	Total Root Length	ss715595487	6	7265304	3.617	0.312
2021	Total Root Length	ss715594876	6	48364034	3.783	0.212
2021	Total Root Length	ss715594878	6	48379671	3.876	0.361
2021	Total Root Length	ss715594883	6	48394685	3.555	0.336
2021	Total Root Length	ss715594885	6	48396005	3.500	0.321
2021	Total Root Length	ss715620046	14	8743445	3.653	0.461
2021	Volume	ss715585103	3	307872	4.638	0.400
2021	Volume	ss715599804	8	1637004	3.579	0.094
2021	Volume	ss715600371	8	19775377	3.619	0.430
2021	Volume	ss715623514	16	1610380	3.848	0.085
2021	Volume	ss715623516	16	1611595	3.848	0.085
2021	Volume	ss715623521	16	1621536	4.445	0.091
2021	Volume	ss715623524	16	1629041	3.848	0.085
2021	Volume	ss715626368	17	1995081	4.327	0.064
2021	Volume	ss715636692	20	1449558	4.502	0.088
2021	Volume	ss715636693	20	1450515	4.407	0.094
2022	Volume	ss715579825	1	49176585	4.319	0.118
2022	Volume	ss715582616	2	4420727	6.435	0.052
2022	Volume	ss715587929	4	42461950	5.202	0.061
2022	Volume	ss715599474	8	1373179	4.072	0.318
2022	Volume	ss715604909	9	48665322	4.994	0.106
2022	Volume	ss715607784	10	48181565	4.317	0.267
2022	Volume	ss715609265	11	25276674	3.500	0.106
2022	Volume	ss715610405	11	32865992	3.872	0.061
2022	Volume	ss715610406	11	32866054	3.872	0.061
2022	Volume	ss715611347	12	1036614	4.721	0.055
2022	Volume	ss715621455	15	2740735	4.966	0.339
2022	Volume	ss715627279	17	37750369	3.679	0.130
2022	Volume	ss715636694	20	1452106	4.502	0.088
2021	Width-to-Depth Ratio	ss715583682	2	5947162	3.707	0.470
2021	Width-to-Depth Ratio	ss715583684	2	5948580	3.707	0.470
2021	Width-to-Depth Ratio	ss715636632	20	1267801	3.530	0.091
2021	Width-to-Depth Ratio	ss715638000	20	39100920	3.946	0.339
2021	Width-to-Depth Ratio	ss715638002	20	39117215	4.088	0.364
2021	Width-to-Depth Ratio	ss715638004	20	39145005	3.661	0.391
2022	Width-to-Depth Ratio	ss715583686	2	5959354	3.707	0.470
2022	Width-to-Depth Ratio	ss715585374	3	33866089	4.049	0.248
2022	Width-to-Depth Ratio	ss715597486	7	36855637	4.512	0.142
2022	Width-to-Depth Ratio	ss715597487	7	36869304	4.474	0.158
2022	Width-to-Depth Ratio	ss715604528	9	45016688	3.588	0.327
2022	Width-to-Depth Ratio	ss715609206	11	24884673	3.646	0.330
2022	Width-to-Depth Ratio	ss715628308	17	8566482	3.703	0.355
2022	Width-to-Depth Ratio	ss715636628	20	1263704	3.818	0.112
2022	Width-to-Depth Ratio	ss715636630	20	1265928	3.789	0.109

Supplemental Table 3.4. 651 Genes in Linkage with SNPs significant at -log(p) > 4.54

Gene stable ID	Chr.	Gene start (bp)	Gene end (bp)	Gene name	GO term name
GLYMA_02G046700	2	4297419	4301373		plasma membrane
GLYMA_02G046800	2	4302936	4312761		catalytic activity
GLYMA_02G046900	2	4314354	4319916		nucleus
GLYMA_02G047000	2	4322834	4324959		catalytic activity
GLYMA_02G047100	2	4329417	4333528		RNA binding
GLYMA_02G047200	2	4337518	4343470		integral component of membrane
GLYMA_02G047300	2	4344431	4351294		cytoplasm
GLYMA_02G047400	2	4356203	4358686		integral component of membrane
GLYMA_02G047500	2	4373609	4374901		nucleic acid binding
GLYMA_02G047600	2	4376285	4379912		oxidoreductase activity
GLYMA_02G047700	2	4384491	4386890		cell surface receptor signaling pathway
GLYMA_02G047800	2	4396176	4398689		RNA binding
GLYMA_02G047900	2	4402299	4403204		
GLYMA_02G048000	2	4407580	4408194		
GLYMA_02G048100	2	4412271	4418176		nucleus
GLYMA_02G048200	2	4419899	4425822		nucleus
GLYMA_02G048300	2	4426937	4434315		protein kinase activity
GLYMA_02G048400	2	4440520	4451775		metal ion binding
GLYMA_02G048500	2	4447769	4448744		
GLYMA_02G048600	2	4449030	4451814		metal ion binding
GLYMA_02G048700	2	4456124	4457800		
GLYMA_02G048800	2	4458411	4459296		integral component of membrane
GLYMA_02G048900	2	4459650	4462929		metal ion binding
GLYMA_02G049000	2	4464177	4467693		integral component of membrane
GLYMA_02G049100	2	4469856	4474398		response to red or far red light
GLYMA_02G049200	2	4479569	4480377		response to auxin
GLYMA_02G049300	2	4486759	4488584		RNA binding

GLYMA_02G049400	2	4490216	4495264	peptide-methionine (S)-S-oxide reductase activity
GLYMA_02G049500	2	4496218	4498814	nucleus
GLYMA_02G049600	2	4500912	4508232	metal ion binding
GLYMA_02G049700	2	4511302	4519700	nucleus
GLYMA_02G049800	2	4522510	4528329	cytoplasm
GLYMA_02G049900	2	4529051	4529206	integral component of membrane
GLYMA_02G050000	2	4529545	4530681	
GLYMA_02G050100	2	4538456	4541907	nucleus
GLYMA_03G001700	3	187374	191041	cortical microtubule organization
GLYMA_03G001800	3	199857	203222	protein-disulfide reductase activity
GLYMA_03G001900	3	204061	205995	nucleus
GLYMA_03G002000	3	206737	209914	carbohydrate metabolic process
GLYMA_03G002100	3	211934	216522	carbohydrate metabolic process
GLYMA_03G002200	3	214631	219469	protein kinase activity
GLYMA_03G002300	3	225254	226405	nucleus
GLYMA_03G002400	3	234217	238375	nucleic acid binding
GLYMA_03G002500	3	239471	245321	integral component of membrane
GLYMA_03G002600	3	252667	254842	RNA binding
GLYMA_03G002700	3	257834	260910	integral component of membrane
GLYMA_03G002800	3	263773	270060	integral component of membrane
GLYMA_03G002900	3	270078	273611	integral component of membrane
GLYMA_03G003000	3	281581	284883	integral component of membrane
GLYMA_03G003100	3	288563	291114	protein kinase activity
GLYMA_03G003200	3	298397	300282	
GLYMA_03G003300	3	300704	303769	protein kinase activity
GLYMA_03G003400	3	313242	317840	nucleus
GLYMA_03G003500	3	319689	323975	nucleus
GLYMA_03G003600	3	324972	330076	integral component of membrane
GLYMA_03G003700	3	332974	334434	integral component of membrane

GLYMA_03G003800	3	343391	347552	
GLYMA_03G003900	3	349245	353081	plant-type cell wall
GLYMA_03G004000	3	357269	360639	alpha-L-arabinofuranosidase activity
GLYMA_03G004100	3	364853	366774	nucleus
GLYMA_03G004200	3	370538	374055	ATP binding
GLYMA_03G004300	3	375732	377625	cytoplasm
GLYMA_03G004400	3	377626	383458	negative regulation of DNA-templated transcription
GLYMA_03G004500	3	391913	396356	
GLYMA_03G004600	3	398842	404874	phosphatidylinositol transfer activity
GLYMA_03G004700	3	406773	408434	
GLYMA_03G004800	3	418391	423868	integral component of membrane
GLYMA_03G004900	3	426042	442555	mRNA processing
GLYMA_04G102500	4	9463356	9464836	
GLYMA_04G102600	4	9480145	9484815	integral component of membrane
GLYMA_04G102700	4	9488775	9494564	integral component of membrane
GLYMA_04G102800	4	9497727	9503510	integral component of membrane
GLYMA_04G102900	4	9509980	9513597	RNA binding
GLYMA_04G103000	4	9530332	9533665	
GLYMA_04G103100	4	9554862	9558678	methyltransferase activity
GLYMA_04G103200	4	9567274	9568529	
GLYMA_04G103300	4	9570059	9571000	
GLYMA_04G103400	4	9611225	9615074	obsolete cell
GLYMA_04G103500	4	9624916	9626694	
GLYMA_04G103600	4	9677545	9680477	catalytic activity
GLYMA_04G103700	4	9701112	9702592	integral component of membrane
GLYMA_04G103800	4	9705282	9705434	
GLYMA_04G167700	4	42079785	42082205	coenzyme A metabolic process
ENSRNA049760745	4	42112591	42112663	tRNA-Ala
GLYMA_04G167800	4	42116363	42119511	membrane

GLYMA_04G167900	4	42124874	42127039	integral component of membrane
GLYMA_04G168000	4	42172882	42174041	
GLYMA_04G168100	4	42174898	42175537	NAD biosynthetic process
GLYMA_04G168200	4	42175994	42176200	
GLYMA_04G168300	4	42191074	42194388	nucleus
GLYMA_04G168400	4	42241347	42242428	
GLYMA_04G168500	4	42248937	42254258	hydrolase activity, acting on ester bonds
GLYMA_04G168600	4	42262556	42263689	ribosome binding
GLYMA_04G168700	4	42278385	42282461	integral component of membrane
GLYMA_04G168800	4	42287869	42290820	GTP binding
GLYMA_04G169000	4	42346861	42348336	nucleus
GLYMA_04G169100	4	42355994	42356600	
GLYMA_04G169200	4	42358456	42360357	nucleus
GLYMA_04G169300	4	42365061	42369247	integral component of membrane
GLYMA_04G169400	4	42380768	42381923	
GLYMA_04G169500	4	42382255	42385930	integral component of membrane
GLYMA_04G169600	4	42389919	42391416	
GLYMA_04G169700	4	42399854	42400021	
GLYMA_04G169800	4	42416557	42417895	
GLYMA_04G169900	4	42428584	42429495	regulation of DNA-templated transcription
GLYMA_04G170000	4	42464752	42467580	integral component of membrane
GLYMA_04G170100	4	42542222	42544189	nucleus
GLYMA_05G030900	5	2678918	2682880	mitochondrion
GLYMA_05G031000	5	2689614	2699278	cysteine-type deubiquitinase activity
GLYMA_05G031100	5	2705628	2711940	mRNA cis splicing, via spliceosome
GLYMA_05G031200	5	2712680	2715373	integral component of membrane
GLYMA_05G031300	5	2720956	2729817	regulation of DNA-templated transcription
GLYMA_05G031400	5	2733265	2735493	ATP binding
GLYMA_05G031500	5	2742497	2744586	nucleus

GLYMA_05G031600	5	2745464	2749487	integral component of membrane
GLYMA_05G031700	5	2753222	2754948	microtubule-based process
GLYMA_05G031800	5	2760249	2763974	regulation of DNA-templated transcription
GLYMA_05G031900	5	2767384	2787627	cytoplasm
GLYMA_05G032000	5	2790581	2794268	protein kinase activity
GLYMA_05G032100	5	2794636	2796021	
GLYMA_05G032200	5	2802638	2804780	nucleus
GLYMA_05G032300	5	2818779	2826218	protein binding
GLYMA_05G032400	5	2835362	2841192	
GLYMA_05G032500	5	2844488	2847302	membrane
GLYMA_05G032600	5	2848695	2852187	microtubule binding
GLYMA_05G032700	5	2864935	2869204	ubiquitin-protein transferase activity
GLYMA_05G032800	5	2870616	2871729	
GLYMA_05G032900	5	2872504	2874006	integral component of membrane
GLYMA_05G033000	5	2882073	2884630	intracellular anatomical structure
GLYMA_05G033100	5	2882782	2883558	
GLYMA_05G033200	5	2894024	2897467	mRNA splicing, via spliceosome
GLYMA_05G033300	5	2899580	2899938	integral component of membrane
GLYMA_05G033400	5	2903718	2907357	nucleus
GLYMA_05G033500	5	2908499	2912457	oxidoreductase activity, acting on the aldehyde or oxo group of donors, l acceptor
GLYMA_05G033600	5	2918077	2918869	
GLYMA_05G033700	5	2928085	2929424	protein binding
GLYMA_05G035300	5	3113055	3118511	proteolysis
GLYMA_05G035400	5	3118491	3120900	integral component of membrane
GLYMA_05G035500	5	3123293	3124468	integral component of membrane
GLYMA_05G035600	5	3129627	3132703	integral component of membrane
GLYMA_05G035700	5	3138855	3145745	ATP binding
GLYMA_05G035800	5	3151303	3153428	integral component of membrane
GLYMA_05G035900	5	3162908	3168262	RNA binding

GLYMA_05G036000	5	3171382	3171876		
GLYMA_05G036100	5	3177057	3183023		cytoplasm
GLYMA_05G036200	5	3186730	3189327		integral component of membrane
GLYMA_05G036300	5	3189678	3192613		catalytic activity
GLYMA_05G036400	5	3200781	3201440		protein binding
GLYMA_05G036500	5	3209765	3213223		integral component of membrane
GLYMA_05G036600	5	3214335	3221205		protein kinase activity
GLYMA_05G036700	5	3224675	3226041		
GLYMA_05G036800	5	3241818	3243016		DNA-binding transcription factor activity
GLYMA_05G036900	5	3260922	3263195		
GLYMA_05G037000	5	3266166	3272260		integral component of membrane
GLYMA_05G037100	5	3279689	3281101		membrane
GLYMA_05G037200	5	3292832	3296192		protein kinase activity
ENSRNA049760111	5	3297116	3297195	tRNA-Leu	
GLYMA_05G037300	5	3299913	3303696		protein binding
GLYMA_05G037400	5	3307818	3315114		peroxisomal membrane
GLYMA_05G037500	5	3318255	3323478		metal ion binding
GLYMA_05G037600	5	3326981	3327574		
GLYMA_05G037700	5	3334270	3337647		NAD+ ADP-ribosyltransferase activity
GLYMA_05G037800	5	3361590	3364100		nucleus
GLYMA_05G037900	5	3366809	3371296		ATP binding
GLYMA_05G038000	5	3377196	3385642		rRNA processing
GLYMA_05G038100	5	3388905	3391023		cytoplasm
GLYMA_05G038200	5	3398047	3399121		protein dimerization activity
GLYMA_05G038300	5	3401960	3408039		integral component of membrane
GLYMA_05G038400	5	3410511	3415753		hydrolase activity, acting on ester bonds
GLYMA_05G038500	5	3418552	3420505		DNA binding
GLYMA_05G038600	5	3431124	3435309		protein binding
GLYMA_07G085400	7	7870356	7876333		ATP binding

GLYMA_07G085500	7	7877189	7883386	integral component of membrane
GLYMA_07G085600	7	7891876	7896291	integral component of membrane
GLYMA_07G085700	7	7910707	7915213	integral component of membrane
GLYMA_07G085800	7	7918483	7922268	ATP binding
GLYMA_07G085900	7	7924353	7928899	
GLYMA_07G086000	7	7942077	7944540	integral component of membrane
GLYMA_07G086100	7	7948705	7949954	
GLYMA_07G086200	7	7964042	7967721	flavin adenine dinucleotide binding
GLYMA_07G086300	7	7997334	7998516	regulation of DNA-templated transcription
GLYMA_07G086400	7	8000996	8002926	nucleus
GLYMA_07G086500	7	8015207	8021014	ATP binding
GLYMA_07G086600	7	8024187	8029402	protein transport
GLYMA_07G086700	7	8031061	8031833	integral component of membrane
GLYMA_07G086800	7	8032435	8034515	mitochondrion
GLYMA_07G086900	7	8037905	8039995	
GLYMA_07G087000	7	8053652	8055911	
GLYMA_07G087100	7	8057372	8058244	
GLYMA_07G087200	7	8063714	8064534	integral component of membrane
GLYMA_07G087300	7	8067710	8068385	
GLYMA_07G087400	7	8068697	8073551	oxidoreductase activity, acting on the aldehyde or oxo group of donors, N acceptor
GLYMA_07G087500	7	8093667	8100429	oxidoreductase activity, acting on the aldehyde or oxo group of donors, N acceptor
GLYMA_07G087600	7	8103388	8104969	oxidoreductase activity, acting on the aldehyde or oxo group of donors, N acceptor
GLYMA_07G087700	7	8111751	8121053	ATP binding
GLYMA_08G217800	8	17676081	17681757	nucleus
GLYMA_08G217900	8	17685997	17702340	mitotic sister chromatid cohesion
GLYMA_08G218000	8	17705556	17711781	
GLYMA_08G218100	8	17723077	17726462	catalytic activity

GLYMA_08G218200	8	17727507	17736077	integral component of membrane
GLYMA_08G218300	8	17746118	17747218	
GLYMA_08G218400	8	17747795	17750917	protein kinase activity
GLYMA_08G218500	8	17769268	17770741	membrane
GLYMA_08G218600	8	17784425	17786833	nucleus
GLYMA_08G218700	8	17787384	17792912	catalytic activity
GLYMA_08G218800	8	17793108	17796564	chloroplast
GLYMA_08G218900	8	17796580	17798681	integral component of membrane
GLYMA_08G219000	8	17813887	17816494	acyltransferase activity, transferring groups other than amino-acyl group
GLYMA_08G219100	8	17818201	17822329	chloroplast
GLYMA_08G219200	8	17824529	17837260	chloroplast
GLYMA_08G219300	8	17837504	17842580	integral component of membrane
GLYMA_08G219400	8	17843671	17845527	membrane
GLYMA_08G219500	8	17847935	17853405	integral component of membrane
GLYMA_08G219600	8	17854666	17856011	
GLYMA_08G219700	8	17857603	17860441	integral component of membrane
GLYMA_08G219800	8	17863774	17864667	protein ubiquitination
GLYMA_08G219900	8	17867478	17873695	integral component of membrane
GLYMA_08G220000	8	17875817	17877391	
GLYMA_08G220100	8	17880513	17887538	metal ion binding
GLYMA_08G220200	8	17889781	17898867	acyltransferase activity, transferring groups other than amino-acyl group
GLYMA_08G220300	8	17900423	17901287	integral component of membrane
GLYMA_08G220400	8	17908440	17911791	regulation of flower development
GLYMA_08G220500	8	17911846	17915248	
GLYMA_08G249000	8	21699042	21700600	
GLYMA_08G249100	8	21725339	21726323	
GLYMA_08G249200	8	21727446	21730345	integral component of membrane
GLYMA_08G249300	8	21743467	21744016	
GLYMA_08G249400	8	21748017	21750483	integral component of membrane

GLYMA_08G249500	8	21764339	21765748	acyltransferase activity, transferring groups other than amino-acyl group
GLYMA_08G249600	8	21767874	21772678	integral component of membrane
GLYMA_08G249700	8	21802765	21806491	integral component of membrane
GLYMA_08G249800	8	21807655	21811474	anchored component of membrane
GLYMA_08G249900	8	21840291	21842869	cytosol
GLYMA_08G250000	8	21849856	21854008	heme binding
GLYMA_08G250100	8	21868222	21870550	nucleus
GLYMA_08G250200	8	21873948	21874889	defense response
GLYMA_08G250300	8	21883792	21885282	
GLYMA_08G250400	8	21893620	21904683	oxidoreductase activity
GLYMA_08G250500	8	21920107	21922538	metal ion binding
GLYMA_08G250600	8	21932682	21934440	nucleus
GLYMA_08G288700	8	40111458	40116627	GTPase activity
GLYMA_08G288800	8	40142225	40145724	integral component of membrane
GLYMA_08G288900	8	40148172	40152533	integral component of membrane
GLYMA_08G289000	8	40175872	40176762	
GLYMA_08G289100	8	40181096	40199847	Golgi apparatus
GLYMA_08G289200	8	40207246	40209420	integral component of membrane
GLYMA_08G289300	8	40220202	40220423	regulation of DNA-templated transcription
GLYMA_08G289400	8	40245455	40249358	nucleic acid binding
GLYMA_08G289500	8	40269544	40273383	
GLYMA_08G289600	8	40293958	40299165	
GLYMA_08G289700	8	40300039	40300645	gluconokinase activity
GLYMA_08G289800	8	40301039	40302939	intracellular membrane-bounded organelle
GLYMA_08G289900	8	40304775	40307300	ATP binding
GLYMA_08G290000	8	40309863	40312592	
GLYMA_08G290100	8	40318384	40327148	nucleus
GLYMA_08G290200	8	40345838	40351483	protein kinase activity
GLYMA_08G290300	8	40353614	40356078	integral component of membrane

GLYMA_09G255000	9	47428922	47432420	catalytic activity
GLYMA_09G255100	9	47439258	47442513	metal ion binding
GLYMA_09G255200	9	47457748	47465103	NAD binding
GLYMA_09G255300	9	47470438	47474331	nucleus
GLYMA_09G255400	9	47475550	47482896	
GLYMA_09G255500	9	47485124	47488455	ribosome
GLYMA_09G255600	9	47493591	47501433	integral component of endoplasmic reticulum membrane
GLYMA_09G255700	9	47507850	47511743	integral component of membrane
GLYMA_09G255800	9	47517468	47520530	
GLYMA_09G255900	9	47520955	47521167	integral component of membrane
GLYMA_09G256000	9	47524747	47530243	protein kinase activity
GLYMA_09G256100	9	47530401	47534434	carbohydrate metabolic process
GLYMA_09G256200	9	47548047	47552180	cytoplasm
GLYMA_09G256300	9	47553262	47558455	integral component of membrane
GLYMA_09G256400	9	47558228	47559081	integral component of membrane
GLYMA_09G256500	9	47562527	47563231	membrane
GLYMA_09G256600	9	47564659	47568053	mitochondrion
GLYMA_09G256700	9	47570343	47583508	intracellular protein transport
GLYMA_09G256800	9	47598004	47598784	integral component of membrane
GLYMA_09G256900	9	47602956	47604833	
GLYMA_09G257000	9	47606735	47616389	integral component of membrane
GLYMA_09G257100	9	47619504	47623279	ubiquitin-protein transferase activity
GLYMA_09G257200	9	47627999	47629509	integral component of membrane
GLYMA_09G257400	9	47632586	47645269	integral component of membrane
GLYMA_09G257300	9	47635541	47638576	integral component of membrane
GLYMA_09G257500	9	47646061	47653232	integral component of membrane
GLYMA_09G257600	9	47650619	47653281	ribosomal large subunit biogenesis
GLYMA_09G257700	9	47657743	47668614	nucleus
GLYMA_09G257800	9	47667497	47670973	ATP binding

GLYMA_09G267600	9	48539846	48541166	
GLYMA_09G267700	9	48541771	48543831	anchored component of plasma membrane
GLYMA_09G267800	9	48545238	48551306	nucleic acid binding
GLYMA_09G267900	9	48553881	48554449	integral component of membrane
GLYMA_09G268000	9	48555363	48562421	DNA-binding transcription factor activity
GLYMA_09G268100	9	48570632	48571980	
GLYMA_09G268200	9	48572511	48576260	lyase activity
GLYMA_09G268300	9	48581218	48593414	ATP binding
GLYMA_09G268400	9	48594875	48606154	cytosol
GLYMA_09G268500	9	48604740	48609090	protein binding
GLYMA_09G268600	9	48610524	48611277	
GLYMA_09G268700	9	48615020	48619110	nucleus
GLYMA_09G268800	9	48625675	48631364	microtubule binding
GLYMA_09G268900	9	48638803	48644136	minor groove of adenine-thymine-rich DNA binding
GLYMA_09G269000	9	48647144	48650471	integral component of membrane
GLYMA_09G269100	9	48651429	48653656	
GLYMA_09G269200	9	48655605	48661519	oxidoreductase activity
GLYMA_09G269300	9	48662130	48667330	integral component of membrane
GLYMA_09G269400	9	48669469	48672113	oxidoreductase activity
GLYMA_09G269500	9	48672715	48675501	oxidoreductase activity
GLYMA_09G269600	9	48678731	48681590	oxidoreductase activity
GLYMA_09G269700	9	48682766	48684260	
GLYMA_09G269800	9	48687027	48692234	integral component of membrane
GLYMA_09G269900	9	48694898	48703255	integral component of membrane
GLYMA_09G270000	9	48704737	48708820	nucleus
GLYMA_09G270100	9	48716835	48724605	integral component of membrane
GLYMA_09G270200	9	48725417	48728520	protein kinase activity
GLYMA_09G270300	9	48733890	48734902	
GLYMA_09G270400	9	48735991	48740879	protein kinase activity

GLYMA_09G270500	9	48745649	48751140	cytoplasm
GLYMA_09G270600	9	48753177	48754562	integral component of membrane
GLYMA_09G270700	9	48758879	48763390	protein binding
GLYMA_09G270800	9	48765962	48770118	mediator complex
GLYMA_09G270900	9	48774489	48775667	calcium ion binding
GLYMA_09G271000	9	48778944	48784665	integral component of membrane
GLYMA_10G221900	10	45339110	45345346	response to light intensity
GLYMA_10G222000	10	45346296	45349474	
GLYMA_10G222100	10	45346323	45349130	response to light intensity
GLYMA_10G222200	10	45351101	45356279	protein kinase activity
GLYMA_10G222300	10	45358021	45358882	
GLYMA_10G222400	10	45366010	45367642	response to oxidative stress
GLYMA_10G222500	10	45373587	45376359	response to oxidative stress
GLYMA_10G222600	10	45378675	45380536	integral component of membrane
GLYMA_10G222700	10	45381000	45381544	nucleic acid binding
GLYMA_10G222800	10	45381577	45387369	nucleus
GLYMA_10G222900	10	45393914	45399095	integral component of membrane
GLYMA_10G223000	10	45400648	45401217	enzyme inhibitor activity
GLYMA_10G223100	10	45404603	45405334	enzyme inhibitor activity
GLYMA_10G223200	10	45415775	45417826	nucleus
GLYMA_10G223300	10	45430584	45438893	nucleic acid binding
GLYMA_10G223400	10	45440350	45443915	ribosome
GLYMA_10G223500	10	45444200	45451455	integral component of membrane
GLYMA_10G223600	10	45458315	45458750	double fertilization forming a zygote and endosperm
GLYMA_10G223700	10	45459518	45462243	
GLYMA_10G223800	10	45464900	45468155	nucleus
GLYMA_10G223900	10	45473669	45476195	integral component of membrane
GLYMA_10G224000	10	45479863	45493565	carbohydrate metabolic process
GLYMA_10G224100	10	45494198	45496872	cytoplasm

GLYMA_10G224200	10	45498206	45500186	nucleic acid binding
GLYMA_10G224300	10	45503642	45505214	
GLYMA_10G224400	10	45509340	45510452	integral component of membrane
GLYMA_10G224500	10	45514702	45516815	integral component of membrane
GLYMA_10G224600	10	45526661	45531424	
GLYMA_10G224700	10	45534516	45534867	
GLYMA_10G224800	10	45537703	45537876	
GLYMA_10G224900	10	45540859	45544972	phosphatidylinositol binding
GLYMA_10G225000	10	45549152	45550892	
GLYMA_10G225100	10	45561745	45564354	
GLYMA_10G225200	10	45579021	45582548	nucleus
GLYMA_12G012500	12	915303	917557	hydrolase activity, hydrolyzing O-glycosyl compounds
GLYMA_12G012600	12	918419	919047	integral component of membrane
GLYMA_12G012700	12	920004	923697	
GLYMA_12G012800	12	925017	925703	integral component of peroxisomal membrane
GLYMA_12G012900	12	928448	932347	mRNA binding
GLYMA_12G013000	12	934229	940832	intracellular protein transport
GLYMA_12G013100	12	946483	947858	
GLYMA_12G013200	12	955725	959879	integral component of membrane
GLYMA_12G013300	12	964404	969175	regulation of DNA-templated transcription
GLYMA_12G013400	12	970258	974669	integral component of membrane
GLYMA_12G013500	12	976612	977910	DNA binding
GLYMA_12G013600	12	980833	989353	DNA binding
GLYMA_12G013700	12	996838	998367	membrane
GLYMA_12G013800	12	999082	1002268	cellular lipid metabolic process
GLYMA_12G013900	12	1005754	1007345	
GLYMA_12G014000	12	1010585	1015652	positive regulation of DNA-templated transcription
GLYMA_12G014100	12	1018924	1022357	integral component of membrane
GLYMA_12G014200	12	1025584	1029095	methyltransferase activity

GLYMA_12G014300	12	1033151	1037054		methyltransferase activity
GLYMA_12G014400	12	1039859	1041301		
GLYMA_12G014500	12	1042638	1045495		resolution of meiotic recombination intermediates
GLYMA_12G014600	12	1045864	1059246		DNA binding
ENSRNA050001912	12	1060610	1060688	snoR117	
GLYMA_12G014700	12	1066217	1070263		ATP binding
GLYMA_12G014800	12	1071368	1079413		integral component of membrane
GLYMA_12G014900	12	1080511	1088935		metal ion binding
GLYMA_12G015000	12	1090328	1090698		cytosol
GLYMA_12G015100	12	1092653	1096887		oxidoreductase activity
GLYMA_12G015200	12	1097666	1098792		
GLYMA_12G015300	12	1100879	1104057		oxidoreductase activity
GLYMA_12G015400	12	1105883	1108270		oxidoreductase activity
GLYMA_12G015500	12	1112166	1114351		oxidoreductase activity
GLYMA_12G015600	12	1117363	1121163		cytoplasm
GLYMA_12G015700	12	1122541	1123618		cellular modified amino acid catabolic process
GLYMA_12G015800	12	1126280	1132370		flower development
GLYMA_12G015900	12	1136900	1140971		membrane
GLYMA_12G016000	12	1142873	1143676		single-stranded DNA binding
GLYMA_12G016100	12	1144398	1148496		anaphase-promoting complex
GLYMA_12G016200	12	1144638	1144811		
GLYMA_12G016300	12	1153697	1156286		
GLYMA_13G037100	13	11622743	11626638		nucleus
GLYMA_13G037200	13	11623501	11623874		
GLYMA_13G037300	13	11627463	11638646		nucleic acid binding
GLYMA_13G037400	13	11674345	11678672		integral component of membrane
GLYMA_13G037500	13	11706406	11706753		protein-disulfide reductase activity
GLYMA_13G037600	13	11706789	11719329		nucleus
GLYMA_13G037700	13	11709400	11713858		

GLYMA_13G037800	13	11749903	11750913		integral component of membrane
GLYMA_13G037900	13	11759194	11762687		integral component of membrane
GLYMA_13G038000	13	11784164	11784597		nucleus
GLYMA_13G038100	13	11786608	11792614		nucleus
GLYMA_13G038200	13	11815808	11818199		nucleus
GLYMA_15G032600	15	2617264	2617590		
GLYMA_15G032700	15	2617841	2620783		nucleus
GLYMA_15G032800	15	2628375	2632765		regulation of DNA-templated transcription
GLYMA_15G032900	15	2635424	2636605		
GLYMA_15G033000	15	2636819	2643592		integral component of membrane
GLYMA_15G033100	15	2652481	2654283		mitochondrial intermembrane space
GLYMA_15G033200	15	2656030	2657795		mitochondrion
GLYMA_15G033300	15	2659168	2659979		integral component of membrane
GLYMA_15G033400	15	2661884	2664401		DNA binding
GLYMA_15G033500	15	2665196	2669410		integral component of membrane
GLYMA_15G033600	15	2675618	2678073		nucleic acid binding
GLYMA_15G033700	15	2686015	2693849		outer membrane
GLYMA_15G033800	15	2693820	2696407		
GLYMA_15G033900	15	2701565	2702716		
GLYMA_15G034000	15	2704676	2719699		metal ion binding
GLYMA_15G034100	15	2722009	2727957		integral component of membrane
GLYMA_15G034200	15	2727304	2729830		nucleic acid binding
GLYMA_15G034300	15	2730657	2737709		ATP binding
ENSRNA050000362	15	2735683	2735760	snoR28	
GLYMA_15G034400	15	2740960	2746344		oxidoreductase activity, acting on the aldehyde or oxo group of donors, acceptor
GLYMA_15G034500	15	2754696	2757556		nucleus
GLYMA_15G034600	15	2765299	2770528		integral component of membrane
GLYMA_15G034700	15	2771938	2774552		metal ion binding
GLYMA_15G034800	15	2776136	2781490		

GLYMA_15G034900	15	2790182	2794119	
GLYMA_15G035000	15	2796277	2798223	
GLYMA_15G035100	15	2800824	2803162	ubiquitin-dependent protein catabolic process
GLYMA_15G035200	15	2803980	2808450	
GLYMA_15G035300	15	2814675	2820897	transcription initiation at RNA polymerase II promoter
GLYMA_15G035400	15	2822350	2822727	
GLYMA_15G035500	15	2825110	2827434	response to abscisic acid
GLYMA_15G035600	15	2830678	2835534	intracellular protein transport
GLYMA_15G035700	15	2836778	2840795	
GLYMA_15G035800	15	2841251	2842819	integral component of membrane
GLYMA_15G035900	15	2843074	2849389	RNA binding
GLYMA_15G036000	15	2855429	2860689	
GLYMA_15G036100	15	2862111	2864041	cytoplasm
GLYMA_15G123800	15	9834252	9837179	proteolysis
GLYMA_15G123900	15	9840544	9844156	nucleus
GLYMA_15G124000	15	9845097	9849312	cytoplasm
GLYMA_15G124100	15	9850904	9858110	integral component of membrane
GLYMA_15G124200	15	9861709	9873220	cytosol
GLYMA_15G124300	15	9875069	9875810	
GLYMA_15G124400	15	9881706	9885816	integral component of membrane
GLYMA_15G124500	15	9888761	9894068	defense response
GLYMA_15G124600	15	9894533	9898193	integral component of membrane
GLYMA_15G124700	15	9904106	9911579	integral component of membrane
GLYMA_15G124800	15	9915745	9916676	
GLYMA_15G124900	15	9917306	9924755	integral component of membrane
GLYMA_15G125000	15	9927434	9929672	integral component of membrane
GLYMA_15G125100	15	9930653	9933697	oxidoreductase activity
GLYMA_15G125200	15	9936226	9942471	integral component of membrane
GLYMA_15G125300	15	9944915	9945451	actin binding

GLYMA_15G125400	15	9948110	9950838		regulation of DNA-templated transcription
GLYMA_15G125500	15	9952666	9956867		regulation of DNA-templated transcription
GLYMA_15G125600	15	9957729	9961129		defense response
GLYMA_15G125700	15	9962401	9965136		protein binding
GLYMA_15G125800	15	9966956	9969650		membrane
GLYMA_15G125900	15	9970216	9977246		integral component of membrane
GLYMA_15G126000	15	9978071	9984000		protein binding
GLYMA_15G126100	15	9986010	9986372	psaJ	integral component of membrane
GLYMA_15G126200	15	9993331	9998476		integral component of membrane
GLYMA_15G126300	15	9993826	9994626		
GLYMA_15G126400	15	10013184	10015082		ubiquitin-protein transferase activity
GLYMA_15G126500	15	10026688	10032754		cytoplasm
GLYMA_15G126600	15	10042824	10045511		integral component of membrane
GLYMA_15G126700	15	10048619	10053791		nucleic acid binding
GLYMA_15G126800	15	10060618	10065342		
GLYMA_15G126900	15	10068929	10072999		defense response
GLYMA_15G127000	15	10069699	10073883		
GLYMA_15G127100	15	10079102	10084397		defense response
GLYMA_15G259000	15	49050970	49051421		
GLYMA_15G259100	15	49109474	49111739		
GLYMA_15G259200	15	49151184	49155711		cytoplasm
GLYMA_15G259300	15	49152690	49153131		integral component of membrane
GLYMA_15G259400	15	49185213	49187748		DNA binding
GLYMA_15G259500	15	49199706	49202722		response to oxidative stress
GLYMA_15G259800	15	49203518	49219334		
GLYMA_15G259600	15	49206962	49211313		regulation of DNA-templated transcription
GLYMA_15G259700	15	49208579	49209658		
GLYMA_15G259900	15	49223458	49224959		
GLYMA_15G260000	15	49225920	49236827		cytoplasm

GLYMA_15G260100	15	49256253	49261623		nucleic acid binding
GLYMA_15G260200	15	49265048	49265746		proteolysis
GLYMA_15G260300	15	49280109	49288192		thiosulfate sulfurtransferase activity
GLYMA_16G072400	16	7292429	7294920		protein-disulfide reductase activity
GLYMA_16G072500	16	7293317	7294097		
GLYMA_16G072600	16	7296986	7301966		integral component of membrane
GLYMA_16G072700	16	7334768	7338117		DNA binding
GLYMA_16G072800	16	7348727	7349581		
GLYMA_16G072900	16	7352635	7353651		
GLYMA_16G073000	16	7363595	7367826		nucleus
GLYMA_16G073100	16	7376670	7381613		integral component of membrane
GLYMA_16G073200	16	7387012	7391186		
GLYMA_16G073300	16	7395155	7396911		
ENSRNA050002662	16	7395263	7395362	snoR1	
ENSRNA050002669	16	7395898	7395980	SNORD24	
GLYMA_16G073400	16	7406652	7407890		
GLYMA_16G073500	16	7414249	7426535		chloroplast
GLYMA_16G073600	16	7433300	7436617		oxidoreductase activity
GLYMA_16G073700	16	7442094	7446398		integral component of membrane
GLYMA_16G073800	16	7451045	7452524		UDP-glycosyltransferase activity
GLYMA_16G073900	16	7451047	7451566		
GLYMA_16G074000	16	7452848	7453324		
GLYMA_16G074100	16	7456787	7457831		
GLYMA_16G074200	16	7465834	7473801		nucleus
GLYMA_16G074300	16	7475096	7482042		protein kinase activity
GLYMA_16G074400	16	7482702	7483896		integral component of membrane
GLYMA_16G074500	16	7489153	7489729		
GLYMA_16G074600	16	7493107	7495937		ribosome
GLYMA_16G074700	16	7504853	7517609		integral component of membrane

GLYMA_16G074800	16	7527171	7533853	integral component of membrane
GLYMA_17G184000	17	23434224	23434797	
GLYMA_17G184100	17	23442643	23443739	nucleic acid binding
GLYMA_17G184200	17	23448768	23450356	nucleic acid binding
GLYMA_17G184300	17	23453051	23456592	integral component of membrane
GLYMA_17G184400	17	23463888	23465508	plasma membrane
GLYMA_17G184500	17	23469456	23471306	plasma membrane
GLYMA_17G184600	17	23487694	23488520	
GLYMA_17G184700	17	23500448	23503711	catalytic activity
GLYMA_17G184800	17	23505148	23507851	ATP binding
GLYMA_17G184900	17	23521954	23528610	cytosol
GLYMA_17G185000	17	23531754	23534400	nucleus
GLYMA_17G185100	17	23547204	23549736	ATPase activator activity
GLYMA_17G185200	17	23552065	23557873	protein binding
GLYMA_17G185300	17	23567602	23568277	mitochondrion
GLYMA_17G185400	17	23569564	23569752	
GLYMA_17G185500	17	23569868	23571255	ribosome
GLYMA_17G185600	17	23571268	23573950	proton transmembrane transporter activity
GLYMA_17G185700	17	23575285	23575714	
GLYMA_17G185800	17	23584802	23586743	integral component of membrane
ENSRNA050000440	17	23584949	23585010	Intron_gpII
GLYMA_17G185900	17	23589596	23589899	
GLYMA_17G186000	17	23590809	23591093	integral component of membrane
GLYMA_17G186100	17	23591200	23591765	oxidoreductase activity, acting on NAD(P)H
GLYMA_17G186200	17	23591968	23592532	membrane
GLYMA_17G237200	17	39256648	39261225	nucleus
GLYMA_17G237300	17	39263011	39264414	integral component of membrane
GLYMA_17G237400	17	39269471	39270222	cell-cell signaling involved in cell fate commitment
GLYMA_17G237500	17	39275410	39276430	mitotic cell cycle

GLYMA_17G237600	17	39285991	39286642	
GLYMA_17G237700	17	39305810	39306678	integral component of membrane
GLYMA_17G237800	17	39314910	39316504	cytoplasm
GLYMA_17G237900	17	39325886	39328062	DNA binding
GLYMA_17G238000	17	39342062	39342974	hydrolase activity
GLYMA_17G238100	17	39349616	39350869	rRNA processing
GLYMA_17G238200	17	39357077	39359079	cytoplasm
GLYMA_17G238300	17	39371870	39373991	integral component of membrane
GLYMA_17G238400	17	39388031	39390247	cytoplasm
GLYMA_17G238500	17	39397559	39397795	nucleic acid binding
GLYMA_17G238600	17	39410033	39415645	
GLYMA_17G238700	17	39424740	39427127	protein ubiquitination
GLYMA_17G238800	17	39431136	39435970	integral component of membrane
GLYMA_17G238900	17	39439399	39442109	
GLYMA_17G239000	17	39449686	39454670	proteolysis
GLYMA_17G239100	17	39462452	39463649	
GLYMA_17G239200	17	39477219	39478708	nucleus
GLYMA_17G239300	17	39486604	39488313	
GLYMA_17G239400	17	39491307	39494566	
GLYMA_17G239500	17	39495438	39511517	ATP binding
GLYMA_17G239600	17	39512498	39518671	
GLYMA_17G239700	17	39528463	39535244	integral component of membrane
GLYMA_17G239800	17	39537994	39541100	integral component of membrane
GLYMA_17G239900	17	39545941	39547083	nucleic acid binding
GLYMA_17G240000	17	39548307	39553633	chloroplast
GLYMA_17G240100	17	39564103	39565209	nucleus
GLYMA_17G240200	17	39574738	39576684	integral component of membrane
GLYMA_17G240300	17	39592153	39593989	nucleus
GLYMA_17G240400	17	39597803	39603019	cytoplasm

GLYMA_17G240500	17	39604375	39609674	nucleus
GLYMA_17G240600	17	39606256	39607334	proteolysis
GLYMA_18G090900	18	9044375	9050844	proteolysis
GLYMA_18G091000	18	9060662	9066712	nucleic acid binding
GLYMA_18G091100	18	9081698	9083625	acyltransferase activity, transferring groups other than amino-acyl group
GLYMA_18G091200	18	9110189	9111657	integral component of membrane
GLYMA_18G091300	18	9117664	9125559	oxidoreductase activity
GLYMA_18G091400	18	9135906	9137438	nucleic acid binding
GLYMA_18G091500	18	9143974	9150438	catalytic activity
GLYMA_18G091600	18	9165090	9166656	nucleus
GLYMA_18G091700	18	9183996	9184634	
GLYMA_18G091800	18	9188322	9191318	defense response
GLYMA_18G091900	18	9231711	9233200	
GLYMA_18G092000	18	9236520	9241505	RNA binding
GLYMA_18G092100	18	9240928	9241197	
GLYMA_18G092200	18	9262392	9267008	nucleus
GLYMA_18G092300	18	9278545	9280545	structural molecule activity
GLYMA_18G215200	18	50219142	50222679	integral component of membrane
GLYMA_18G215300	18	50246446	50247549	DNA binding
GLYMA_18G215400	18	50255282	50260137	cytosol
GLYMA_18G215500	18	50262516	50267358	protein kinase activity
GLYMA_18G215600	18	50266705	50269603	hydrolase activity, hydrolyzing O-glycosyl compounds
GLYMA_18G215700	18	50279788	50283686	carbohydrate metabolic process
GLYMA_18G215800	18	50287921	50291401	integral component of membrane
GLYMA_18G215900	18	50295562	50300258	protein-disulfide reductase activity
GLYMA_18G216000	18	50303953	50307600	ATP binding
GLYMA_18G216100	18	50311058	50319639	
GLYMA_18G216200	18	50319842	50323452	integral component of membrane
GLYMA_18G216300	18	50326165	50331008	cortical microtubule organization

GLYMA_18G216400	18	50338826	50346088		integral component of membrane
GLYMA_18G216500	18	50354555	50355369		integral component of membrane
GLYMA_18G216600	18	50355487	50359944		protein ubiquitination
GLYMA_18G216700	18	50369166	50369708		
GLYMA_18G216800	18	50371768	50388753		integral component of membrane
GLYMA_18G216900	18	50401763	50406217		acetyltransferase activity
GLYMA_18G217000	18	50427219	50437453		integral component of membrane
GLYMA_18G217100	18	50440342	50444873		integral component of membrane
GLYMA_18G217200	18	50451061	50454354		integral component of membrane
GLYMA_18G217300	18	50451299	50451568		
GLYMA_18G217400	18	50463930	50466563		protein dimerization activity
GLYMA_20G099500	20	34275736	34292214		
GLYMA_20G099600	20	34295547	34302938		ATP binding
GLYMA_20G099700	20	34307301	34308845		integral component of membrane
GLYMA_20G099800	20	34310977	34312408		integral component of membrane
GLYMA_20G099900	20	34312783	34318966		integral component of membrane
GLYMA_20G100000	20	34320945	34324107		regulation of DNA-templated transcription
GLYMA_20G100100	20	34325559	34327943		defense response
GLYMA_20G100200	20	34329531	34336381		hydrolase activity
GLYMA_20G100300	20	34338338	34339114		integral component of membrane
GLYMA_20G100400	20	34346064	34357352		integral component of membrane
ENSRNA050030386	20	34369815	34369933	5S_rRNA	
GLYMA_20G100500	20	34388983	34390790		protein binding
GLYMA_20G100600	20	34391133	34392975		nucleus
GLYMA_20G100700	20	34398890	34402882		
GLYMA_20G100800	20	34408300	34420130		ATP binding
GLYMA_20G100900	20	34421932	34423966		proteolysis
GLYMA_20G101000	20	34430192	34439087		methyltransferase activity
GLYMA_20G101100	20	34439997	34441373		cytoplasm

GLYMA_20G101200	20	34443522	34447013		regulation of alternative mRNA splicing, via spliceosome
GLYMA_20G101300	20	34448047	34448376		oxidoreductase activity, acting on the CH-CH group of donors, NAD or
GLYMA_20G101400	20	34449093	34454758		integral component of membrane
GLYMA_20G101500	20	34454972	34459221		integral component of membrane
GLYMA_20G101600	20	34462051	34466726		integral component of membrane
GLYMA_20G101700	20	34467936	34475476		integral component of membrane
GLYMA_20G101800	20	34482678	34487576		
GLYMA_20G101900	20	34483296	34484294		vacuole
ENSRNA050030384	20	34484058	34484253	U2	
ENSRNA050030391	20	34486612	34486762	U4	
GLYMA_20G102000	20	34490052	34492059		
GLYMA_20G102100	20	34497052	34498857		
GLYMA_20G102200	20	34500889	34502958		
GLYMA_20G102300	20	34523300	34524470		
GLYMA_20G102400	20	34529273	34531173		ubiquitin-dependent protein catabolic process
GLYMA_20G102500	20	34538883	34540903		ubiquitin-dependent protein catabolic process